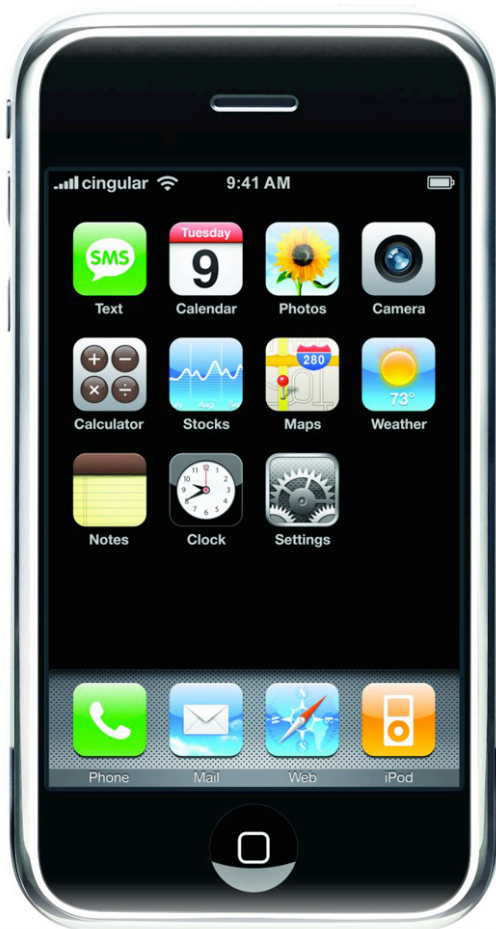


# Antennas for Small Mobile Terminals

Jordi Masip Montserrat, Jordi Obrador Ruíz, Romain Pozzo di Borgo

Mobkom group 08gr118, Aalborg University

June 4th, 2008



# Abstract

Digital Video Broadcasting for Handheld Terminals (DVB-H) is a service based on DVB-T (for terrestrial broadcasting). Some differences and changes must be considered to adapt the existing DVB-T technology to the experimental DVB-H one. The purpose of this master thesis is to design the best possible antenna for DVB-H. In order to achieve this, some scenarios are considered such as the influence of the human hand and wood or metal planes (emulating tables).

As this antenna must be inside a handheld device, its size will be a very limiting factor. This is worsened by the fact that the wavelength is bigger than the size of the handheld device and so this constraint will add more problems related with small bandwidth, impedance matching, received power, etc.

Thanks to the simulations, two planar monopole antennas have been chosen and explained in detail under the different scenarios. It will be seen that these two antennas are small enough to fit in a handheld device and that they can overcome all the problems related with the wavelength, received power, human body interference, etc.

# Preface

This report is the result of the 10th semester project work carried out between February 4th and June 4th 2008 by the students in group no. 08gr1118 at the Department of Communication Technology, Aalborg University, Denmark. This project report documents the study and investigation on small antenna for Digital Video Broadcasting for Handheld terminals. It includes the understanding of the basics DVB-H, its technology and problems. Initially, the core concepts are developed in a theoretical analysis in order to define the problem definition. Then, different scenarios are proposed for a normal utilization of a DVB-H terminal, and antennas designed are implemented in a software simulator using MATLAB.

Mobile Communication group 08gr1118

June 4th, 2008

Aalborg University

# Acknowledgments

We want to dedicate this thesis to a lot of people but first of all and more specially we would like to express our gratitude to our supervisor, Gert Froelund Pedersen, for his valuable guidance and time throughout this project. Also we want to thank Ondrej Franek for his time and his help.

As we said there is a lot of people we want to thank so, here they go:

To Pacco for being the best cook ever, to Serena for all the support and the Italian coffee, to Sergio for not letting Jop sleep, to Sam for being pretty gay, to Gosia for all the jelly shots, to Kasagrande for being the real architect, to Pepe for all the fishing, to Shela for all the burgers, to Stefan for programming all night long without loud music, to Bérénice for being the best drunk girl ever, to David because he never tries and never follows to the next step, to Milos because he is really goooing, to Lutz for ... , to Richard for being DJ.Drunk, to Flora for all the sandwiches, to Marcelo for the lousy laughing, to Borja for being always falling of the bike, to Gunter for all the great songs, to Inga for being from Sweden, to Adriana, Esther and Karolina.

And of course, to our families and friends.

Jop, Jordi and Romain

# Contents

<b>1</b>	<b>DVB-H</b>	<b>4</b>
1.1	Time Slicing . . . . .	5
1.1.1	Consumption . . . . .	6
1.2	MPE-FEC Error Correction . . . . .	7
1.2.1	Filling the matrix before transmission . . . . .	8
1.2.2	Reception and decoding of the matrix . . . . .	8
1.3	OFDM fundamentals . . . . .	9
1.4	2k, 4k and 8k OFDM modes . . . . .	13
1.5	Operation Bandwidth . . . . .	14
<b>2</b>	<b>Infrastructure layout: Network topology</b>	<b>15</b>
2.1	Reception Scenarios . . . . .	15
2.2	Network topology . . . . .	16
2.2.1	DVB-H Shared Network . . . . .	16
2.2.2	DVB-H Hierarchical Network . . . . .	17
2.2.3	DVB-H Dedicated Network . . . . .	18
2.2.4	Topology . . . . .	20
2.3	Coverage area . . . . .	20
<b>3</b>	<b>Antenna Design</b>	<b>28</b>
3.1	Electromagnetism fundamentals for antennas . . . . .	28
3.2	Types of antennas . . . . .	30
3.2.1	Dipole . . . . .	31
3.2.2	Loop . . . . .	31
3.2.3	Microstrip . . . . .	31
3.2.3.1	Planar Antennas . . . . .	31
3.2.4	Switched Antennas . . . . .	32
3.3	Required Antenna Performance . . . . .	32
3.4	Previous work done on DVB-H antennas . . . . .	33
3.4.1	Jari Holopainen . . . . .	33
3.4.2	Fredrik Persson & Mattias Wideheim . . . . .	34
3.4.3	Mauro Pelosi . . . . .	34
3.4.4	Zena Fourzoli & Radwan Charafeddine . . . . .	34
3.4.5	Yue Gao & Chao Chiap Chiau & Xiaodong Chen . . . . .	34
3.4.6	Fractus . . . . .	34

3.5	FDTD Theory . . . . .	35
3.6	FDTD Software . . . . .	37
<b>4</b>	<b>Antenna Design and Simulations</b>	<b>40</b>
4.1	Patch Antennas . . . . .	40
4.2	Meandered Monopole Vertical Antenna . . . . .	41
4.2.1	Smith Chart . . . . .	42
4.2.2	Radiation Pattern . . . . .	43
4.2.3	Hand Simulations . . . . .	45
4.2.4	Hands simulations in horizontal position . . . . .	48
4.2.5	Wood Influence . . . . .	49
4.2.6	Metal influence . . . . .	50
4.2.7	S11 and radiation efficiency . . . . .	51
4.2.8	Q at resonance and BW resonance . . . . .	53
4.2.9	Conclusions . . . . .	53
4.3	Meandered Monopole Book-Type Antenna . . . . .	54
4.3.1	Smith Chart . . . . .	54
4.3.2	Radiation Pattern . . . . .	55
4.3.3	Hands Simulations . . . . .	57
4.3.4	Wood influence . . . . .	58
4.3.5	S11 and radiation efficiency . . . . .	59
4.3.6	Q at resonance and BW resonance . . . . .	61
4.3.7	Conclusions . . . . .	62
<b>A</b>	<b>List of receiver chips of DVB-H by manufacturer</b>	<b>73</b>
<b>B</b>	<b>List of cell-phones with DVB-H capability by manufacturer</b>	<b>81</b>
<b>C</b>	<b>Radio-propagation models</b>	<b>83</b>
<b>D</b>	<b>Smith Chart</b>	<b>98</b>
<b>E</b>	<b>Resonant frequency in PIFA antennas</b>	<b>100</b>
<b>F</b>	<b>Antenna Matching</b>	<b>103</b>
<b>G</b>	<b>Design and Simulation of different antennas</b>	<b>105</b>

# Introduction

For many years a fast evolution of video devices has been taking place. It began with the television boom after the second world war and since then a lot of improvements have occurred: color TV, progressive improvement of image sound and quality, reduction of the device's size, flat screens, digital TV and finally the TV on handheld devices.

This Master Thesis main objective is to design the best Digital Video Broadcasting for Handheld devices (DVB-H) antenna possible and to simulate and evaluate the effect of the human hand on the antenna when holding the device. To decide which antenna is best, different parameters have been considered. The first thing considered was that the antennas size was not to big. Then, it was checked if the antenna's impedance could be matched to  $50 \Omega$  for all the frequency range (the lowest DVB-H band: 470 MHz to 702 MHz). And finally it was pursued that the bandwidth was as big as possible and the radiation pattern as omnidirectional as possible.

On this thesis different types of antenna are evaluated including PIFA antennas but finally the conclusion is that the most suitable ones for DVB-H are the Switchable Meandered Monopole Antennas. The simulations have been done using a simulator developed at Aalborg University based on FDTD theory. Some interesting antennas are found both for vertical ground plane antennas and horizontal ground plane antennas and they are evaluated in different scenarios such as holding the handheld device with one hand, both hands, or laying on a surface (i.e. wood).

On Chapter 1 one can read a short summary about how the DVB-H system works. Chapter 2 explains the network topology and shows some calculations about the coverage area of the DVB-H system as well as explaining the possible reception scenarios. Chapter 3 shows the different basic types of antenna and explains the theory behind them. Also on Chapter 3 it can be found a summary on the FDTD theory and the software used for the simulations. Finally, Chapter 4 includes all the designs and all the results of the simulations of the antennas. Additional information can be found through appendixes A to G.

# Chapter 1

## DVB-H

The DVB-H standard is based on the DVB-T standard and so the main characteristics are almost the same for both. It is not intended in this project to explain all the details of DVB-T and neither of DVB-H and so the lecture of documents such as [1], [2] and [3] are recommended to continue reading on this subject. In any case a short summary of the three texts mentioned can be read in this chapter, which focuses mainly in the new characteristics that DVB-H adds to DVB-T.

DVB-T (Digital Video Broadcast-Terrestrial) is an initiative to standarize the digital television emissions around the world. This standard was created in 1993 and, by 1995 it was almost finished and become operational. The adopted source coding methods are MPEG-2 and, more recently, H.264/MPEG-4. This system transmits in different orthogonal subcarriers a compressed digital audio/video stream, using OFDM modulation. This system was created to work with 6, 7 and 8 MHz bandwidth for each TV channel. Within DVB-T exist two different OFDM modes: 2k and 8k as is described in the following sections.

DVB-H is the evolution of DVB-T to supply digital video to handheld devices. Although DVB-T could also supply the handheld devices, the problem was that the handheld devices consumed too much power. This is due to the fact that DVB-T is a streaming system and the receptor has to have the antenna always turned on which is a serious battery problem for portable devices. The solution to this problem is DVB-H which uses time slicing and an additional error correction system (MPE-FEC) to lower the power consumption. In fact, only the time slicing is implemented as a way to lower power consumption as the additional error correction system is optional to DVB-H, although its use is recommended. These two additional features are implemented at the link layer and so the DVB-T physical layer is not affected by the DVB-H system, which is really important because then both systems can coexist. The counterpart of using time slicing is that using MPEG-2 packets like in DVB-T to carry the information is no longer an option because they work as a whole streaming system, and so IP datagrams are used to send the DVB-H data in a packet based way. In order to insert IP datagrams into MPEG-2 packets the MPE (Multi Protocol Encapsulation) system is used.

Another thing that is also new in DVB-H with respect to DVB-T is an additional 4k FFT mode (apart from the 2k and 8k that exist in DVB-T) that is a trade-off between the mobility of the user (speed) and the extension of the SFN (Single Frequency Network) cell. This 2k, 4k and 8k modes are



discussed in section 1.4. Figure 1.1 shows a schematic description of how the DVB-H system interacts with the DVB-T system.

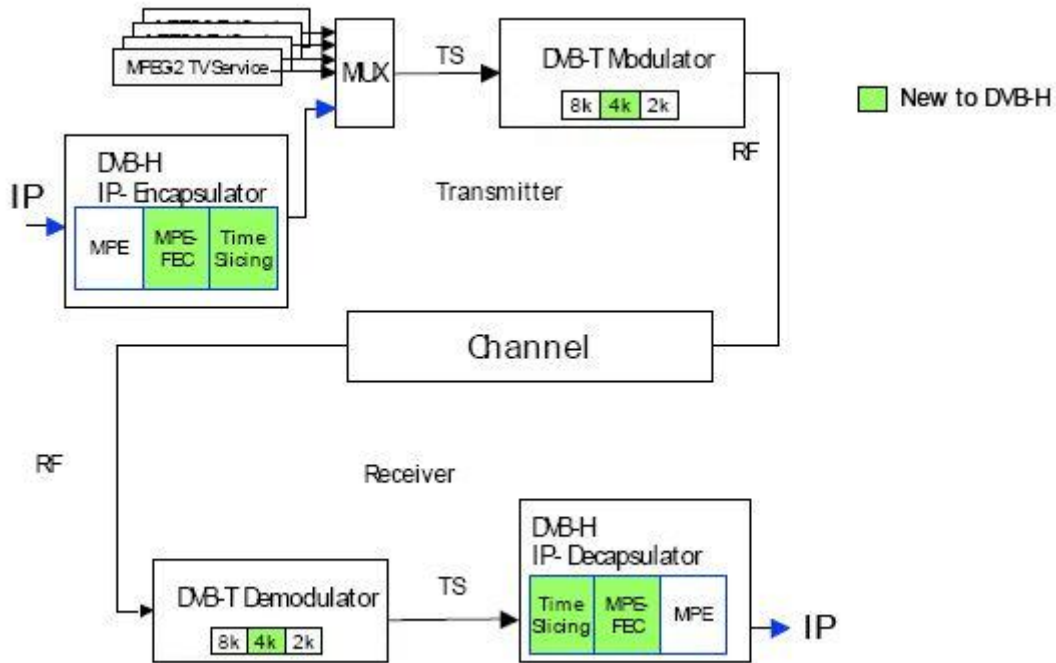


Figure 1.1: Schematic description of the DVB-H system operating over a DVB-T system. The original figure comes from [3].

Another problem that appears on DVB-H terminals is the need of a certain power at the reception antenna which could be difficult to achieve. In fact, it is possible to achieve in an outdoor scenario but it could be difficult in indoor and in-car scenarios. These problems are discussed in Chapter 2.

## 1.1 Time Slicing

The DVB-H way of inserting IP datagrams into DVB-T's MPEG-2 Transport Stream (TS) is to use multiprotocol encapsulation (MPE) and so each IP datagram is encapsulated into one MPE section. A stream of MPE sections are then put into an elementary stream (ES). Each MPE section has a 12-Byte header, a 4-Byte cyclic redundancy check (CRC-32) tail and a payload length, which is identical to the length of the IP datagram, which is carried by the MPE section.

A DVB-H handheld device scenario may be able to receive audio/video services transmitted over IP on ESs having a low bitrate, although the MPEG-2 TS may have a high bitrate, and so the particular ES of interest only occupies a fraction of the total MPEG-2 TS bitrate. Additionally, to reduce the power consumption you would only like the receiver to demodulate the ES instead of the whole

MPEG-2 TS, which can be done thanks to that with time slicing the MPE sections of a particular ES are sent in high bitrate bursts instead of with a constant low bitrate.

The counterpart of this system is that the receiver will have to know when to power on to receive only the ESs. This precise timing between ESs is achieved by signaling in each ES when the next one will start. Thanks to this system, there is no need to have a constant bitrate or fixed burst size (no fixed time between bursts needed). And obviously, the receiver should wake up a little time before the burst arrival to be sure of the correct reception of it.

The actual parameters used for Time Slicing are a compromise between power consumption and other factors, such as service access time and RF performance, but they are not going to be further discussed as it is not this thesis objective.

### 1.1.1 Consumption

In a DVB system, the normal consumption of the system receiver is around 1W [1]. This power drain is too high for a handheld terminal because the power in battery is around 2.5 W and thus, the talk time and the watch time will be small.

The method to reduce this consumption is to use Time Slicing. This system achieves, depending on the Burst Bitrate, a reduction of the consumption between 60% and 93% as shown in figure 1.2. In applications with DVB-H, the typical Constant Bitrate that achieved is 350 Kbps, thus the power saved is around 93%. With this reduction, it could be possible to achieve a power consumption less than 100mW.

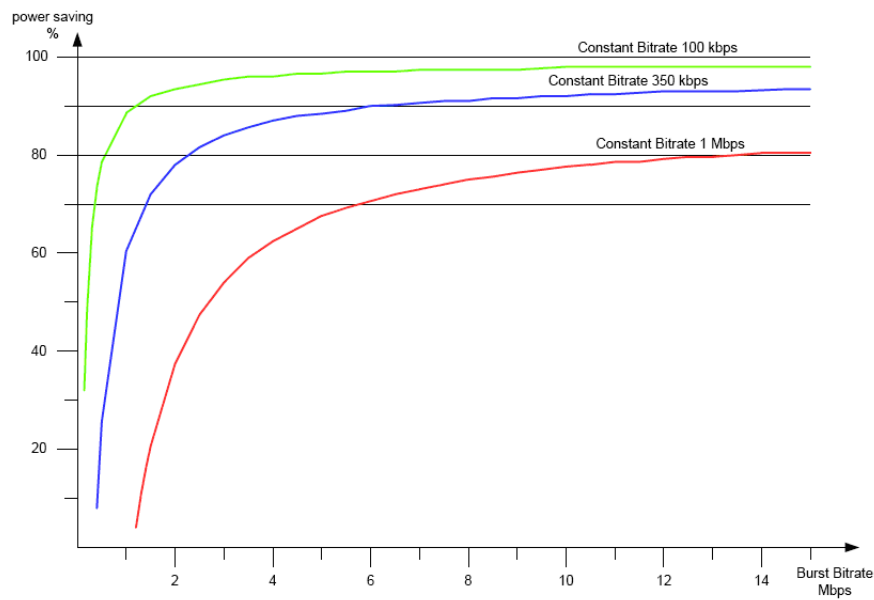


Figure 1.2: Relation between burst bitrate and power saving [1]

## 1.2 MPE-FEC Error Correction

The MPE-FEC system uses the Reed–Solomon parity data (RS data) to protect the IP datagrams of each time sliced burst. The RS data is encapsulated into MPE-FEC sections, which are also part of the burst and are sent immediately after the last MPE section of the burst in the same ES, which enables the receiver to discriminate between the two types of sections in the ES.

To make it more understandable for the reader, its implementation is shortly explained. The first thing is to understand that this system is based on a matrix system, and so all the data is organized as a matrix. This matrix has exactly 255 columns and an undetermined number of rows. This undetermined number of rows is due to the fact that the code has to have some flexibility. Although it is undetermined, the number of rows has limits and so it can only vary between 1 and 1024. Each position in the matrix holds one byte and so the maximum case scenario would be of 255x1024 bytes which is about 2Mbits. The exact matrix structure can be seen in Figure 1.3.

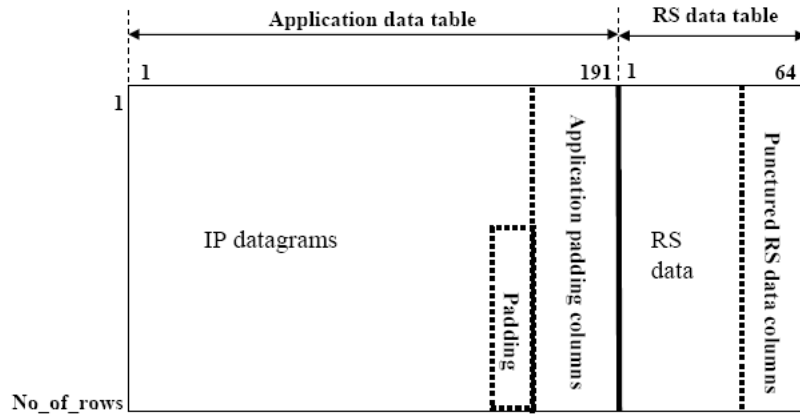


Figure 1.3: Structure of MPE-FEC error correction matrix. Obtained from [1]

The first 191 columns are dedicated to IP datagrams and possible padding, and is called the Application data table. The other 64 columns are dedicated to the parity information of the FEC code and is called the RS data table.

### 1.2.1 Filling the matrix before transmission

IP datagrams are transmitted datagram-by-datagram, starting with the first column of the matrix shown on figure 1.3 and going downwards the first column. Immediately after the end of one IP datagram the following IP datagram starts. As explained before, the length of the IP datagrams may vary arbitrarily from datagram to datagram and so if an IP datagram does not end precisely at the end of a column it continues at the top of the following column. When all IP datagrams have entered the Application data table any unfilled byte positions are padded with zero bytes.

Once the first 191 columns are filled, it is possible then for each row to calculate the 64 parity bytes for the 191 bytes of IP data (including the padding). The code used is the Reed-Solomon RS (255, 191). With this, the matrix is completely filled up.

### 1.2.2 Reception and decoding of the matrix

The IP data is carried in the MPE sections even if MPE-FEC is not being used. This makes reception fully compatible with receivers that don't have MPE-FEC capabilities. A section includes only one IP datagram and it also carries the information about the place where the IP datagram starts and so it indicates the first byte position inside the Application data table. This address is signaled in the MPE header and with it the receiver is able to put the received IP datagram in the right byte position in the Application data table. It is also important to notice that every transmitted section uses a CRC-32 check code to make sure that the reception of the section is reliable.

After the reception of all the sections, there can be a certain number of lost sections. All the correctly received bytes can then be marked as "reliable" and all byte positions in the lost sections can be marked as "unreliable", and so all bytes within the matrix will be marked as either reliable or unreliable. Now the RS decoder proceeds to correct the whole frame and the correction works by rows instead of by columns. The RS decoder is able to correct up to 64 unreliable bytes per each 255 bytes row and if more than 64 bytes are unreliable, the decoder will not be able to restore any lost information. On the other hand, if the correction is only partially achieved, the decoder will know where the error is and act in consequence (i.e. discarding the datagram, using it, etc.).

One of the consequences of using this error correcting system is that in the worst scenario, 2 Mbits of memory is needed and about 100 Kbytes are also necessary to process the data [1]. Another effect is that this error correction method allows a large reduction in the required C/N on mobile channels. Actually, in [3] it can be seen that the resulting C/N performance is similar to what can be achieved using antenna diversity.

### 1.3 OFDM fundamentals

DVB-H system needs a high data rate to transmit videos, music or to get Internet access. In high data rate transmissions some distortion can occur which can damage the communication quality. It is possible to recover the damaged signal thanks to complex receiver structure and elaborated algorithms. However, OFDM (Orthogonal Frequency Division Multiplexing) can simplify this problem. OFDM based systems were born during the second world war for American military usages. Nevertheless, the first patent was obtained many years later in 1970. Lots of improvement about OFDM were done between 1970 and 1990 such as dispersion reduction and higher data rate. Finally, the first commercial use was in 1987 with the Digital Audio Processing.

This multi-carrier transmission is a solution based on the fact that all the subcarriers are orthogonal to each other. In fact, OFDM converts a high data rate channel to many low data rate channels (subcarriers). The problem of high data rate is that a large bandwidth is required to avoid some losses during the transmission (due to multi-path environment). To solve it, information is split into small parts which are frequency constant. Each subcarrier is modulated at its own frequency and is separated by a time space interval. Orthogonal signals can be transmitted by overlapped spectrum and so a large amount of bandwidth can be saved (see Figure 1.4). This spared frequency range has many advantages such as increasing the capacity of the channel (more simultaneous users). OFDM makes overlapping possible by splitting the information into N channels spaced out of a multiple of  $\frac{1}{T_{Symbol}}$  time. The bandwidth saved might be used for other channel uses.

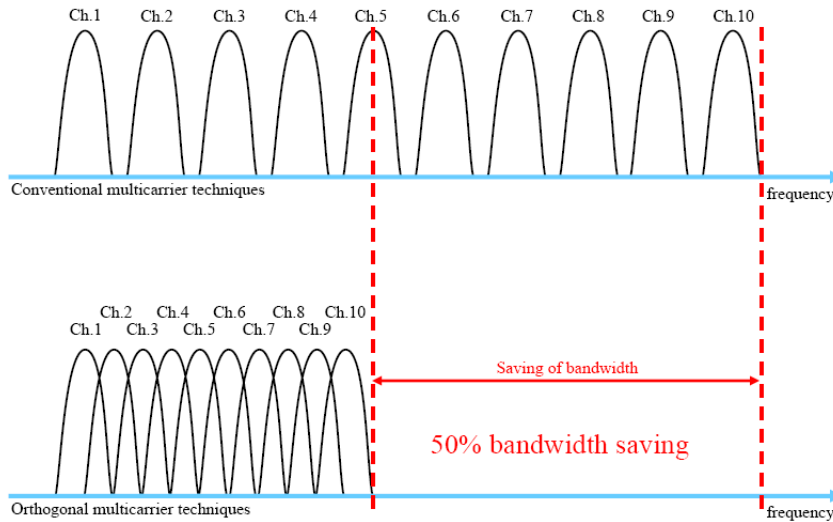


Figure 1.4: Spectral efficiency of OFDM signals [20][21]

OFDM method can also reduce some distortion parameters such as ISI (inter symbol interference) and ICI (inter carrier interference). To avoid ISI, the symbol duration  $T_{symbol}$  must be larger than the delay spread. By this way, delayed information is contained into the symbol period and does not overlap the next symbol (see Figure 1.5).

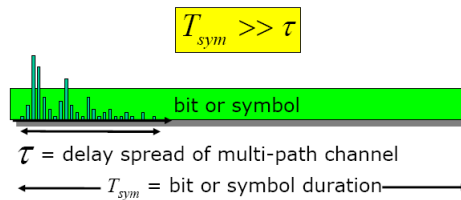


Figure 1.5: Delay spread and symbol duration [20][21]

Delay spread occurs because of multi-path channel. Specially when the line-of-sight is obstructed between the transmitter and the receiver, radio waves arrive from different directions with different amplitudes, phases and time-delay. The latter could create some distortions which are responsible of interference between a given symbol and the next one, which is illustrated in 1.6.

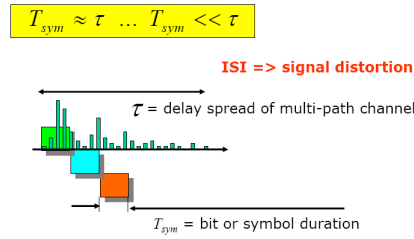


Figure 1.6: Inter-symbol interference[20][21]

In Figure 1.6, the echo of a given symbol is damaging the next one. The guard interval is a solution to solve the ISI effect. It is a signal time interval added between each symbol to avoid overlapping. The guard interval must be greater than the expected delay spread. This method is illustrated in Figure 1.7.

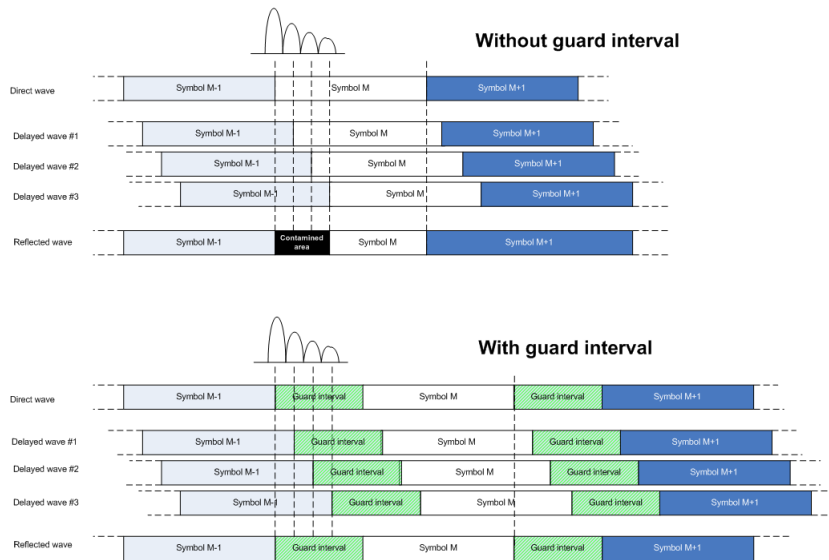


Figure 1.7: Guard time interval

However, the guard interval must be cyclically extended to avoid ICI. The guard interval is a cyclic extension of OFDM symbols, which provides orthogonality over dispersive channels. This ensures that delayed waves of a given OFDM symbol always have an integer number of cycles inside the FFT interval. However, this cyclic prefix (CP) occurs a loss of signal energy but removes the ICI.

Currently, Forward Error Control Correction (FEC) and interleaving are added in OFDM system in order to improve the robustness and protect it against burst errors. This enhanced OFDM system is called Coded OFDM (COFDM). In the following graph, the transceiver is equipped with a FEC and interleaving systems. Once the input binary data is collected into the transceiver, FEC coded the

information using convolutional codes. This code is interleaved to obtain diversity gain. Interleaver places the adjacent outputs far apart in frequency domain, meaning that two close outputs will be separated far away from each other in frequency domain. This technique improves the BER (error bits over total transmitted bits) of the system and so the communication efficiency.

The next step is to convert the serial data into parallel ones. During this stage, known pilots symbols are inserted with the known mapping schemes. Pilots symbols are added in order to estimate the channel transfer function. Thanks to them, it is possible to measure the channel transfer functions for each subcarriers. Then, a cyclic prefix is added to limit the ICI and ISI effects. Finally, we convert the digital signal into an analog one and send the information by radio frequencies modulation. At this point, OFDM modulation is ready to be transmitted. Information is sent from the emitter to the receiver through the wireless channel. The received signal follows the inverse procedure: analog to digital conversion, demodulation, parallel to series and finally FEC decoding and de-interleaving. All these steps are sum up in Figure 1.8.



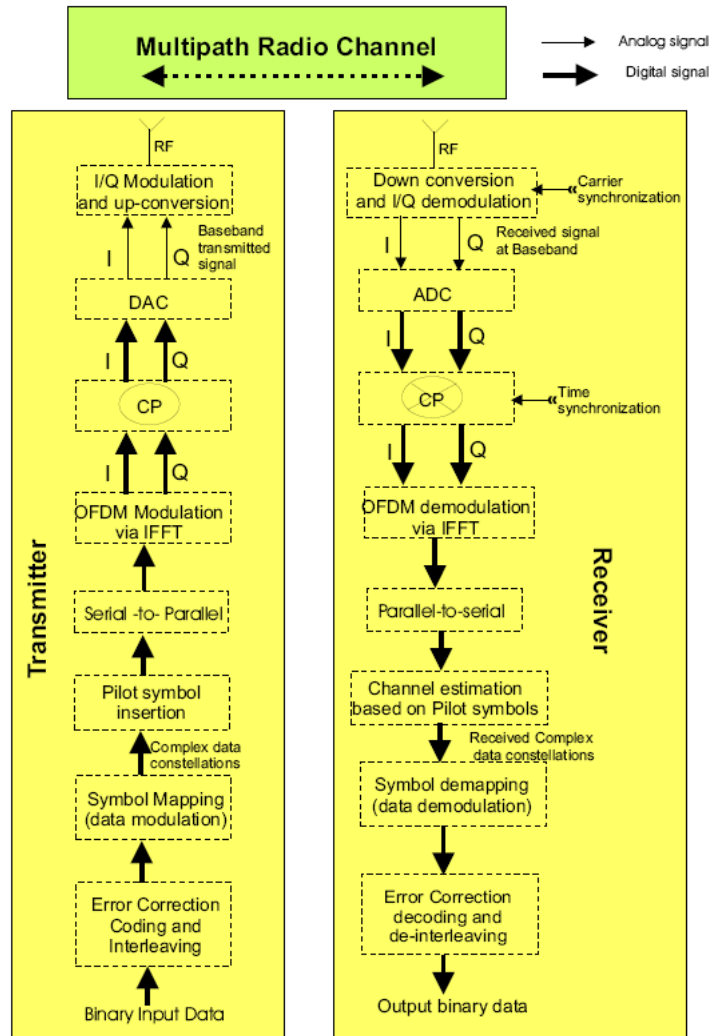


Figure 1.8: OFDM transceiver model [20][21]

### 1.4 2k, 4k and 8k OFDM modes

One of the extension of the physical layer is a new 4K OFDM mode. This mode is complementing the 2K and 8K existing mode and is a trade off mobility and single frequency network cell size. Its purpose is to provide an additional degree of flexibility for network planning. To understand the advantages of each modes, some performance measurements had been done with the different modes.

The most usable modulation method for mobile and portable reception is the 16QAM with code rate of 2/3. This code requires moderate C/N and provides sufficient transmission capacity for DVB-H

applications. In this modelisation, we will estimate the mobile performances in a urban environment with a transmitter working at  $f=500$  Hz. Thanks to these information, we can estimate the maximum speed of our mobile receptor, according to the modes (2k, 4k or 8k). All measurements had been done in [16] and are sum up in Figure 1.9.

4K mode expected mobile performances in TU6 channel profile															
GI = 1/4				2K				4K				8K			
Code Rate	Bitrate	C/N		C/N min	Fd max	At C/N min + 3dB		C/N min	Fd max	At C/N min + 3dB		C/N min	Fd max	At C/N min + 3dB	
		Rayleigh				Fd	500 MHz			Fd	500 MHz			Fd	500 MHz
QPSK	1/2	4,98 Mbps	5,4 dB	13,0 dB	201 Hz	169 Hz	365 km/h	13,0 dB	133 Hz	112 Hz	242 km/h	13,0 dB	65 Hz	55 Hz	119 km/h
QPSK	2/3	6,64 Mbps	8,4 dB	16,0 dB	167 Hz	135 Hz	291 km/h	16,0 dB	111 Hz	90 Hz	194 km/h	16,0 dB	55 Hz	45 Hz	97 km/h
16-QAM	1/2	9,95 Mbps	11,2 dB	18,5 dB	142 Hz	114 Hz	246 km/h	18,5 dB	96 Hz	77 Hz	166 km/h	18,5 dB	50 Hz	40 Hz	86 km/h
16-QAM	2/3	13,27 Mbps	14,2 dB	21,5 dB	113 Hz	96 Hz	207 km/h	21,5 dB	74 Hz	63 Hz	136 km/h	21,5 dB	35 Hz	30 Hz	65 km/h
64-QAM	1/2	14,93 Mbps	16,0 dB	23,5 dB	90 Hz	75 Hz	162 km/h	23,5 dB	60 Hz	50 Hz	108 km/h	23,5 dB	30 Hz	25 Hz	54 km/h
64-QAM	2/3	19,91 Mbps	19,3 dB	27,0 dB	62 Hz	39 Hz	84 km/h	27,0 dB	38 Hz	27 Hz	58 km/h	27,0 dB	20 Hz	15 Hz	32 km/h

Figure 1.9: Comparison of the OFDM modes [3]

These results clearly show that the 2K mode is 4 times more Doppler resilient than the 8K mode, meaning that this mode is well suitable for mobility conditions (better receiving capability at high speed). In fact, with a standard modulation method, the maximum speed at 2K is more than 200 km/h whereas it is getting down at 65 km/h with a 8K mode. However, the 2K cell size is really small compared to the 8K mode.

## 1.5 Operation Bandwidth

In DVB-H network it is possible to operate with bandwidths of 6 MHz, 7 MHz, 8 MHz and also 5 MHz. Operating with the last one, a reduction of the operation bandwidth can be achieved. This reduction may affect at the system in different ways like [1, section 9.5]:

- Increase the symbol period, therefore it should be possible to reduce the system payload.
- Tolerance to phase noise. The frequencies bellow at carrier spacing can be mitigated with phase error correction in the receiver. However, when the frequencies of the phase noise exceed the carrier spacing, the inter-carrier interference cannot be eliminated. Using the band of 5 MHz, it place a tighter tolerance on phase noise that it can reduce this effect.
- Doppler shift. The effect of using 5 MHz in the system is that it will provide the mobile receivers with a better reception signal. The Doppler Effect can be mitigated through different ways such as increasing the amount of applied MPE-FEC. Using this method, the payload of the system will be reduced. In order to mitigate this reduction it could be possible to use different convolution code rate in the system. Depending of the network characteristic a compromise between each parameters can be found.

## Chapter 2

# Infrastructure layout: Network topology

One of the most important things in DVB coverage is that it has a very rapid transition from near perfect reception to no reception at all. This is a very limiting factor and it is the perfect element to consider in order to define the cell's size. Additionally to this, when considering the particular case of DVB-H one can realize that it is even more demanding as the DVB-H receiver is expected to be in really bad radio propagation conditions such as moving at high speeds, indoor reception, etc. Therefore DVB-H is very demanding in terms of network planning and usually, to provide service to the sensitive zones (places where the power received from the base station is minimal) it is necessary to increase the transmitter power or to provide the network with more transmitter sites, etc.

As DVB-H has to be fully compatible with DVB-T and to be able to operate over DVB-T networks, both of their network topologies should be the same. However, even considering this fact, there are some exceptions as a whole new DVB-H network could be deployed if wanted. On the other hand, when working over a DVB-T network it is possible to use some signal repeaters or other mechanisms in order to give coverage to the whole population.

In the following sections of this chapter, the different utilization conditions for the user (reception scenarios such as indoor, outdoor, etc.) will be explained and developed. Also the coverage area and the needed field strength will be discussed.

### 2.1 Reception Scenarios

Considering the reception scenarios for DVB-H, it has to be considered the places where a subject will be more susceptible to watch TV. The typical scenarios can be classified as:

- Indoor
- Outdoor
- In-car/In-bus/In-train

These scenarios are independent from other conditions but one can consider the fact that outdoors or in-car/in-train, the user can be traveling at high speeds (more than 3 km/h according to the DVB-H specification [1] and [2]) and then there will be losses due to the Doppler effect as shown in chapter 1.

Another possible classification according to the DVB-H implementation guidelines [1] is depending on the speed of the receptor device. The classification is:

- Portable reception: is defined as the reception at no speed or very low speed (lower than 3 km/h).
- Mobile reception: is defined as the reception at medium to high speed (higher than the 3 km/h).

It should be noted that the  $C/N$  performance in mobile channels is nearly constant until the maximum possible speed (corresponding to a 3dB power loss in the  $S_{11}$  parameter due to the Doppler effect) is reached, but it should be taken into account that MPE-FEC has an important impact on the minimum  $C/N$  value and the maximum Doppler shift. However, the Doppler effect is not the main issue for DVB-H. In fact the frequency shift (modification of the operational frequency because of the Doppler effect) is negligible. For example, at 702 MHz and 300 Km/h the Doppler shift is only 195 Hz. In fact, it is to be expected that there will be more significant power variation on reception caused by the environment of the mobile terminal (outdoors or in-vehicles, etc). For more information about this, it is recommended to read Section 2.3.

## 2.2 Network topology

There are three kinds of network configurations that can be used to deploy a DVB-H network, depending on the coexistence between DVB-H and DVB-T. Using one configuration or another will determine the network topology that will have to be used.

### 2.2.1 DVB-H Shared Network

As it has been shown in Chapter 1, DVB-H can share the DVB-T infrastructure by using the same DVB-T multiplex, see Figure 2.1.

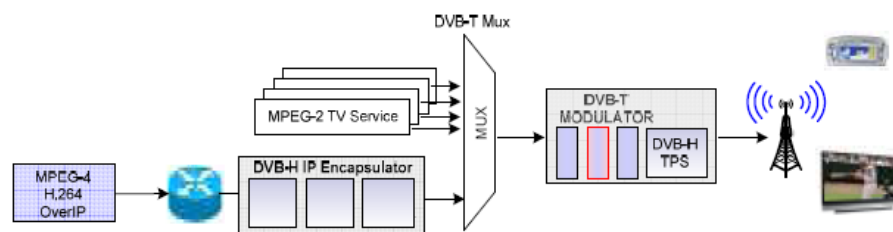


Figure 2.1: DVB-H on a Shared Multiplex

Although this network scenario reuses the existing DVB-T infrastructure, the network does not support the 4k mode and this drawback will involve a lower service availability and quality of service in scenarios such as indoor reception. Additionally, as mentioned earlier the DVB-T transmission is

meant for stationary TV sets with a large antenna on the rooftops which can be directed toward the transmitter. By contrast, the DVB-H signal needs to reach the mobile handsets with small built in antenna in a (unstable) mobile environment. Due to these factors, the required transmitted power in DVB-H should be much higher than in DVB-T [24] (same antenna height is considered). Nevertheless, in a shared scenario, as the transmitting system is the same for both DVB-T and DVB-H, the power transmitting the DVB-H signal will be the same as the DVB-T signal.

Re-using DVB-T infrastructure reduces the overall cost of DVB-H network implementation [25].

### 2.2.2 DVB-H Hierarchical Network

DVB-H can also be shared with DVB-T in a hierarchical way (see Figure 2.2). Unlike the DVB-H shared network where the DVB-T and DVB-H streams are combined in a single transport stream, in a hierarchical network the DVB-H and DVB-T streams are transported separately. This is achieved using a hierarchical modulation which consists of two streams, where the DVB-T stream is modulated as high priority, and the DVB-H stream is modulated as low priority [24].

The high priority stream codifies the quadrant in which the group of symbols will be carried whereas the low priority stream codifies the bits inside the quadrant. This can be seen in Figure 2.3 where the blue dots represent the low priority bits and the yellow zones represent the high priority bits. Also, Figure 2.3 shows an example using a 64-QAM modulation which is formally in fact the modulation which is used but, in the hierarchical interpretation, it is viewed as the combination of 16-QAM and 4-PSK modulation. This is referred to as “4-PSK in 64-QAM”. The bit-rates of the two partial streams together are the same as the bit-rate of a 64-QAM stream [39].

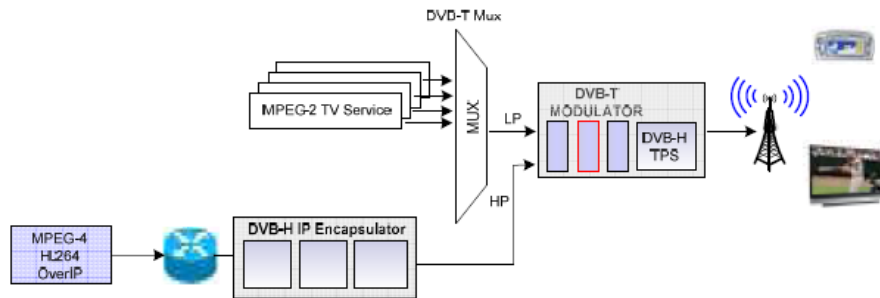


Figure 2.2: DVB-H using Hierarchy

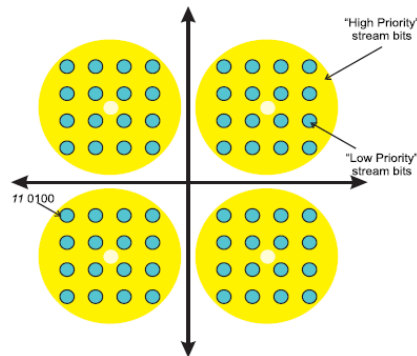


Figure 2.3: Hierarchical modulation example [40]

The advantage of this network scenario over the multiplexing scenario is that different modulation parameters can be set for fixed DVB-T as well as for DVB-H reception. This option will lead to a better bandwidth usage. The disadvantage of this network scenario however, is that the amount of bandwidth that is reserved for DVB-H services should be fixed, which decreases network flexibility. Also and similar to DVB-H shared network the optional 4K mode cannot be used in this network configuration. Moreover, introducing DVB-H service hierarchically into existing DVB-T network will reduce the required network resources and hence a lower implementation cost of the DVB-H network.

### 2.2.3 DVB-H Dedicated Network

DVB-H can also be built from scratch using dedicated network (see Figure 2.4). In this network configuration, the carrier is used exclusively for DVB-H transmission and so the network will have maximum flexibility. It is designed and deployed to support as many users as wanted and to have all the desired coverage area without any constraints imposed by DVB-T. This network configuration can take also advantage of using the 4k mode [24].

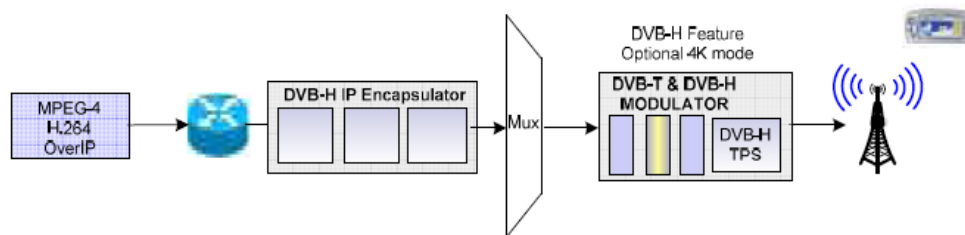


Figure 2.4: Dedicated DVB-H Network

Some researches have been done to compare the network shared and the network dedicated performances. According to Aurelian Bria and David Gómez-Barquero [27], with the same transmission power, the coverage area is larger in the dedicated DVB-H network than in a shared network (see Figures 2.5 and 2.6).

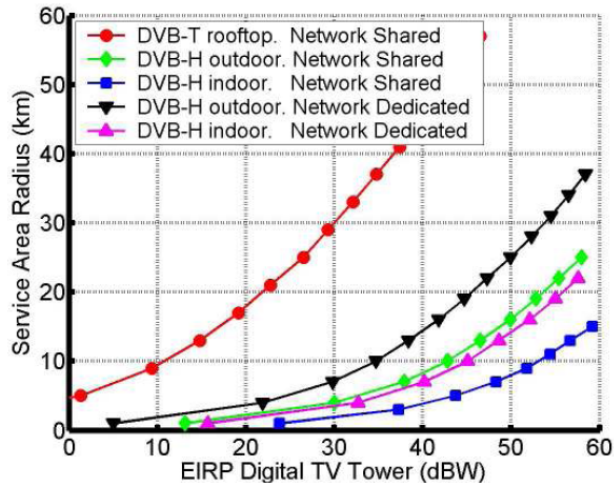


Figure 2.5: Service Area vs Transmitted Power

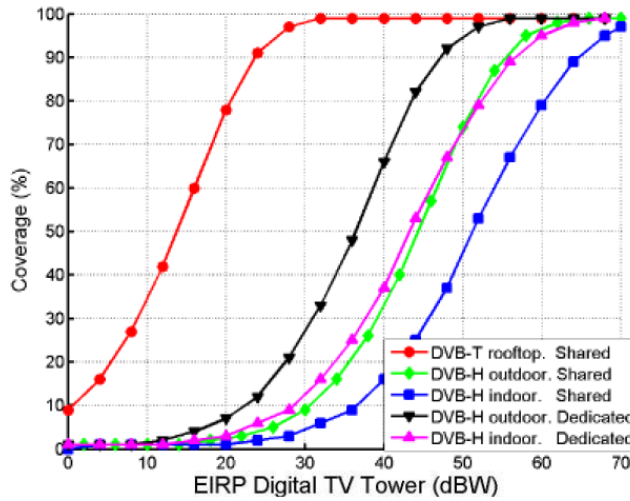


Figure 2.6: Area Coverage vs Transmitted Power for a 150 m high antenna and a 25 km service area

The main drawback, except the fact that in this network deployment there will be no DVB-T signal transmitted, is that on a financial aspect, this network scenario is more expensive in terms of initial capital investment than the previously discussed network architectures (assuming you already had a DVB-T network deployed). This is because it needs new core network equipment as well as a separate frequency channel [25].

### 2.2.4 Topology

If the network configuration used is a shared or a hierarchical configuration then the typical topology of the network will be a group of single-frequency macrocells using each one a different carrier frequency. Additional gap fillers could be added to strengthen the signal power to the most shielded zones, specially in large cities. This configuration already exists in an Italian DVB-H network, which is shown in Figure 2.7.

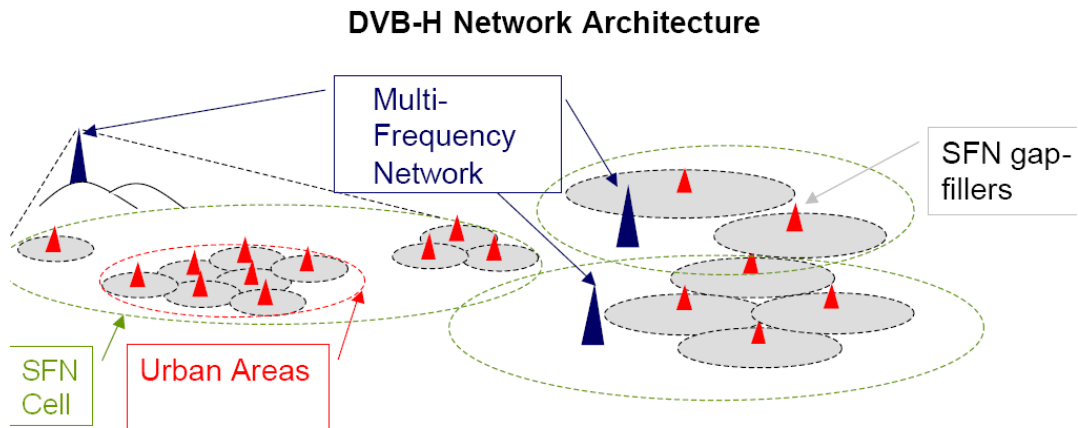


Figure 2.7: Topology of the Italian DVB-H network. Obtained from [4]

If the network configuration used is a dedicated one, the rural and some suburban areas could be deployed using macrocells and the cities could be covered using microcells, typical more of a GSM or UMTS network than a TV network.

## 2.3 Coverage area

To make an overview of the coverage area of the DVB-H system, a comparison between different models will be done. Firstly, a macrocell model is used (Okumura-Hata [14] [15], 2-ray model [13]) and then microcell models are evaluated (Egli [13] [15]). The results are compared to the Free Space model and relative to each other.

The first thing to be pointed out is that the Okumura-Hata model is used to design macrocells whose radius is between 1 km and 20 km [31]. It was developed through works of Y. Okumura [30] and M. Hata [31] and is based on the results of extensive measurements in certain urban and suburban areas of Japan. Its use is only valid in urban and suburban zones of (big) cities as it was developed in central Tokyo [32]. It is also important to notice that although it is a realistic model to design macrocells which include a big city, a lot of points without coverage will appear in the ground level of the city and thus it will not be a perfectly valid model for DVB-H inside cities.



This problem can be solved using microcells inside a city which have a size of less than 1 km and whose propagation model (i.e. Egli model) is based on the line of sight (LOS). Another model used for macrocells is the 2-ray model. This model has a breakpoint, which is the distance point (from the transmitter) in which the propagation loss stops behaving as an inverse of the quadratic distance to start behaving as an inverse of the distance powered to 4. This breakpoint means that at a known distance the loss due to the propagation will increase rapidly.

The procedure followed to evaluate the different models can be seen in Appendix C. The different values used to evaluate the models are as follows:

Minimum receiver power: -93.2 dBm [3] [1, section 10.3.3, worst case scenario]  
 Maximum transmitter power: 5 kW [17] [18] (almost best case scenario)  
 Transmitter antenna gain: 12.5 dB (2 bay antenna) [19, 2nd worst case scenario]  
 Receiver antenna gain: -10 dB [1] (at frequency 702MHz, worst case scenario for the antenna gain)  
 Transmitter antenna height: 100 m (normally placed outside the city)  
 Receiver antenna height: 1.5 m [1]  
 In-building penetration loss: 15 dB [1, section 11.2.2.2 (a), worst case scenario]  
 In-car penetration loss: 7 dB [1, section 11.2.2.3 (c)]  
 Frequency: 702 MHz.

It is interesting to point out that the received power is proportionally inverse to the frequency (as far as the antenna gain is considered constant), and so the higher the frequency, the lower the propagation loss. This also implies that the propagation loss will be higher, and so this is the worst case scenario.

As seen in [1], the losses due to being inside a car are of about additional 7 dB and the additional ones due to being inside a building are between 7 dB and 15 dB and thus the cell size is going to be smaller when this loss is considered. When designing the network (placement of the antennas and maximum coverage area expected) the fact of considering the losses due to being inside a building or vehicle in the design is up to the network designer. In this project, one of the worst scenario is thought to be more accurate and realistic and so in the evaluation of the different models, these losses are included.

The different cell sizes (radius) for each different model are shown in table 2.1, which also shows the different effects of being inside a car or in a building to the cell size for different propagation scenarios and models. This table has been calculated using the equations of each propagation model shown in Appendix C using a numeric solving software such as Derive [23]. In the case of the In-Car Scenario, an extra 7 dB have been subtracted from the power received and in the case of an Indoor Scenario an extra 15 dB have been subtracted. It can also be seen that the breakpoint for the 2-ray model does not change. If, for example, 7 dB are subtracted from the 2-ray model, they will also be subtracted from the free space model, and so the intersection point will be the at the same distance but with 7 dB less of power. Some representations of this fact have been included in Appendix C.

Figure 2.8 shows the color code that is used in Figures 2.9, 2.10, 2.11 and 2.12 which show the decrease of received power as a function of the distance between the transmitter and the receiver on the different Hata models for macrocells and considering also the cases of being inside a car or inside a building.

Model	Outdoor Distance	In-car Distance	Indoor Distance
Free Space	207.3 km	92.6 km	36.8 km
Okumura Hata Urban	4.1 km	2.4 km	1.4 km
Okumura Hata Suburban	7.96 km	4.8 km	2.7 km
Okumura Hata Rural	24.2 km	14.5 km	8.1 km
2-ray/Egli Breakpoint	4410 m		
2-ray	30.3 km	20.2 km	12.8 km
Egli	7.3 km	4.8 km	3.1 km

Table 2.1: In-car and Indoor effects on the coverage area

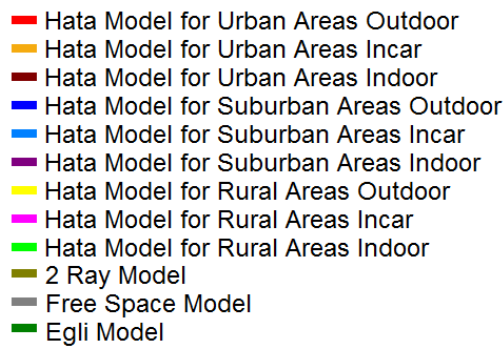


Figure 2.8: Color code for the Hata model representations

Figure [2.13] shows the 2-ray model propagation for an outdoor receiver, and Figure 2.14 shows the 2ray model at outdoor reception compared to the Okumura-Hata model for outdoor rural reception and the Egli model.

From all this propagation models it can be extracted that both the 2-ray model and the Okumura-Hata for rural areas could be used to model the cells in a countryside (assuming always LOS). For cities, it can be seen in Figure 2.15, which shows a comparison between the Egli model and the Okumura-Hata model for Urban areas, that the Okumura model proposes a worst case scenario than the Egli model. Therefore, for large cities the Okumura-Hata model is a better choice but for not really big cities it can be a better option to use the Egli model.

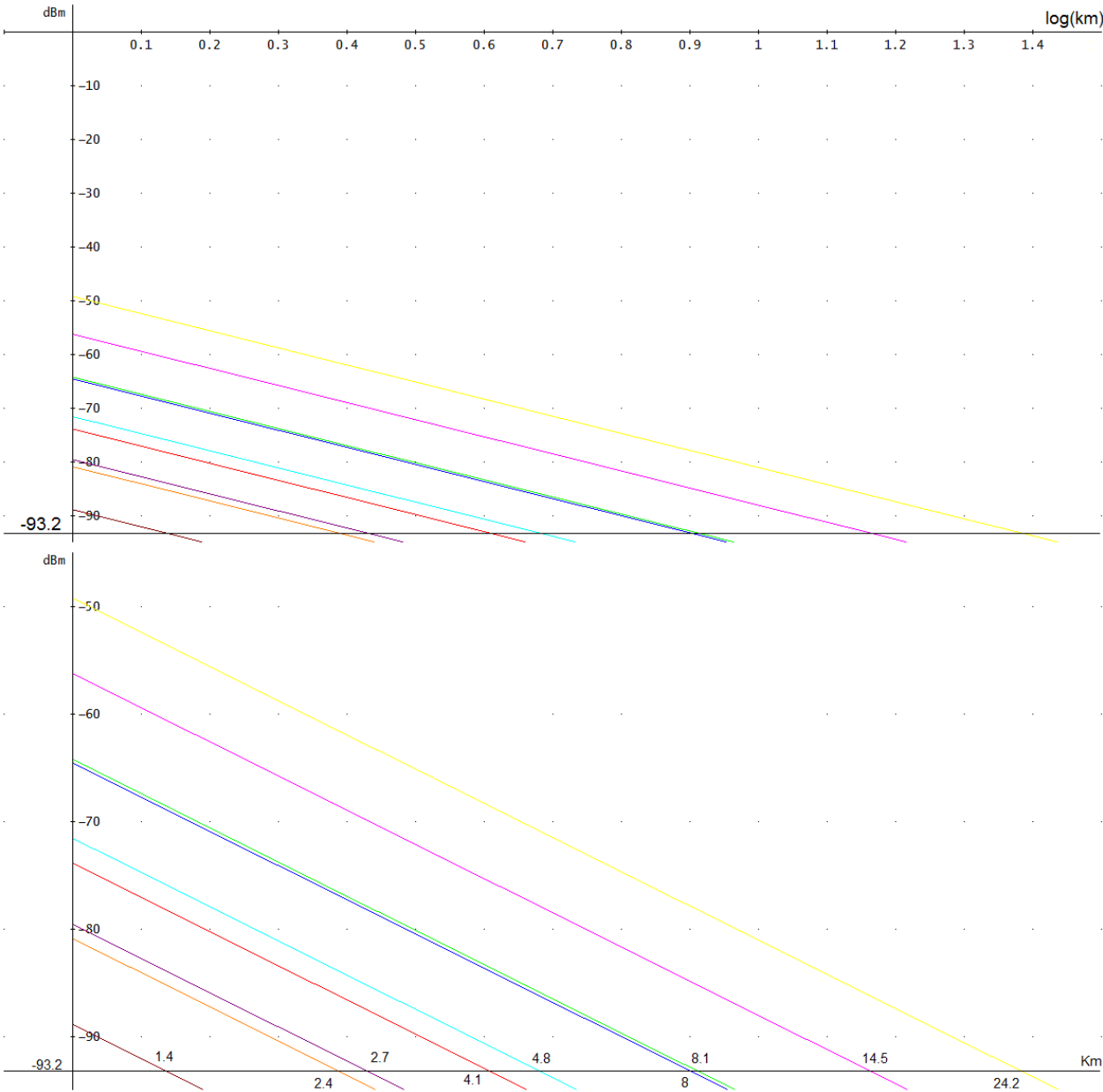


Figure 2.9: In-car and indoor effects on Hata propagation model

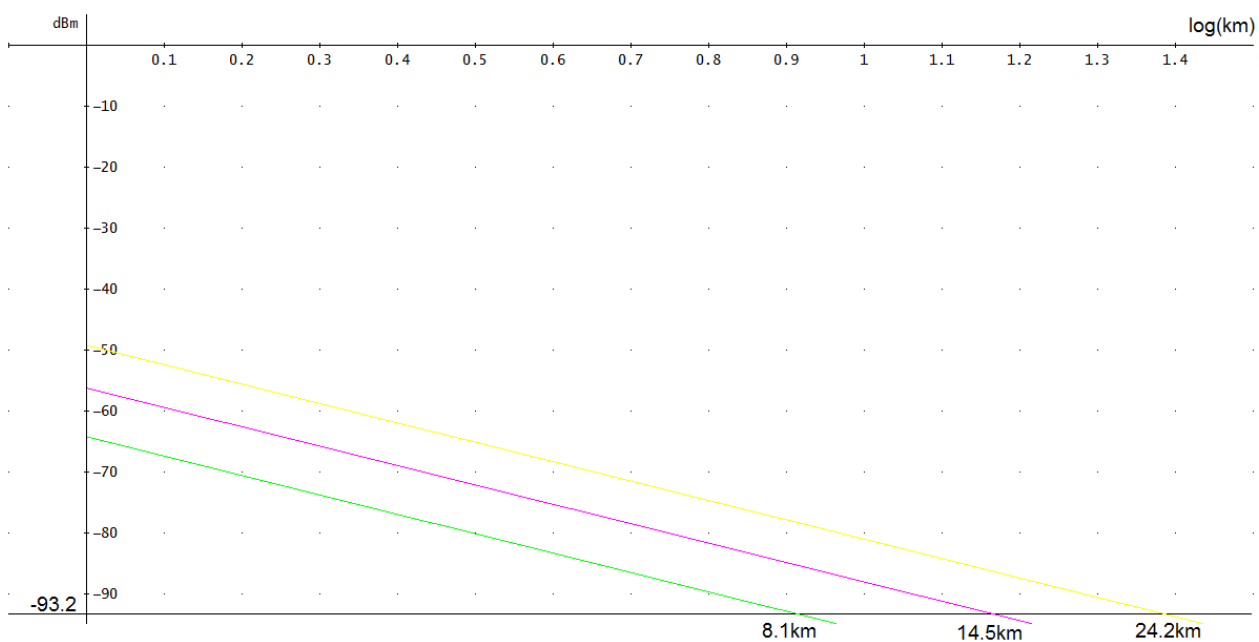


Figure 2.10: In-car and indoor effects on Hata propagation model for rural areas

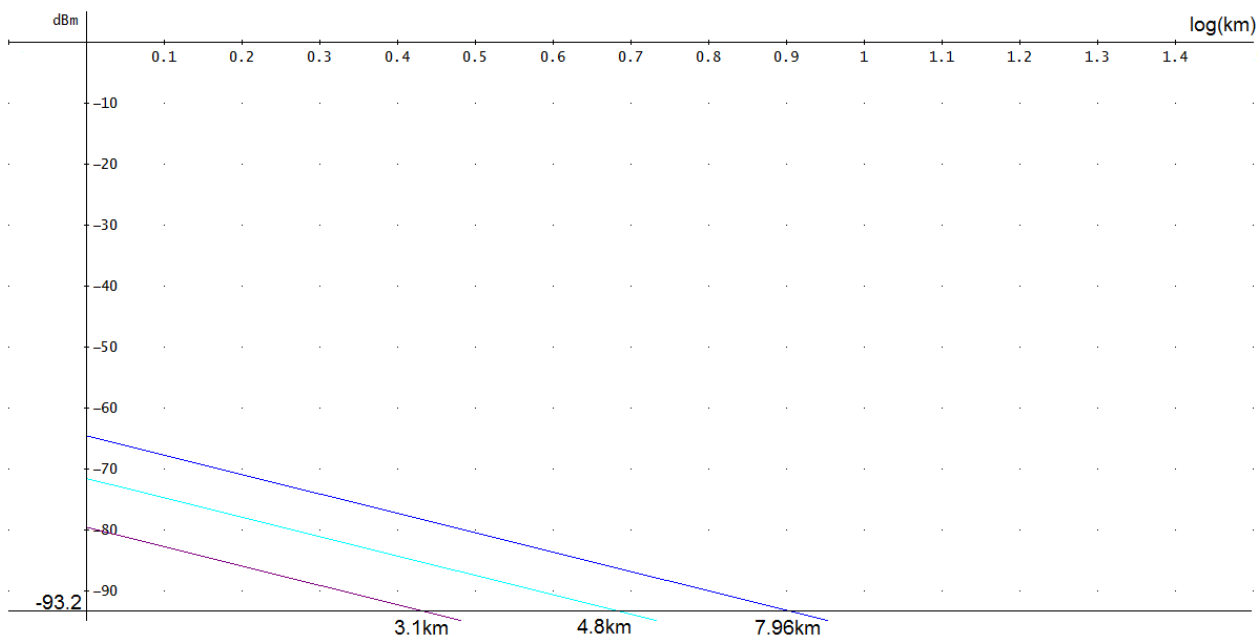


Figure 2.11: In-car and indoor effects on Hata propagation model for suburban areas

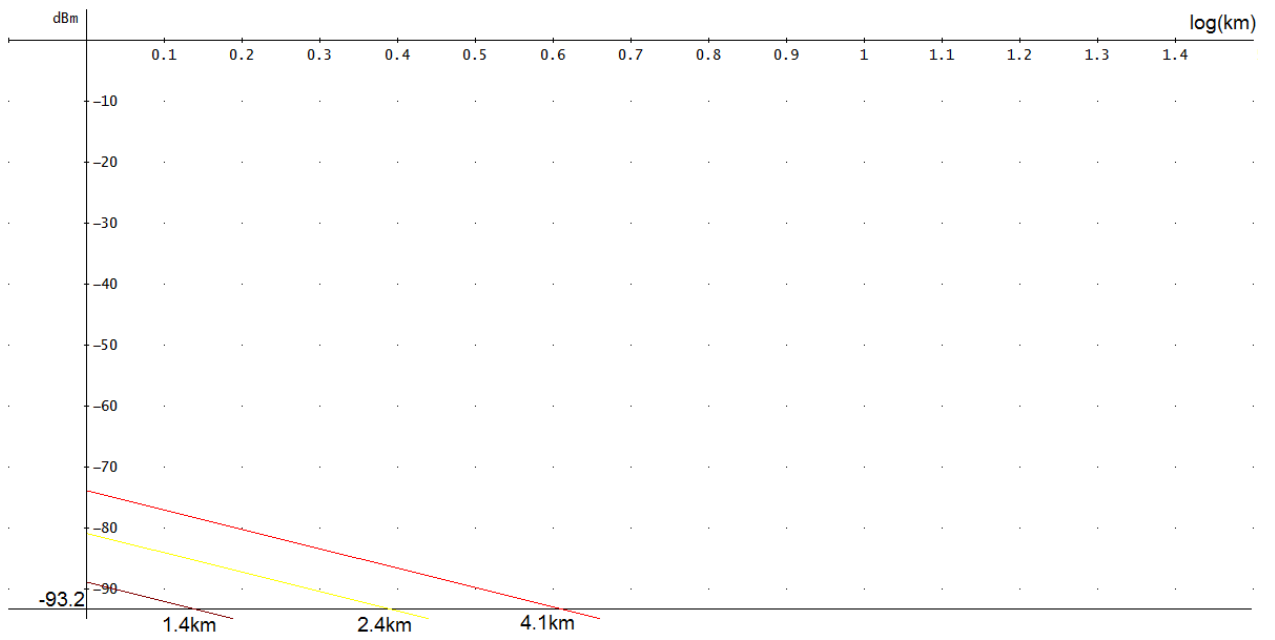


Figure 2.12: In-car and indoor effects on Hata propagation model for urban areas

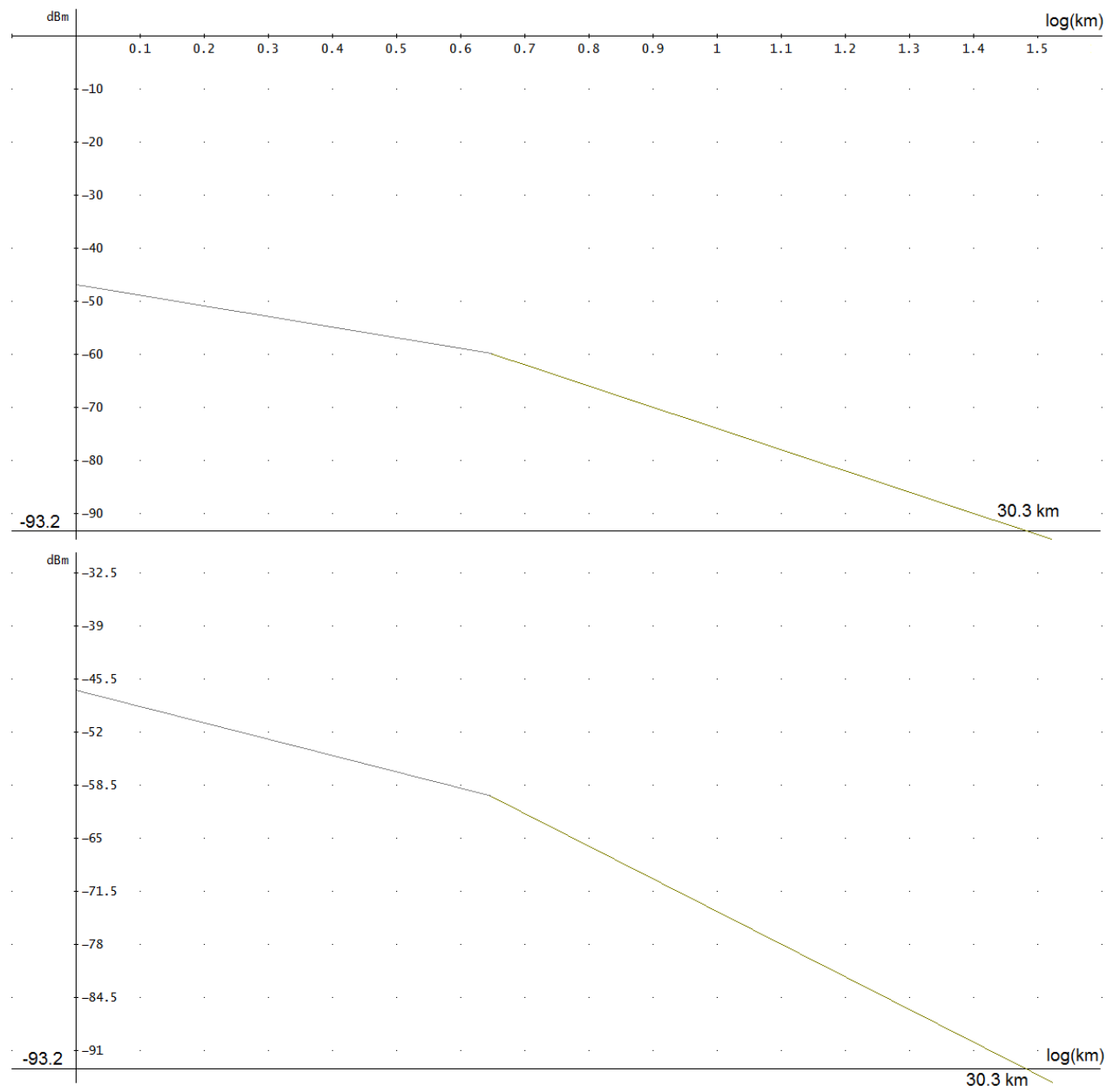


Figure 2.13: 2-Ray model (high) and 2-Ray model with zoom (down)

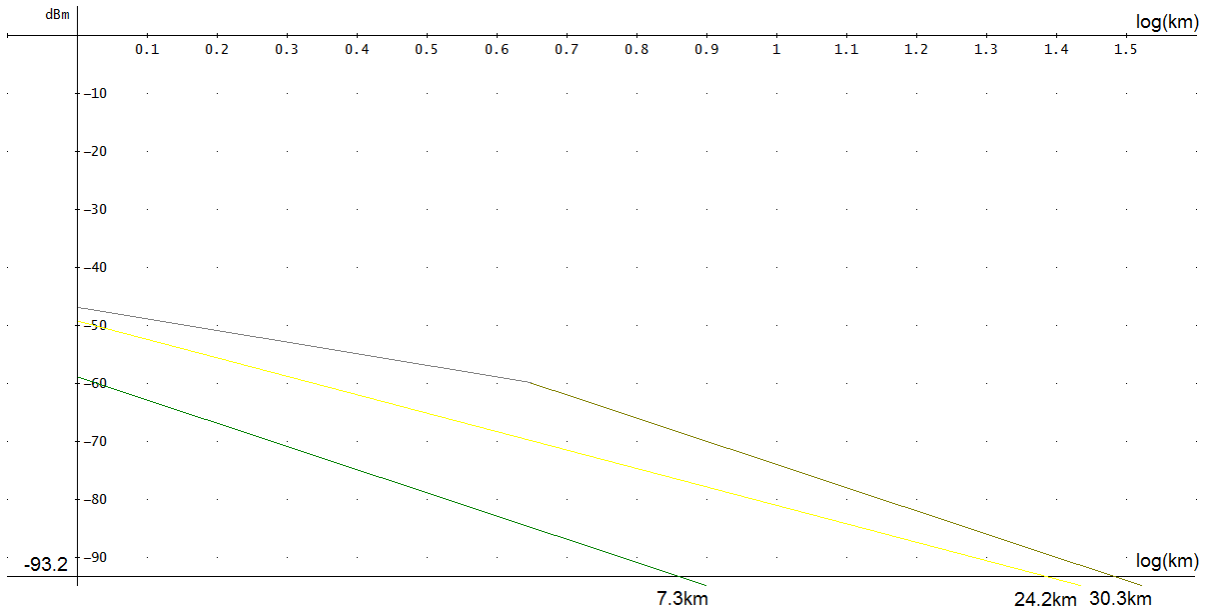


Figure 2.14: Comparison between the Okumura Model (outdoor, rural) and the 2-ray model (outdoor) and the Egli model (outdoor)

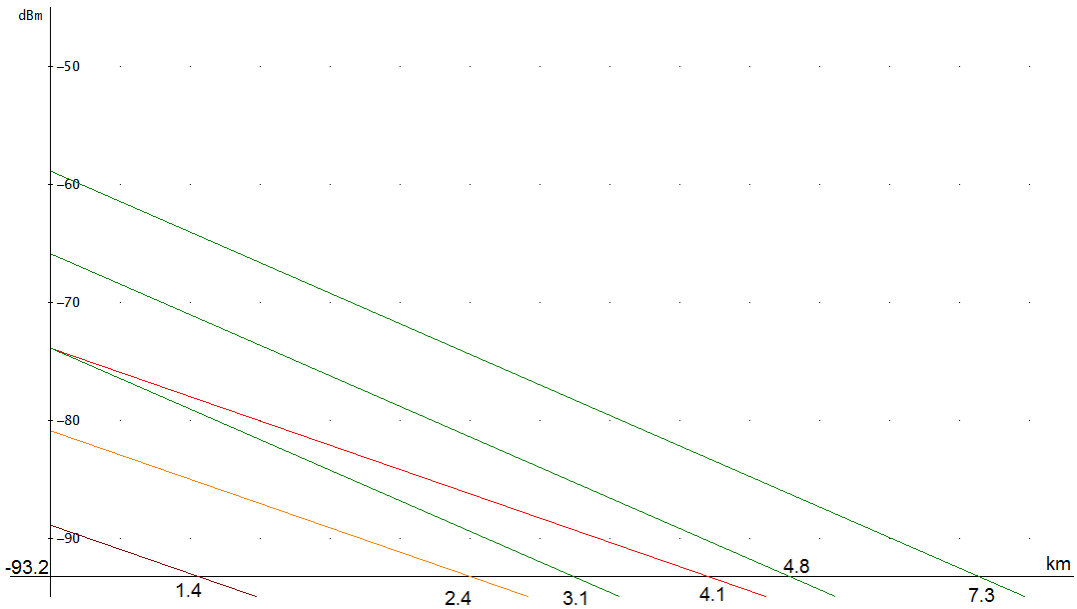


Figure 2.15: Egli Model (green: outdoor at top, indoor bottom, incar in the middle) versus Okumura-Hata Model for Urban areas

## Chapter 3

# Antenna Design

In this chapter the questions about antenna design will be shown. Firstly, it will be introduced a short summary about electromagnetism fundamentals. From this point the different types of antenna will be shortly explained. Then, all the antenna requirements for DVB-H will be summarized and also the previous work done about DVB-H antennas that has been found will be explained. Finally the FDTD software used will be presented and the different designed antennas in this thesis will be exposed, evaluated and compared.

### 3.1 Electromagnetism fundamentals for antennas

In order to understand the experiments and results of small antennas in the following parts, it is necessary to remind the main parameters of an antenna.

An antenna is usually defined as a metallic device for radiating or receiving radio waves. It can also be said that an antenna is the transition device between free-space and transmission line (figure 3.1). This line is connected to a source and carries energy from it (guided antenna) or to the receiver (receiving antenna).



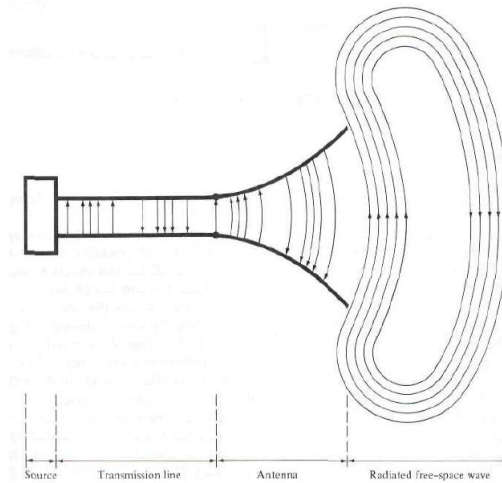
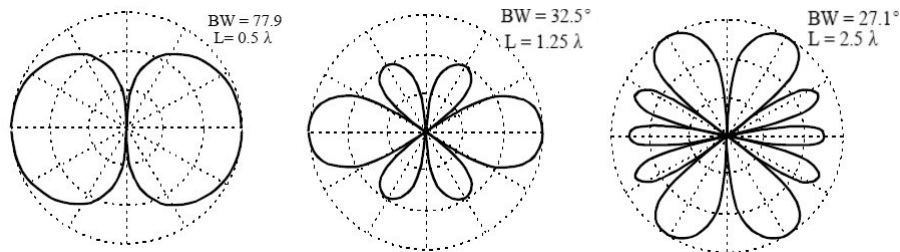


Figure 3.1: Antenna as a transition device [10]

The first important parameter is the radiation pattern, which is a mathematical function or a graphical representation of the radiation properties of the antenna as a function of space coordinates. In most cases, this pattern is represented as a function of the directional coordinates. Figure 3.2 shows that the radiation patterns are modified according to the antenna size.

Figure 3.2: Radiation pattern according to the wavelength  $\lambda$  [33]

In this thesis, the dimensions of the antenna are changing between  $\frac{\lambda}{4}$  and  $\lambda$  and so the pattern will have few big lobes (left graph of Figure 3.2) instead of having a big group of narrow lobes (right graph of Figure 3.2). It can also be seen that when the antenna becomes small (compare to the wavelength  $\lambda$ ), lobes are wider and spread in many directions.

The antenna parameters are different according to the observation point. Antennas do not have the same properties as if you are close to it or far away. The space surrounding an antenna is usually divided into three regions:

1. the reactive near-field region is the area surrounding the antenna and where the reactive field predominates.

2. the radiating region is the area between the reactive near-field and the far field wherein the radiation fields predominate and wherein the angular field distribution is dependent upon the distance from the antenna.
3. the far-field region is the area where the angular field distribution is independent of the distance from the antenna. All the simulations done in this thesis are in this area, which is further away than one wavelength ( $\lambda = 50$  cm with a frequency equal to 600 MHz).

Impedance is an important parameter who characterizes the antenna. It is defined as the ratio of the electric to magnetic fields. There are two types of impedances: self and mutual ones. If the antenna is radiating in a unbounded medium (no other objects around it), it was only considered the self impedance, which is also the input impedance in this case. However, if the antenna is surrounded by other objects, the input impedance is modified and becomes a function of self and mutual impedances.

Impedance is a sum of resistance (real part) and reactance (imaginary part). It is defined by:

$$Z_A = R_R + R_L + jX_A$$

where:

- $Z_A$  is the impedance of the antenna
- $R_R$  is the radiation resistance
- $R_L$  is the loss (dissipated) resistance
- $X_A$  is the reactance (reactive power)

Impedance depends on the frequency of operation, antenna geometry, method of excitation and the proximity of surrounding objects. This parameter can be represented with a Smith Chart (see Appendix D).

Each antenna operates at a given frequency and more accurately at a given range of frequencies. The bandwidth of an antenna is the range of frequencies within the antenna is working. This range is surrounding the central frequency on both sides, where the antenna characteristics (impedance, gain, radiation...) occur.

The perfect and lossless antenna does not exist. The losses of a given antenna can be calculated with the quality factor  $Q_t$ , which is representative of the amount of antenna losses (radiation  $Q_{rad}$ , conduction  $Q_c$ , dielectric  $Q_d$  and surface waves  $Q_{sw}$  losses). This parameter is defined by:

$$\frac{1}{Q_t} = \frac{1}{Q_{rad}} + \frac{1}{Q_c} + \frac{1}{Q_d} + \frac{1}{Q_{sw}}$$

## 3.2 Types of antennas

This chapter shown the different kind of antennas to receive TV within portable terminals such as small television or mobile phones. Not all types of antennas have been simulated since the thesis's main goal was to design a small antenna which could fit inside a handheld device and some of this kinds of antennas are too big.

### 3.2.1 Dipole

This is the most basic kind of antenna. This antenna resonant at the frequency where the conductor length is a half wavelength [10]. The length to work with a DVB-H range is 427mm (at 702MHz) and 638mm (at 470MHz). Thus, the length of  $\lambda/4$  will be between 213.7mm and 319mm depending on the chosen frequency to design the antenna.

Quarter-wave monopole is formed replacing one half of a dipole antenna with a ground plane. The ground plane is very important because if it is large enough will work like dipole [11].

### 3.2.2 Loop

Loop antennas are one of the antennas that can take many different forms as rectangle, square, triangle, ellipse, circle and many other configurations. It is possible to classify two different categories: electrical small and electrical large. The electrical small antennas are those whose overall length (number of turns times circumference) is around  $\lambda/10$  (sometimes less than  $\lambda/10$ ). The electrically large loops are those whose circumference is about a free-space wavelength. The most typical applications in the antennas loops are, HF (3 - 30 MHz), VHF (30 - 300 MHz) and UHF (300 - 3000 MHz) bands. This kind of antenna are normally used such as receiving because are very poor radiators due to loop antennas with electrically small circumferences have small radiation resistances that are usually smaller than their loss resistance [10].

### 3.2.3 Microstrip

Microstrip antennas can be used in different applications such as satellite, mobile radio or wireless communications. These antennas are low-profile and mechanically robust because there is not external elements. The radiating patch may be square, rectangular, circular, elliptical or any other configuration. Major operational disadvantages of microstrip antennas are their low efficiency, low power and high Q [10].

There are numerous substrates that can be used for the design in microstrip antennas. The value of these dielectric constant can vary between  $2.2 \leq \epsilon_r \leq 12$ . The better value of for antennas performance are thick substrate whose dielectric constant is in the lower end of the range because they provide better efficiency or larger bandwidth [10].

#### 3.2.3.1 Planar Antennas

The planar antennas are the solution for wireless communications nowadays. These kinds of antennas are easily to integrate in the mobile phone and give the possibility to reduce the size of the phone, reduce cost and do it more attractive. Also, it is possible to implement in the same antenna different system for mobile communications like GSM (890 - 960 MHz), DCS (1710 - 1880 MHz), PCS (1850 - 1990 MHz) or UMTS (1920 - 2170 MHz) [12].

#### PIFA

A planar inverted-F antenna (PIFA) is in general achieved by short-circuiting its radiating patch or wire to the antenna's ground plane with a shorting pin and can resonate at a much smaller antenna size for a fixed operating frequency.

PIFA have the advantage that it has a very small backwards radiation through the mobile phone thus, the electromagnetic energy absorption by the user is reduced [12].

### MONOPOLE ANTENNAS

Within this kind of antennas we find the very-low-profile monopole for small devices. These antennas are very suitable for integration within the mobile phone housing and operation built-in or concealed antenna [12].

As mentioned in the last point, the monopole antennas also can provide lower specific absorption rate (SAR) thus, the energy absorption by the user is reduced. In [12] it can be seen some example about how to reduce the backward radiation in the design of different antennas.

#### 3.2.4 Switched Antennas

Some types and designs of antenna do not usually have a big bandwidth and this can be a problem if a big frequency range is to be covered by the antenna. Additionally one can consider the fact that using a matching circuit to adapt one frequency point to the feeding line of the antenna (normally  $50\Omega$  of impedance) makes the resonance frequency change to that point (even if it is not the real resonance frequency of the antenna before the matching circuit). If those two ideas are put together it is factible to think that if you make different matching circuits and switch from one to another all the frequencies of the band can be covered (if the radiator/receiver part of the antenna can cover it too, of course). Appendix F shows more information about impedance matching.

One particular case is the Switched Monopole Planar Antennas, because they tend to have a really narrow bandwidth and by means of switching the matching circuits the whole frequency band is usually matched. The trade-off of this kind of antennas is that for small devices it is difficult to include a lot of matching circuits because of the space that the capacitors and inductors need.

### 3.3 Required Antenna Performance

The design of the antenna that it is going to be shown has the requisite of being able to be integrated in the new mobile phones in order to receive DVB-H. Before deciding the approximated size of the antenna and/or gain that the phone needs to receive DVB-H, we made a study about these different parameters as it is shown in Appendix A and Appendix B.

The size of the mobile phone is one of the most important things during the development of the antenna as the size of the phone limits the antenna. As it is shown in Figure [B.1] the standard size of the different mobile phone is around 100mm x 40mm x 10mm. However, the design of the phone will be always as small as possible in order to reduce also the cost of the antenna.

The antenna is just designed to receive DVB-H. The working range is from 470MHz to 702MHz and the power gain is -10dB and -7dB [1] respectively as shown in figure 3.3. The antenna has to be as similar as possible to an omnidirectional antenna in order to be able to receive the signal of the transmitter.

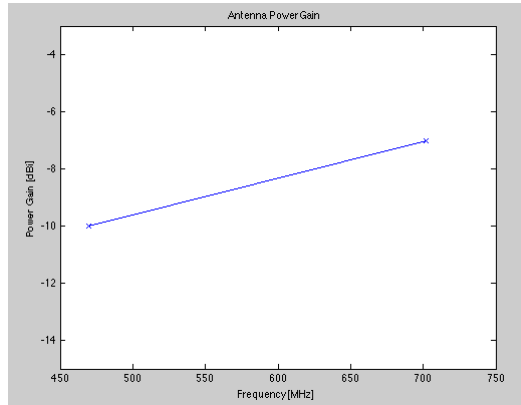


Figure 3.3: Required antenna power gain

Another important parameter to be checked in the simulations is the impedance of the antenna (see appendix D about smith chart) in order to be sure that the antenna can be matched to  $50 \Omega$  of the receiver. In fact, to be able to adapt the antenna, the impedance representation in the smith chart should not be close to the most external circle (representing infinite imaginary part), because the most extreme values in the smith chart are not matchable as there are no commercial values either of capacitors and inductors. More detailed information about this can be found in Appendix F.

Looking more into the  $S_{11}$  parameter, it informs us about the transferred power from the input to the output and in its representation it can also be seen the resonant frequency and the bandwidth of the antenna. Finally it is important to be sure that the resonance frequency is the correct one and that the bandwidth is enough to allocate at least one DVB-H channel (8 MHz maximum). The factor that will give us this information in a fast way is the antenna quality factor (see section 3.1).

## 3.4 Previous work done on DVB-H antennas

Some studies, projects and master thesis have been done involving DVB-H antennas. Following the more significant of them are shortly explained.

### 3.4.1 Jari Holopainen

Jari Holopainen developed three main prototypes [41]. The best one is called by him as DVB3 and we think that the antenna is too big (135 x 75 mm) although the performance is quite good. He also designs a switchable matching L-network (see Appendix F) but in order not to use a lot of matching circuits they assume a compromise and so, reducing the number of matching circuits (by modifying

the values of the components of the L-network), they achieve a bigger bandwidth at the same time that they have more power loss (due to the fact that the matching is not perfect).

### 3.4.2 Fredrik Persson & Mattias Wideheim

On this thesis [42], different types of antennas are discussed and analyzed. First of all, they analyze a folded dipole antenna, then a PIFA antenna, then a folded patch antenna, then they follow with a loop antenna and they finish analyzing a switched monopole antenna. They discard some of the antennas because they are too big or because the performance is not so good. In the end the more interesting antennas they design are the Loop Antenna and the Switched Monopole Antenna.

The problem of the Loop Antenna is that it has a 3 cm diameter and must be placed in an external flap or something similar (not in contact or near the ground plane of the phone) and so it can be easy for it to get broken. On the other hand, the Switched Monopole Antenna is a quite good antenna but its radiation pattern is a bit irregular and a fixed size of 110 mm x 70 mm is quite large.

### 3.4.3 Mauro Pelosi

Mauro Pelosi's thesis [43] focuses in making modifications to the designed antennas using lumped elements in order to modify the resonant frequency. From his numerous different analysis a lot of interesting conclusions can be obtained. In the thesis it is also designed a switched monopole antenna with a quite good performance. In fact, similarly to Jari Holopainen's thesis, in Mauro's thesis an L-matching network is also designed for the antenna and, due to the need of a lot of matching circuits in the switch, it is also studied the possibility of trading-off some power signal to improve the bandwidth and reduce the needed amount of matching circuits.

### 3.4.4 Zena Fourzoli & Radwan Charafeddine

This thesis [44] consists of analyzing some antennas designed before (Mauro Pelosi's antenna, Fredrik Persson and Mattias Wideheim antenna, etc.) and after comparing them they choose Mauro Pelosi's antenna and they enhance it using a new adaptation network based on a Chebyshev bandpass impedance matching network.

### 3.4.5 Yue Gao & Chao Chiap Chiau & Xiaodong Chen

In this short paper [45] they summarize how they designed an antenna whose ground plane is 134 mm x 80 mm and the radiator component of the antenna is 60 mm x 18 mm x 13.5 mm. The radiation pattern simulated in terms of omnidirectionality is very irregular and actually it is not a really good one. The antenna's bandwidth is of 23 MHz considering a -6 dB return loss minimum. Additionally they make a quick evaluation of the hand effect on the antenna.

### 3.4.6 Fractus

Fractus is an antenna designing company that has created an antenna [46] whose size is 40 mm x 5 mm x 4.8 mm and which works fine in an omnidirectional way for both the UHF band (470 to 702 MHz) and L band (GSM band at 1800 MHz). Additionally with only 4 lumped components (3 inductors and 1 capacitor) they are able to adapt the antenna using a double matching L-network to 50  $\Omega$ . Finally to make the measurements they used an evaluation board whose surface is of 104 mm x 42 mm.

### 3.5 FDTD Theory

Finite Difference Time Domain is a very common technique in computing and modelling wide frequency range. Thanks to its simplicity of implementation, it can solve a lot of electromagnetic problems with a single simulation. With the increasing performance of computers, this method are been widely developed in the last decades. This huger amount resources had allowed to obtain more precision coupling with a shorter simulating time. This model is classified as a deterministic scenario, based on Maxwell's equations (time and space dependent domains) as seen on Figure 3.4. In these equations, we can note that there is a relation between the electric field ( $\vec{E}$ ) and the magnetic field ( $\vec{H}$ ). At any point, the update in time of either  $\vec{E}$  or  $\vec{H}$  field occurs the update in space of the other one.

$$\begin{aligned}\frac{\partial \vec{E}}{\partial t} &= -\nabla \times \vec{H} - \vec{J}_m \\ \frac{\partial \vec{H}}{\partial t} &= \nabla \times \vec{E} - \vec{J}_e \\ \nabla \cdot \vec{D} &= 0 \\ \nabla \cdot \vec{B} &= 0\end{aligned}$$

$\vec{E}$  : electric field (volts · meter<sup>-1</sup>)

$\vec{D}$  : electric flux density (coulombs · meter<sup>-2</sup>)

$\vec{H}$  : magnetic field (amperes · meter<sup>-1</sup>)

$\vec{B}$  : magnetic flux density (webers · meter<sup>-2</sup>)

$S$  : arbitrary three – dimensional surface

$d\vec{S}$  : normal vector of surface  $S$  (meter<sup>2</sup>)

$l$  : closed curve bounding the surface  $S$

$d\vec{l}$  : unit path length vector of the curve  $C$  (meter)

$\vec{J}_e$  : electric conduction current density (amperes · meter<sup>-2</sup>)

$\vec{J}_m$  : magnetic conduction current density (volts · meter<sup>-2</sup>)

Figure 3.4: Maxwell's equations

Thanks to this dependency, Yee compiled an algorithm (which is describe on the next page). A computational domain is defined, describing the geometrical objects inside the study domain and also their electrical composition (permittivity, conductance...). Once the source is modeled, information about  $\vec{E}$  and  $\vec{H}$  fields are extrapolated to obtain the required parameters such as input impedance, far-fields, surface currents, etc.

Advantages of the FDTD method

- Large possibilities of modellization (3D, human body influence on waves...).
- Accuracy of the computational domain (objects properties, permittivity and permeability dependent on the frequency...).
- Since  $\vec{E}$  and  $\vec{H}$  fields are calculated everywhere in the computational domain, they are easy to display which is helpful for the analysis of the simulation.

Weaknesses of the FDTD method

- Because of the extreme accuracy of the environment, it is necessary to have a fine grid to “see” all the details of the simulations. This huge amount of data requires large resources (more capacity

with more computers) and also a longer simulation time. Specifically for far-field calculations, the computational domain is larger and so the time duration is significantly increased.

- The E and H fields are calculated into the finite computational domain. This latter must be defined and it is necessary to use some material which simulate an infinity area at the edges of the domain.

Based on the Maxwell's equations above and to [43], we obtain the propagation wave equation:

$$\frac{\partial^2 u}{\partial t^2} = c^2 \frac{\partial^2 u}{\partial x^2}$$

where  $u = u(x, t)$  is a function of both space and time and  $c$  is the speed of the light in the vacuum. This equation is the basis of the Yee algorithm which solves  $\vec{E}$  and  $\vec{H}$  components in time and space.

Yee's algorithm

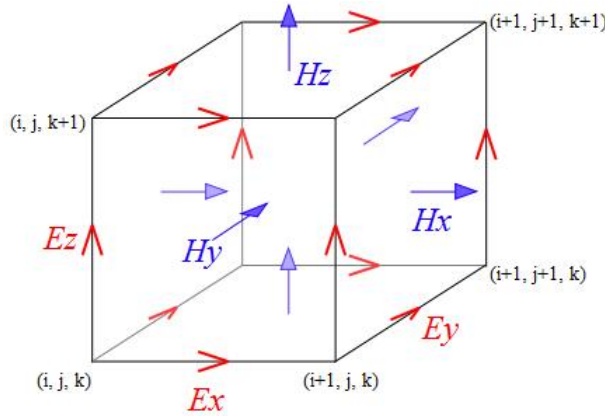


Figure 3.5: Yee cell

In 1966, Yee creates a new method to solve the Maxwell's equations in an isotropic media. The idea was to develop a simple and powerful algorithm which can solve both electric and magnetic fields in space and time. This algorithm is very robust because it uses both  $\vec{E}$  and  $\vec{H}$  information rather than either alone. It can be explained with the unit cell in Figure 3.5, where "every  $\vec{E}$  component is surrounding by four circulating  $\vec{H}$  components, and every  $\vec{H}$  component is surrounding by four circulating  $\vec{E}$  components" [48]. This method provides a simple picture of three-dimensional space being filled by an interlinked array of Faraday's and Ampere's laws contours.

As illustrated in Figure 3.6, the Yee algorithm also centers its  $\vec{E}$  and  $\vec{H}$  components in time which is called a leapfrog arrangement.



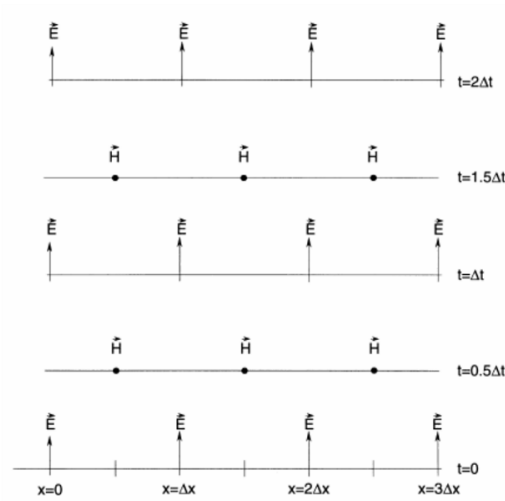


Figure 3.6: Leapfrog chart

At a given time point, all the  $\vec{E}$  computations are completed and stored in memory using  $\vec{H}$  data previously saved in the computer memory. Then, the  $\vec{H}$  components are also completed and stored thanks to the previous stored  $\vec{E}$  component. We repeat this process until time-stepping is concluded.

### 3.6 FDTD Software

Our simulations are realized with a software developed by some scientists of Aalborg University. This program allows to design antenna and then generates the main output parameters in electromagnetic (radiation patterns, impedance, smith chart...). The code is based on the FDTD method which is used in the deterministic scenarios to simulate small scale electromagnetic problems. The Finite Difference Time Domain (FDTD) uses the Maxwell's equations to obtain the required output parameters. The environment around our object imitates an open-space by using the Perfectly Matched Layers on the boundaries. The software runs over Matlab although the kernel is written in FORTRAN, which is faster compared in the compilation duration compared to the Matlab language. The use of powerful servers available at the university has been used to gain some time in our simulations. The main window is represented on Figure 3.7:

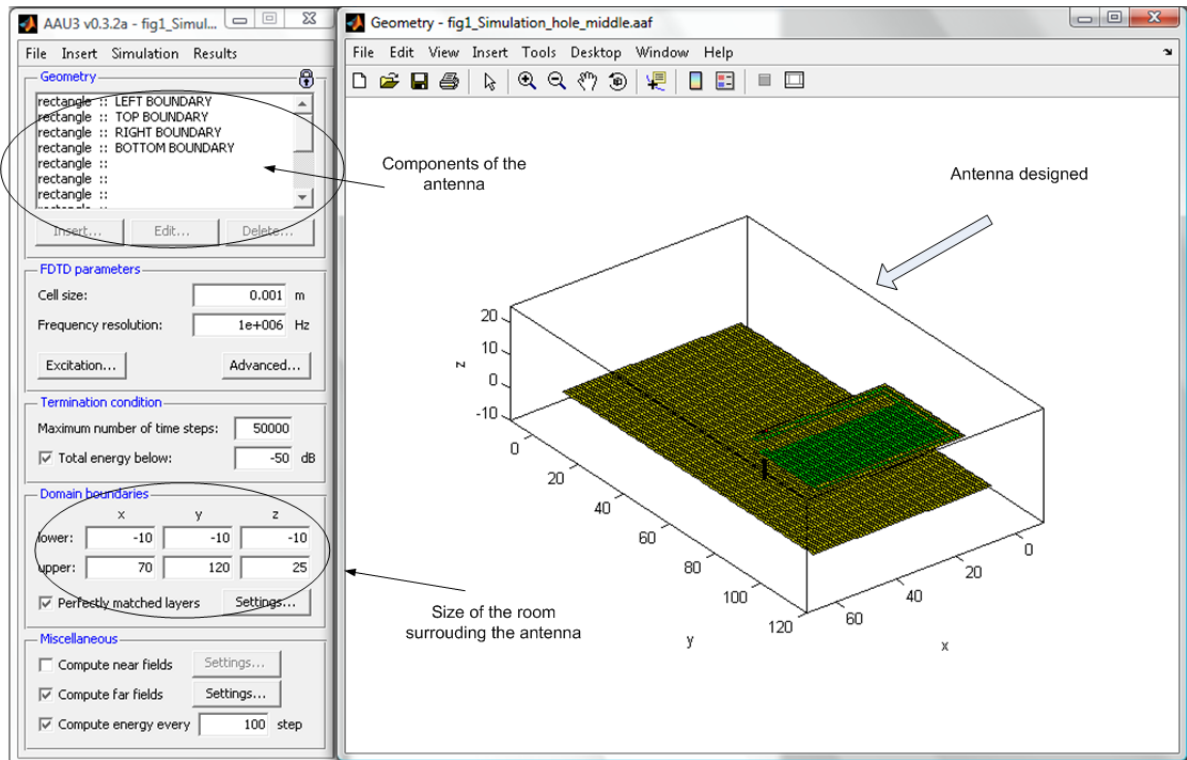


Figure 3.7: FDTD main window

The results menu is the most interesting part and gives us all the information needed to analyze an antenna. It can be seen on Figure 3.8.

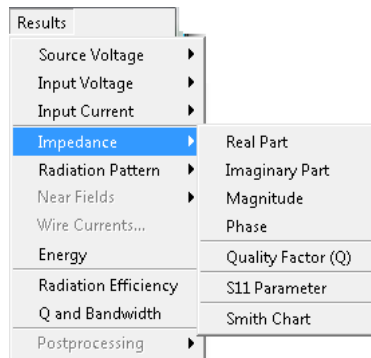


Figure 3.8: Results menu

The forces of this software are:

- its accuracy based on the FDTD method (directly compiles with the Maxwell equations) which can generate pattern in 2D and 3D.
- its simple usage thanks to a well designed interface,
- an infinity number of possibilities proposed to design an antenna in a given environment.

## Chapter 4

# Antenna Design and Simulations

In this chapter the results of the simulations are shown. Firstly, it will be introduced a short section about the simulations done involving Planar Inverted F Antennas. Then the Monopole Antennas simulations are shown. In this Monopole Antenna part, it will also be shown the results obtained under the influence of human hands holding the device. Additionally, the influence of some materials such as wood or metal emulating the phone laying on a table is also simulated. Furthermore, it will be shown how the different parameters of the antenna (such as radiation pattern, smith chart, S11, radiation efficiency, quality factor and bandwidth at resonance frequency) change.

### 4.1 Patch Antennas

The first antennas that were simulated are the patch antennas. This kind of antennas have a good radiation pattern always above the minimum required [1] as is shown in Figure 4.1, and thus the mobile phone can be hold in different positions depending of the final design, horizontal or vertical position. However, the patch antennas have a problem in their size, as in comparison with other antennas such as monopole, the total volume is much bigger.

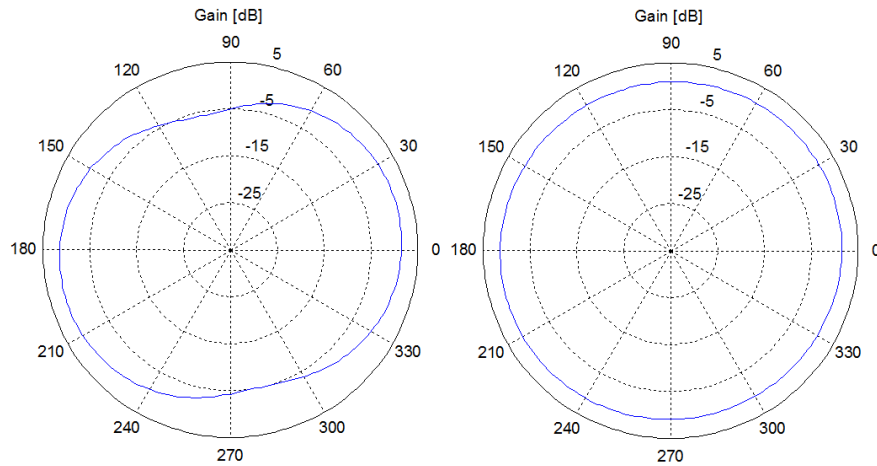


Figure 4.1: Radiation Pattern of the Patch Antenna with a Ground Plane of 62 x 51mm, gap of 40 mm and the antenna with a dimensions of 36 x 51 mm. Plane X-Y (left) and X-Z (right) of the radiation pattern.

Patch antennas are usually used to receive different bands of frequency such as GSM and UMTS in the same antenna receiver in order to reduce the size of the antenna. One of the patch antennas that was simulated following what can be seen in Appendix E has a Plane of 62x51 mm, the gap between the antenna and the ground plane is 40 mm and the dimensions of the antenna are 36x51 mm.

### Conclusions

The design of PIFA antennas is a good solution for mobile phones that want to integrate in a same antenna receiver different bands of frequency such as GSM or UMTS. Next section shows different solutions using monopole antennas, which have a similar behavior as PIFA antennas although they have a smaller size.

## 4.2 Meandered Monopole Vertical Antenna

This section shows the results for the “Meandered Monopole Vertical Antenna”. This antenna has been simulated with two different ground plane sizes, 100 mm and 90 mm.

This antenna was simulated with the feed point in different positions (as shown in Appendix G) in order to find a better impedance for all frequencies. Also this antenna has been simulated with a capacitor in parallel in order to see how the smith chart changes with the different values of it. In Appendix G the results are shown.

The radiation pattern of the antenna has also been studied in order to find the maximal power levels in the received signal. In figure [4.2] it is shown the dimensions of the antenna that has been chosen for the study of this section. The position of the feed point in this case has been moved 5 mm from the original position (which is considered to be the beginning of the meandered) and the size of

the ground plane is 90 mm.

The design of the antenna's resonant frequency was find around  $\frac{\lambda}{2}$ . This antenna has been designed for use in mobile phones that can be hold in vertical or horizontal position.

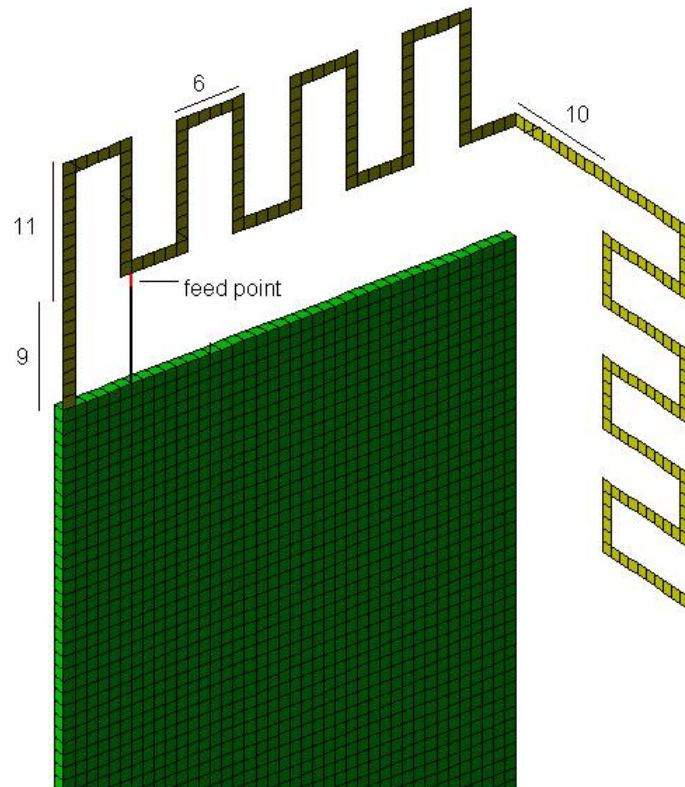


Figure 4.2: Meandered Monopole Vertical Antenna (values in mm)

#### 4.2.1 Smith Chart

Figure [4.3] shows the result of the antenna's simulated Smith Chart. In this figure it can be seen how the points of 470 MHz and 702MHz are close to the line of  $0\Omega$ . To verify if it is possible to match the values to  $50\Omega$ , Appendix F has been used. The impedance of 470 MHz can be matched using two capacitor, C1: 1,69 nF (in parallel) and C2: 3,05 pF (in series). The point of 702 MHz can be adapted using two capacitors, C3: 0,10 nF (in parallel) and C4: 3,73 pF (in series). These values are inside the range of commercial values of surface mount components (see Appendix F).

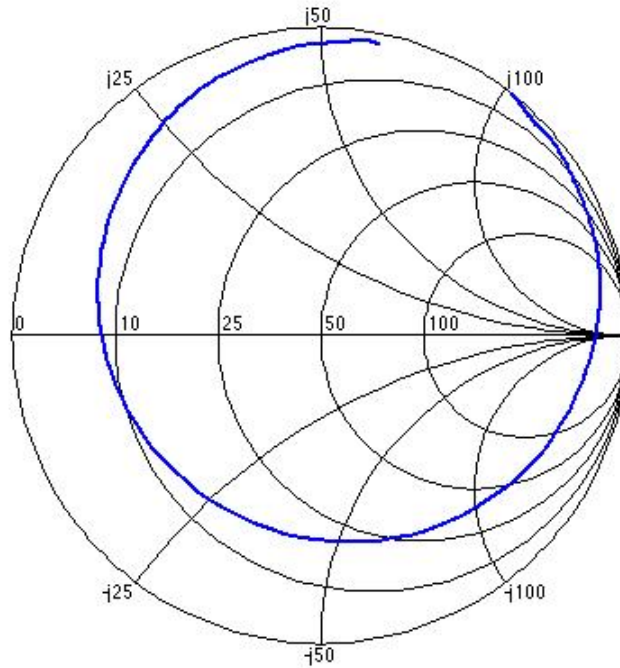


Figure 4.3: Smith Chart for the Meandered Monopole Vertical Antenna

### 4.2.2 Radiation Pattern

In order to ensure a good signal quality in the cell phone the radiation pattern has to be studied. As is shown in Figure 4.4 the radiation pattern has a good omnidirectional shape in all the directions. In order to know the exact gain in the different directions of the radiation pattern, the table in Figure 4.5 has been made, which shows the gain in  $0^\circ$ ,  $90^\circ$ ,  $180^\circ$ ,  $270^\circ$  and also the directions where the gain is minimal. Looking at these results one can conclude that the mobile phone can be held in vertical or horizontal position because the gain is better than the minimal recommended (Figure 3.3) in every direction.

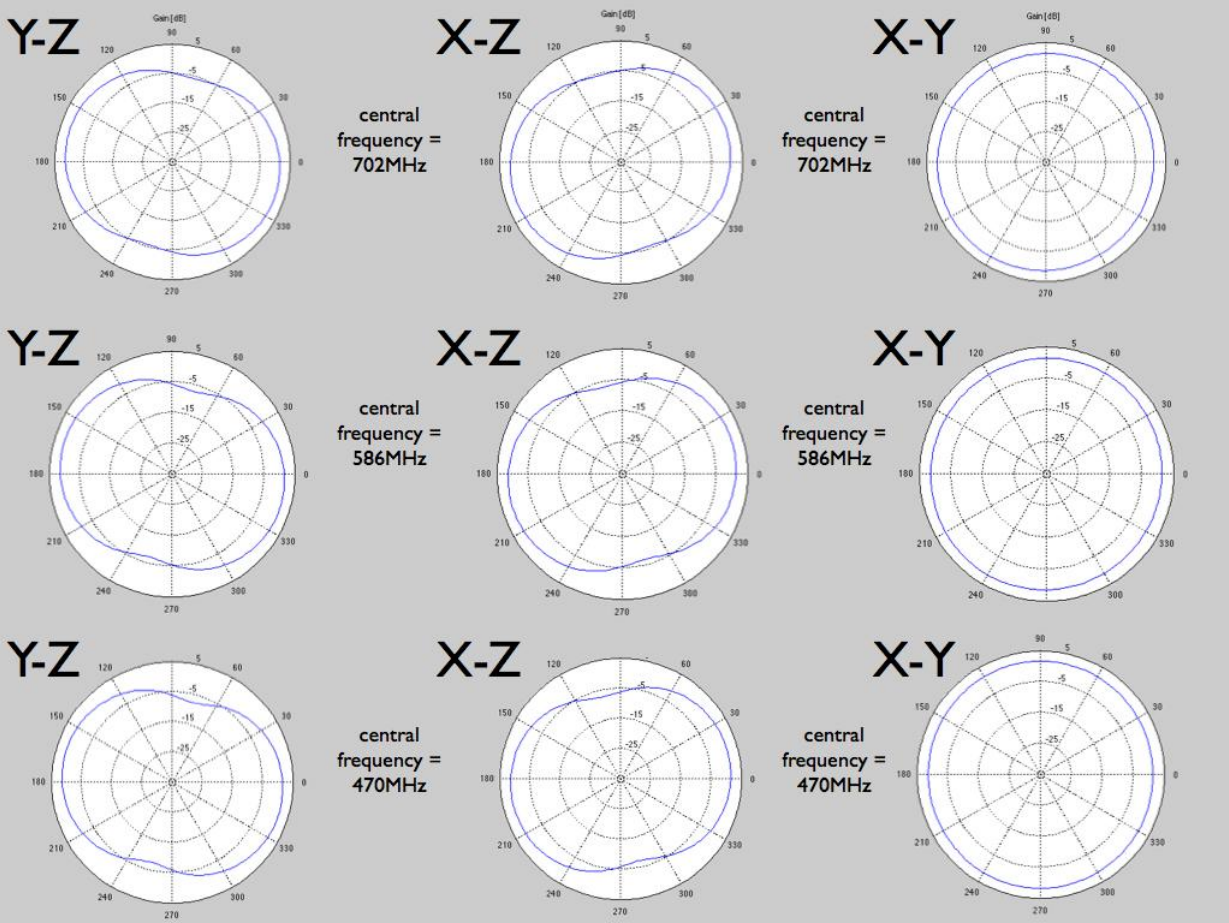


Figure 4.4: Radiation pattern of the antenna in the X-Y, Y-Z and X-Z planes in the extremes of the frequency band (470 MHz and 702 MHz) and also in the middle of it (586 MHz).



PLANE X-Z	0°	90°	180°	270°	90°<X<120°	270°<X<290°
Central freq(470MHz)	1,325	-6,059	1,45	-5,978	-7,117	-7,243
Central freq(586MHz)	1,2	-5,624	1,442	-5,469	-6,611	-6,918
Central freq(702MHz)	0,9624	-4,699	1,382	-4,442	-5,464	-6,039
PLANE X-Y	0°	90°	180°	270°	115°<X<145°	290°<X<320°
Central freq(470MHz)	1,325	1,465	1,45	1,441	1,239	1,122
Central freq(586MHz)	1,2	1,478	1,442	1,436	1,215	0,9987
Central freq(702MHz)	0,9624	1,44	1,382	1,327	1,105	0,707
PLANE Y-Z	0°	90°	180°	270°	75°<X<105°	165°<X<195°
Central freq(470MHz)	1,465	-6,059	1,441	-5,978	-7,67	-7,67
Central freq(586MHz)	1,478	-5,624	1,436	-5,649	-7,081	-7,062
Central freq(702MHz)	1,44	-4,699	1,327	-4,442	-5,74	-5,832

Figure 4.5: Values (dB) of the radiation pattern in 0°, 90°, 180° and 270° for the Meandered Monopole Vertical Antenna, also including the minimum gain of each plane.

### 4.2.3 Hand Simulations

As it can be seen in Section 4.2.2, the antenna's gain is always higher than the minimal recommended, and in order to investigate the losses that the human hand introduces, a simulation of it has been done. In Figure 4.6 it can be seen the model of the hand that was used for the simulations. This model represents a typical position to hold the mobile phone as if the user was looking the screen.



Figure 4.6: Position of the hand holding the cell phone

Figure 4.7 shows a comparative between the radiation pattern with and without the influence of the hand. As it can be seen, the shape of it changes with the influence of the hand.

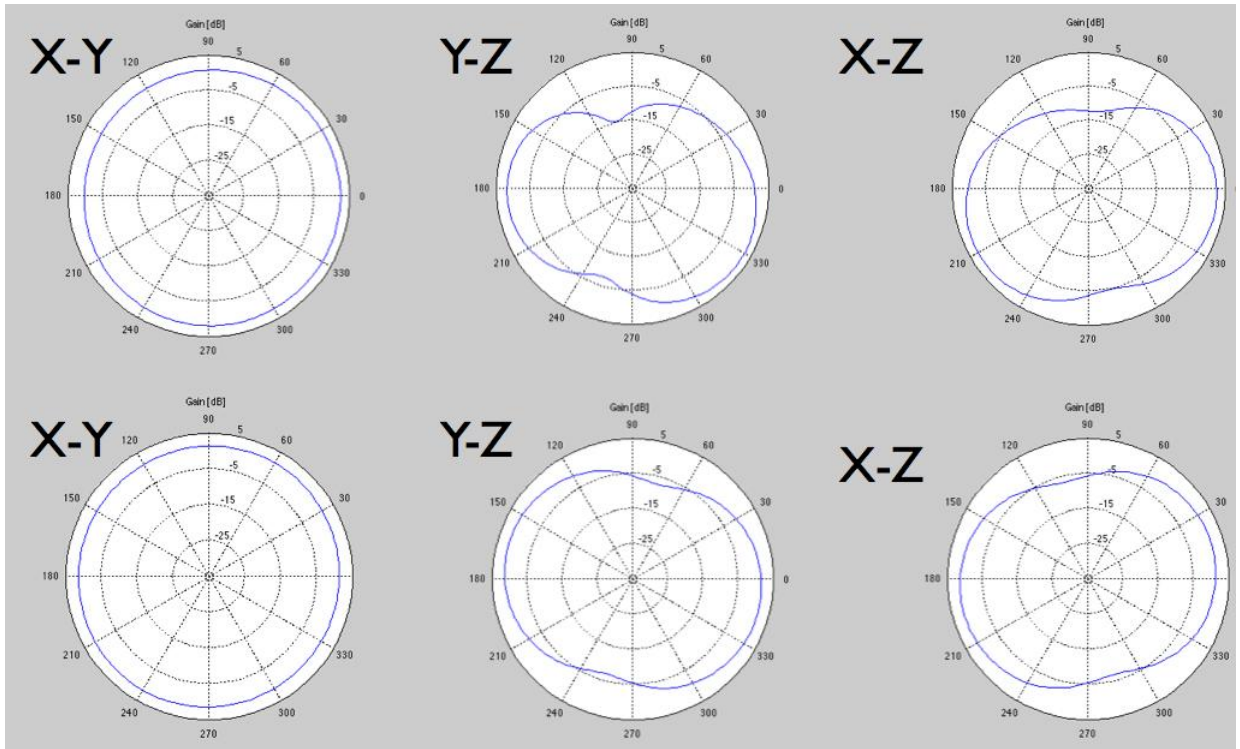


Figure 4.7: Comparative of the radiation pattern with and without the influence of the hand at 586MHz. The results of the first row are with the hand and the second row without hand.

As it can be seen in the table on Figure 4.8, a comparison between the results of the simulations with and without the hand is showed.

PLANE	0°	90°	180°	270°
X-Y (Antenna/Antenna+Hand)	1,325/ 2,428	1,465/ 0,8103	1,45/ 0,4696	1,441/1,883
X-Z (Antenna/Antenna+Hand)	1,2/ 2,428	-5,624/-12,14	1,442/0,4696	-5,469/-3,803
Y-Z (Antenna/Antenna+Hand)	1,478/ 0,8103	-5,624/ -12,14	1,436/ 1,883	-5,649/-3,803

Figure 4.8: Comparative table of the simulations with and without the hand

The radiation pattern of the antenna has some parts that are lower than the minimal required to receive a good level of signal. Thus between the angles  $90^\circ < X < 120^\circ$  in the plane Y-Z, there is a minimum of -14.578 dB. Also it can be seen in the plane X-Z a minimum of -12,19 dB at  $90^\circ$ . This losses could be studied in future investigations in order to improve the performance of the antenna under the influence of the human hand.

#### 4.2.4 Hands simulations in horizontal position

As is seen in 4.2.2, the antenna signal reception is always better than the minimum required (see Figure 3.3). For this reason it should be possible to watch the TV in horizontal position. Therefore a study of the hand's influence has been done. In Figure 4.9 it can be seen the model of the hand that was used for the simulations.

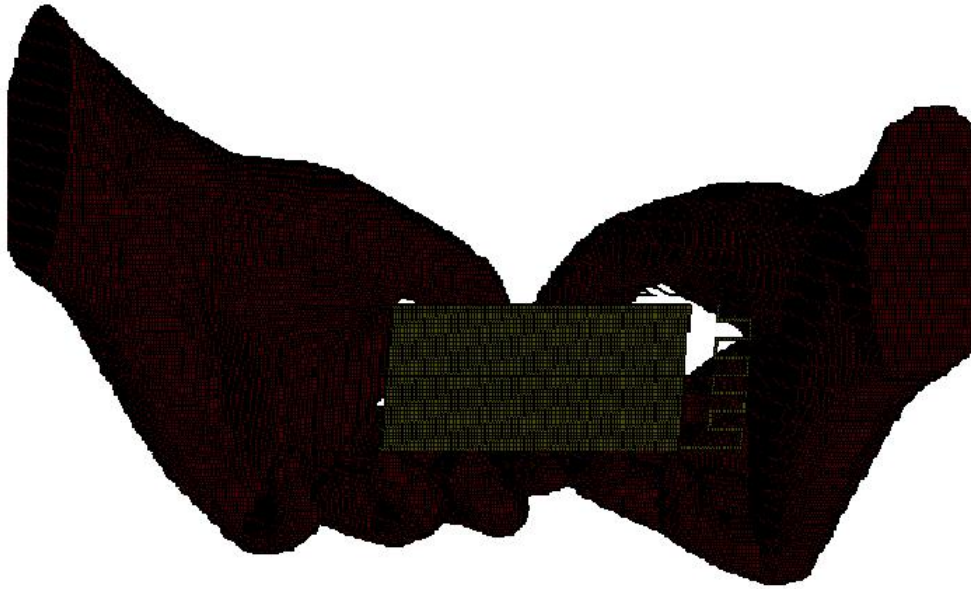


Figure 4.9: Position of the hands holding the mobile phone

Figure 4.10 shows a comparative between the radiation pattern with and without the influence of the hand. As expected, the shape of it changes with the influence of the hand.

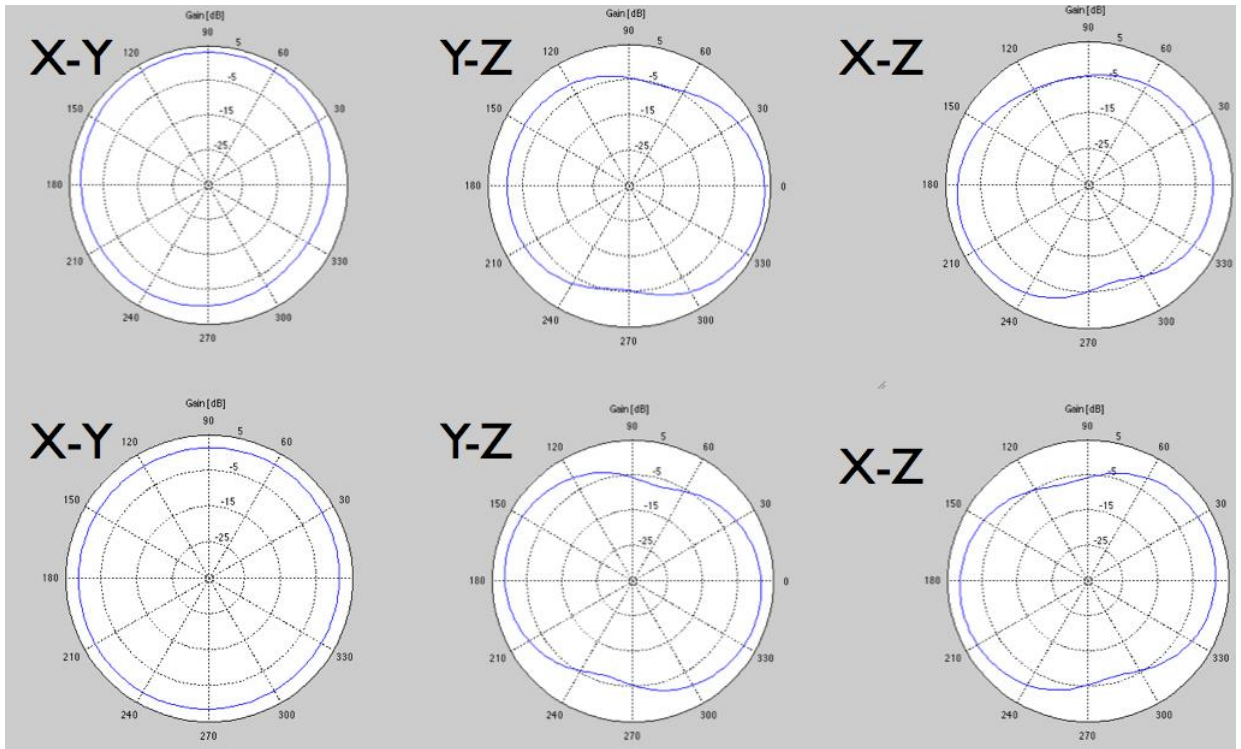


Figure 4.10: Comparative of the radiation pattern with and without the influence of the hand at 586MHz. The results of the first row are with the hand and the second row without hand.

In this simulation, oppositely as it was shown in 4.2.3, the radiation pattern with the hands change the shape but it cannot be seen parts with significant losses. It suppose that depends of the position of the hands the losses in the antenna will change.

#### 4.2.5 Wood Influence

It was also considered the possibility of a user watching DVB-H TV who, instead of holding the phone, let it laying over a table.

Therefore, in this section the antenna has been simulated being 5 mm over a wood plane. The plane is 30 cm x 20 cm x 0.1 cm with a relative permittivity of 2 and a conductivity of  $10^{-15}$  [47]. The antenna is over the middle point of the plane. Further, it has also been simulated the same plane with 3 cm of width.

In the table on Figure 4.11 is shown a comparison between the results of the antenna without the wood plane and with it (both width).

PLANE	0°	90°	180°	270°
X-Y (Antenna/Antenna+Wood Plane(0.1 cm)/Antenna+Wood Plane(3 cm))	1,325/1,209/1,212	1,465/1,488/1,431	1,45/1,449/1,712	1,441/1,429/1,743
X-Z (Antenna/Antenna+Wood Plane(0.1 cm)/Antenna+Wood Plane(3 cm))	1,2/1,209/1,212	-5,624/-5,681/-7,088	1,442/1,449/1,712	-5,469/-5,482/-6,269
Y-Z (Antenna/Antenna+Wood Plane(0.1 cm)/Antenna+Wood Plane(3 cm))	1,478/1,488/1,431	-5,624/-5,681/-6,269	1,436/1,429/1,743	-5,649/-5,482/-6,269

Figure 4.11: Comparative table with and without wood for the Meandered Monopole Vertical Antenna

As it can also be seen in the table on Figure 4.11, the influence of the plane in terms of reception gain is almost null with the plane with a width of 0.1 cm but it can be seen how with a width of 3 cm the gain changes.

#### 4.2.6 Metal influence

In order to follow the study with different materials the antenna has been simulated being 5 mm over a metal plane with a width of 1 cm. The plane is 30 cm x 20 cm x 1 cm.

In the table on Figure 4.12 and also in Figure 4.13 it is shown a comparison between the results of the antenna and the results with the metal ground plane. It can also be seen that the influence of the metal plane in the antennas behavior is more significant than the wood plane.

PLANE	0°	90°	180°	270°
X-Y (Antenna/Antenna+Metal Plane)	1,325/ 1,044	1,465/ -4,842	1,45/ 0,5358	1,441/0,5358
X-Z (Antenna/Antenna+Metal Plane)	1,2/1,044	-5,624/0,4805	1,442/0,5358	-5,469/0,9229
Y-Z (Antenna/Antenna+Metal Plane)	1,478/ -4,842	-5,624/ 0,4805	1,436/ -2,182	-5,649/0,9229

Figure 4.12: Comparative table of radiation pattern results (in dB) with the antenna under the influence of a metal plane

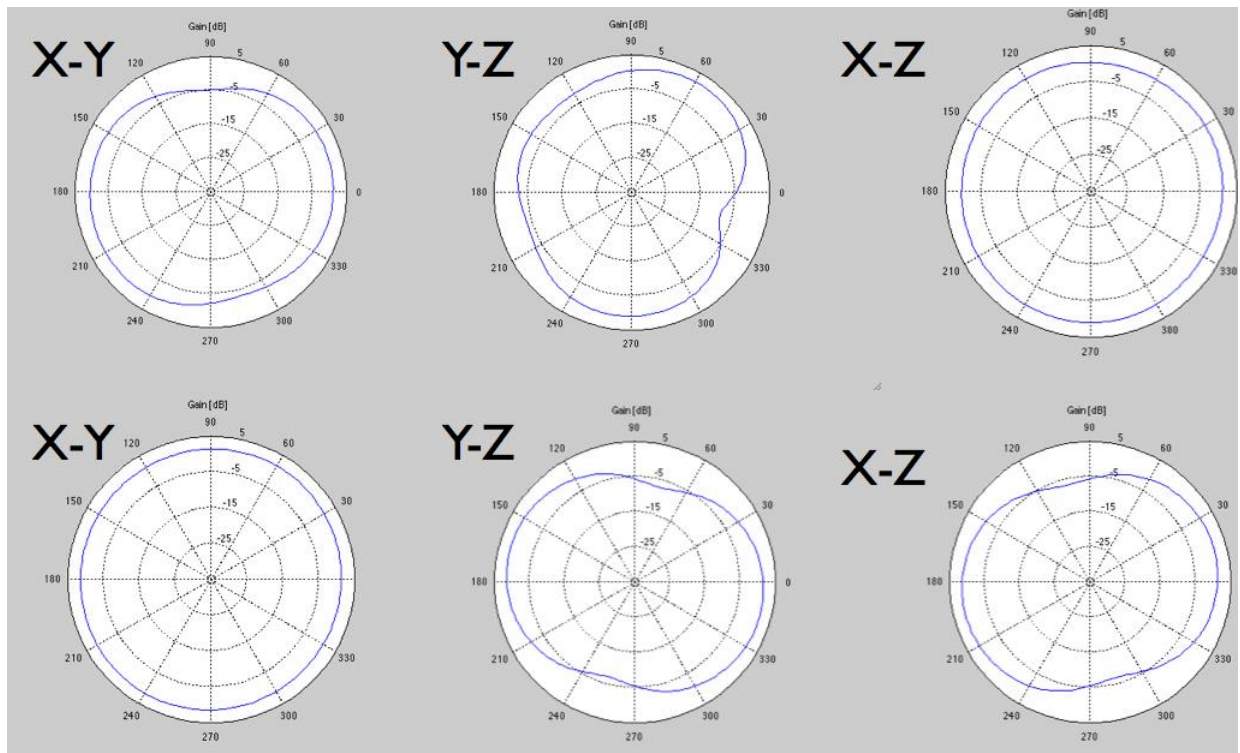


Figure 4.13: Radiation patter of the antenna under the influence of a metal plane

#### 4.2.7 S11 and radiation efficiency

In this point the S11 parameter has been studied in the different scenarios that have been shown in the previous points. Figures 4.14 and 4.15 show the results.

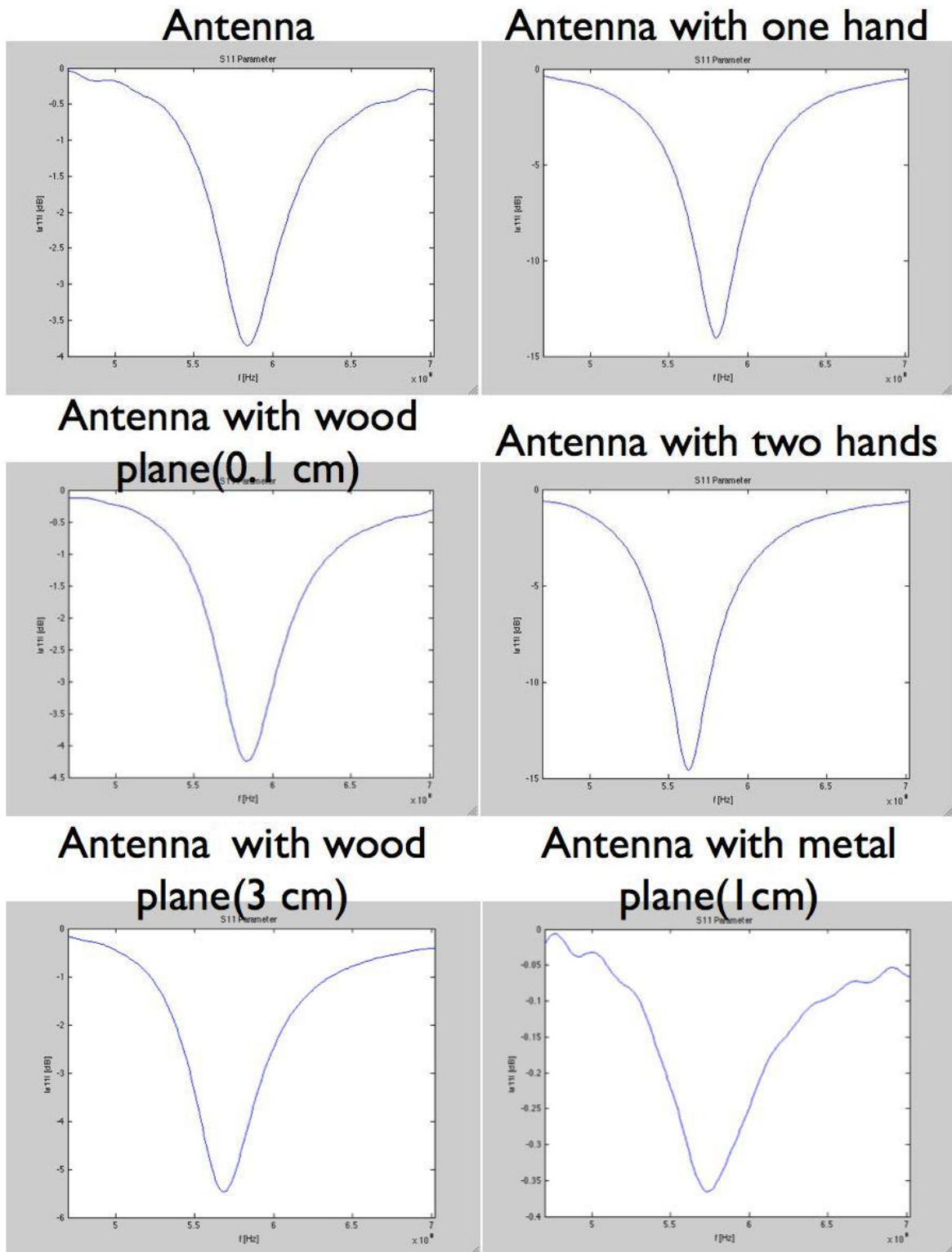


Figure 4.14: S11 parameter variation depending on the different scenarios studied for a 586 MHz frequency. The simulations have been done using a 30 x 20 mm plane (wood and/or metal).



PLANE X-Z	Central frequency(MHz)	Radiation efficiency
Antenna	584	1,2022(0,799dB)
Antenna with one hand	580	0,83919(-0,76138dB)
Antenna with two hands	563	0,64398(-1,9113dB)
Antenna with wood plane (0.1 cm)	584	1,0976(0,4045dB)
Antenna with wood plane (3 cm)	569	1,0929(0,38576dB)
Antenna with metal plane(1 cm)	574	1,064(0,27dB)

Figure 4.15: Radiation efficiency and central frequency variation on the different scenarios

As can be seen in the table on Figure 4.15, the radiation efficiency is worse when is under the influence of the hand. It can also be seen how it depends on the material and its width. Anyway the losses that introduce the hand or the different materials that have been studied, are not so big in comparison with the losses caused by the head's interference. These losses can reach up to 10dB [49]. The central frequency also varies depending on the material.

#### 4.2.8 Q at resonance and BW resonance

As is shown in Appendix G the quality factor and the bandwidth depend on the position of the feeding point.

This study focuses on finding an antenna bandwidth bigger than the maximum channel BW found in DVB-H (which is of 8 MHz [1]) in order to include the maximum number of channels in the bandwidth at resonance frequency. By doing so, it is possible to reduce the number of L-matching circuits needed if the antenna was to be used as a switched monopole antenna (see Section 3.2.4 and Appendix F).

As is it can be seen in Appendix G the BW at resonance frequency of this antenna is 11,64 MHz, and so it is possible to put one channel in it. This implies that one L-matching circuit is necessary for each TV channel. To improve these results it is possible to tune the values of the components of the different L-matching circuits in order to achieve a better BW at resonance frequency by means of trading-off some signal quality (power) at the intended matching frequency (which is also the resonance frequency after the matching). This tuning is not implemented in this thesis but some examples of it can be seen in [41] and [43].

#### 4.2.9 Conclusions

In this section it has been seen one of the proposed solutions for a DVB-H antenna. As it was shown the behavior of the antenna changes depending on different elements like the human hands or the influence of some materials such as wood or metal. Therefore, in future projects it could be interesting to make a more extended study about the different positions of the hand holding the cell phone or about the influence of materials such as metal (that it has been seen that introduces a big return loss). To conclude it can be said that this kind of antennas have a small bandwidth at the resonance frequency and so it is necessary to use a lot of L-matching circuits to adapt the different channels.

### 4.3 Meandered Monopole Book-Type Antenna

This section shows the results for the “Meandered Monopole Book-Type Antenna”, which has been simulated with two different ground plane sizes, 100 mm and 90 mm.

This antenna was simulated with the feed point in different positions (as shown in appendix G) in order to find a better impedance for all the band frequencies. Additionally this antenna has also been simulated with a capacitor in parallel with the source in order to see how the smith chart changes with different values of it. Appendix G shows the results.

The radiation pattern of the antenna has also been studied in order to find the maximal power levels of the received signal. In Figure 4.16 it is shown the dimensions of the antenna that has been chosen for the study of this section. The position of the feed point in this case has been moved 1 mm from the original position and the size of the ground plane is 90 mm.

The design of the antenna’s resonant frequency was find around  $\lambda$ . This antenna has been designed for book type mobile phones.

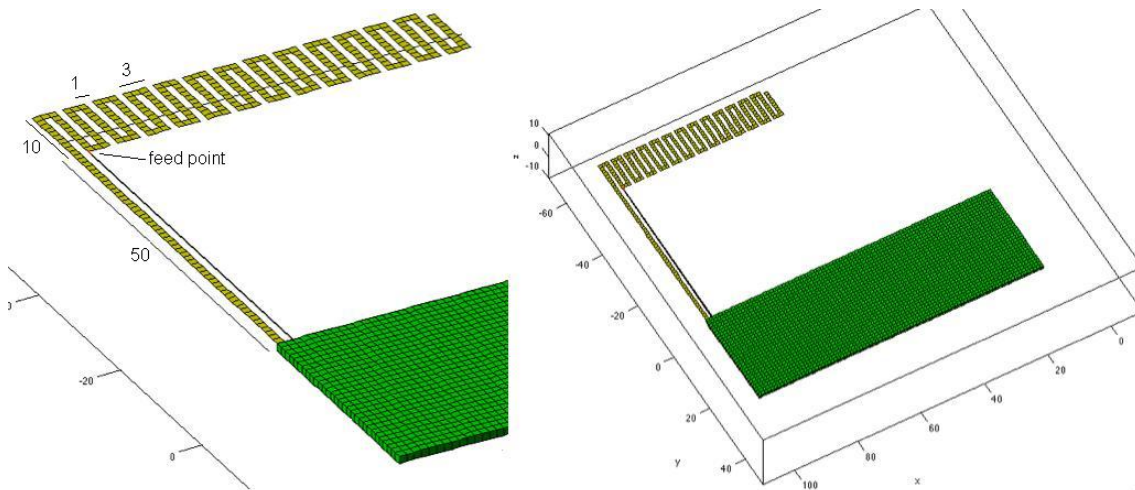


Figure 4.16: Meandered Monopole Book-Type Antenna

#### 4.3.1 Smith Chart

Figure 4.17 shows the antenna’s simulated Smith Chart. In this figure it can be seen how the points of 470 MHz and 702 MHz in the smith chart are close to the curve of  $0\Omega$ . To verify if it is possible to match the values to  $50\Omega$ , Appendix F has been used. The impedance at 470 MHz can be matched using two capacitors, C1: 3,72 nF (in parallel) and C2: 2,4 pF (in series). The point of 702 MHz can be adapted using two capacitors, C3: 14 nF (in parallel) and C4: 1,4 pF (in series). These values are inside the range of commercial values of surface mount components (see Appendix F).

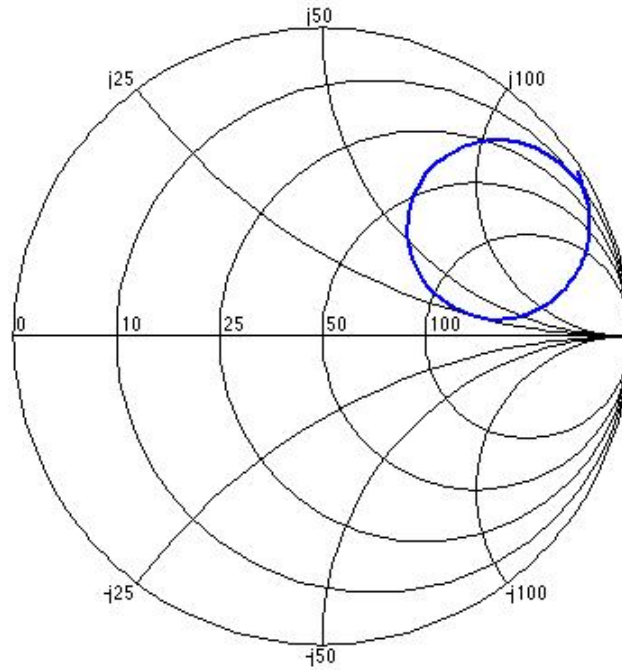


Figure 4.17: Smith Chart for the Meandered Monopole Book-Type Antenna

### 4.3.2 Radiation Pattern

In order to ensure a good signal quality in the cell phone the radiation pattern has to be studied. As is shown in Figure 4.18 the radiation pattern has a good omnidirectional shape in all directions and also a level of gain higher than the minimum specified by DVB-H standard as is shown in Figure 3.3. To guarantee this level of gain in the whole frequency band, simulations with the central frequency in 470 MHz and 702 MHz have been done. In order to know the exact gain in the different directions of the radiation pattern the table in Figure 4.19 has been made. This table shows the gain at  $0^\circ$ ,  $90^\circ$ ,  $180^\circ$  and  $270^\circ$ .

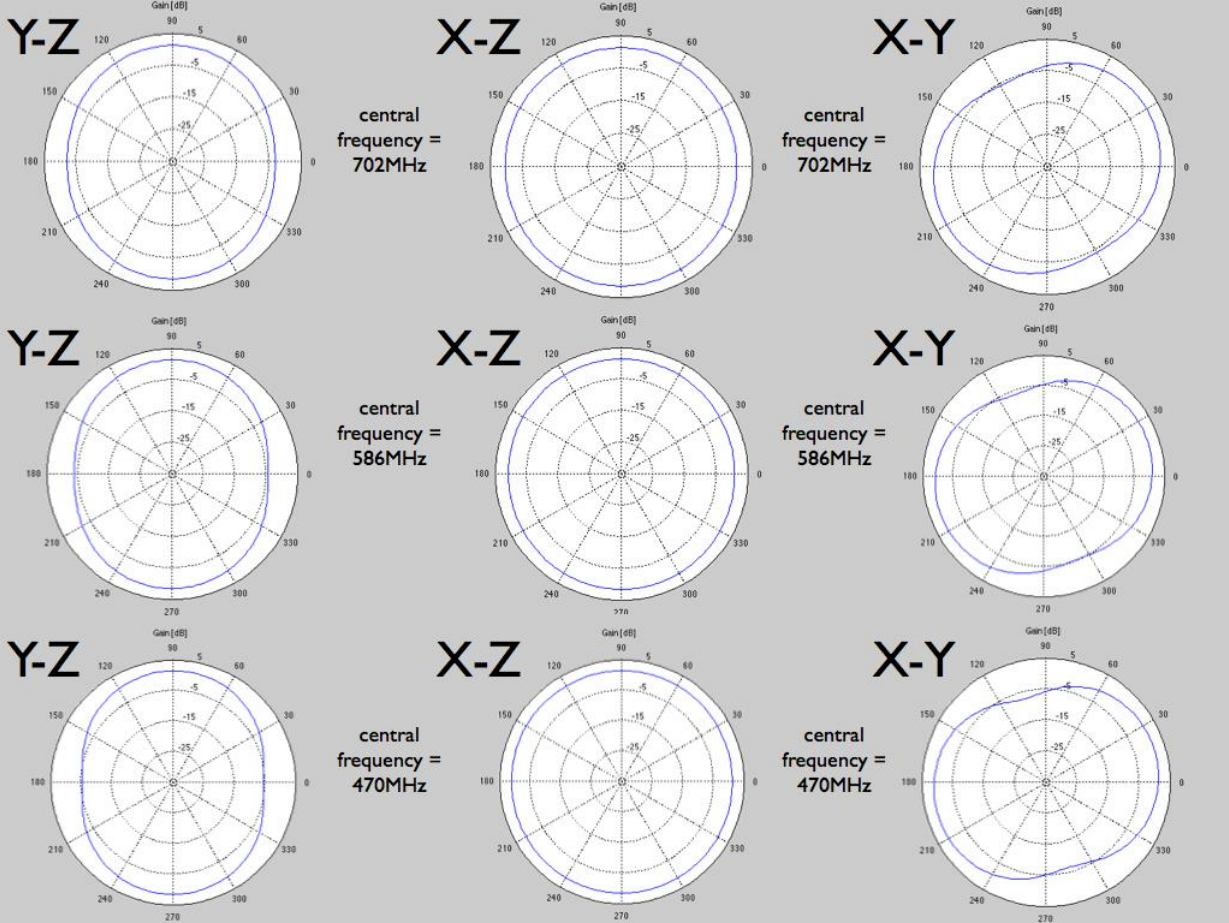


Figure 4.18: Radiation pattern of the antenna in the X-Y, Y-Z and X-Z planes in the extremes of the frequency band (470 MHz and 702 MHz) and also in the middle of it (586 MHz).

PLANE X-Z	0°	90°	180°	270°
Central freq(470MHz)	1,086	1,514	1,175	1,514
Central freq(586MHz)	0,7526	1,456	0,9108	1,455
Central freq(702MHz)	0,2184	1,38	0,4833	1,377
PLANE X-Y	0°	90°	180°	270°
Central freq(470MHz)	1,086	-5,566	1,175	-5,182
Central freq(586MHz)	0,7526	-4,369	0,9108	-3,673
Central freq(702MHz)	0,2184	-3,197	0,4833	-2,062
PLANE Y-Z	0°	90°	180°	270°
Central freq(470MHz)	-5,566	1,514	-5,182	1,514
Central freq(586MHz)	-4,369	1,456	-3,673	1,459
Central freq(702MHz)	-3,197	1,38	-2,062	1,377

Figure 4.19: Values (in dB) of the radiation pattern in 0°, 90°, 180° and 270° comparative table

### 4.3.3 Hands Simulations

As it can be seen in Section 4.3.2, the antenna's gain is always higher than the minimal recommended. Similarly to what has been done in Section 4.2.4, a study about the losses introduced because of holding the phone with two hands has been simulated. In figure 4.20 it can be seen the model of the hand that has been used for the simulations. The model of the hand is one of the position that is possible to hold the mobile phone to watch the television in it.

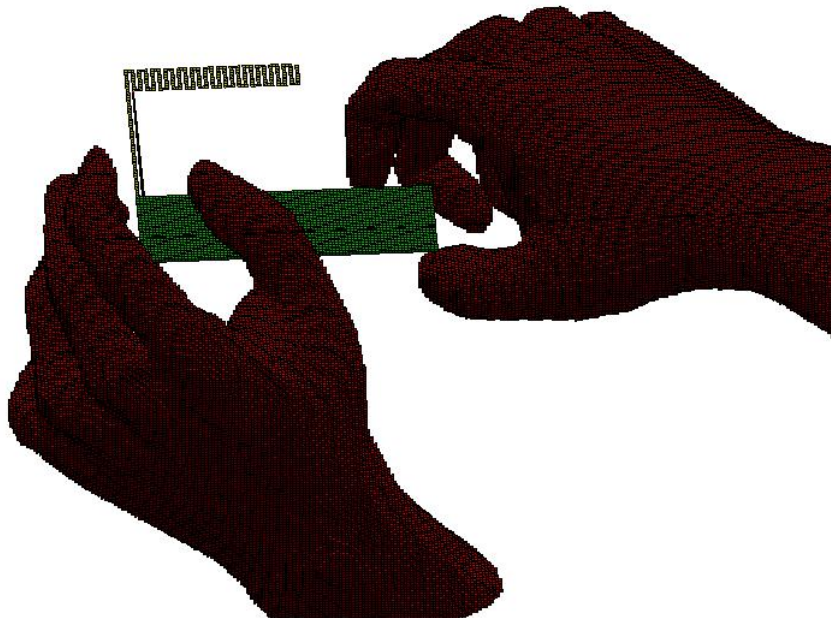


Figure 4.20: Book Type Antenna with Hands

Figure 4.21 shows a comparative between the radiation pattern with and without the influence of the hand. As it can be seen, the shape of it changes with the influence of the hand.

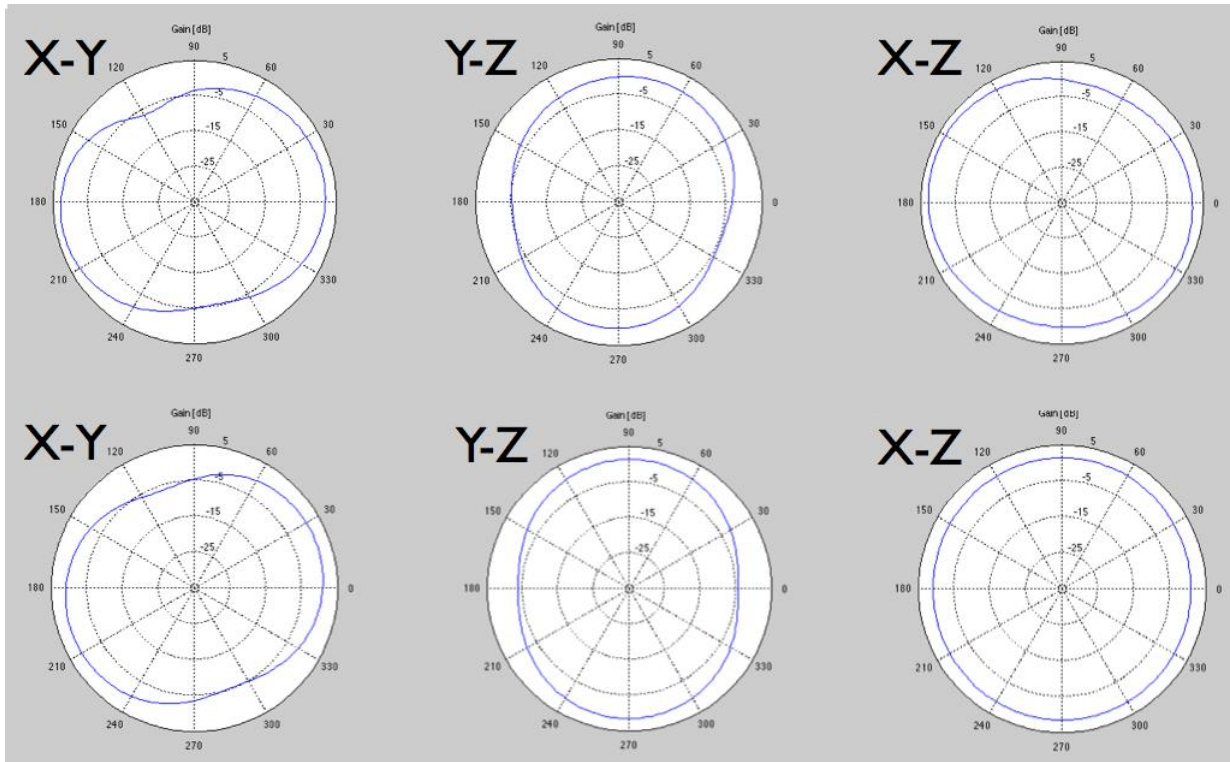


Figure 4.21: Comparative of the radiation pattern with and without the influence of the hands at 586MHz. The results of the first row are with the hands and the second row without hand.

The radiation pattern of the antenna has some parts with less reception gain. However, this gain is always better than the minimal required (see section 3.3). In future studies should be interesting to study the influence of different positions of the hand in order to find the worst position for it.

#### 4.3.4 Wood influence

As it has been done in Section 4.2.5, simulations with a wood plane have also been done for the book-type antenna.

The antenna has been simulated being 5 mm over a wood plane. The plane is 30 cm x 20 cm x 0.1 cm with a relative permittivity of 2 and a conductivity of  $10^{-15}$  [47]. Further, it has also been simulated the last plane but with 3 cm of width.

In the table on Figure 4.22 it is shown a comparison between the results of the antenna with a wood plane with two different widths, and without wood plane.

PLANE	0°	90°	180°	270°
X-Y (Antenna/Antenna+Wood Plane(0,1 cm)/Antenna+Wood Plane(3 cm))	0,7526/ 0,7494/ 0,5955	-4,369/ -4,396/ -3,804	0,9108/ 0,918/ 0,951	-3,673/ -3,678/ -2,52
X-Z (Antenna/Antenna+Wood Plane(0,1 cm)/Antenna+Wood Plane(3 cm))	0,7526/ 0,7194/ 0,5955	1,456/ 1,461/ 0,9534	0,9108/ 0,918/ 0,951	1,455/ 1,456/ 1,453
Y-Z (Antenna/Antenna+Wood Plane(0,1 cm)/Antenna+Wood Plane(3 cm))	-4,369/ -4,396/ -3,804	1,456/ 1,461/ 0,9534	-3,673/ -3,678/ -2,52	1,459/ 1,456/ 1,453

Figure 4.22: Gain in dB's for each plane depending on the angle

As is seen, the influence of the plane in terms of reception gain is almost null for a width of 0.1 cm, but with a width of 3 cm the gain changes depending on which radiation plane (X-Y, X-Z or Y-Z) is considered.

### 4.3.5 S11 and radiation efficiency

As expected after observing the results for the vertical monopole antenna (see Section 4.2.7), it can be seen in Figure 4.23 how the influence of the wood is almost null in the return loss.

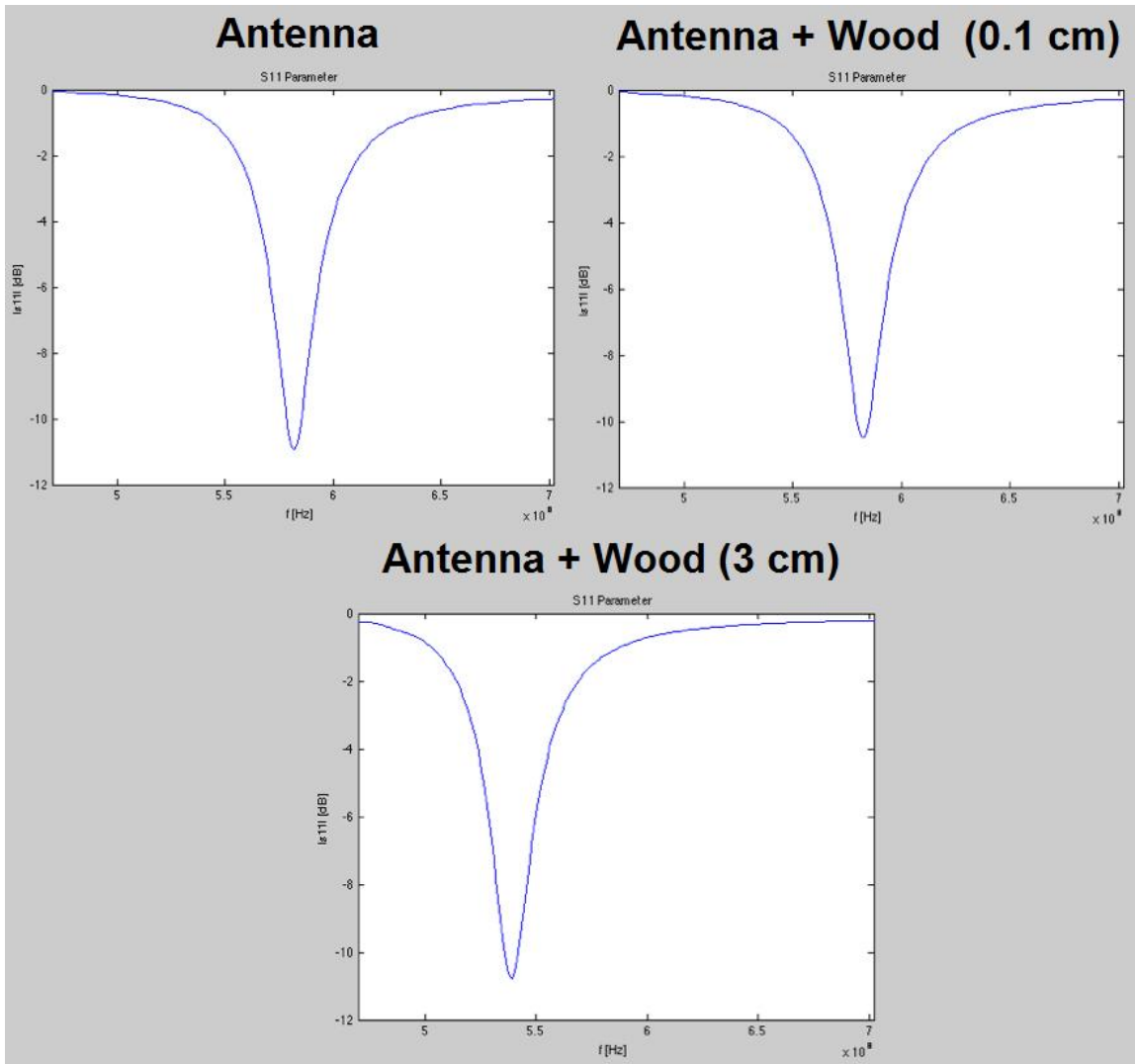


Figure 4.23:  $S_{11}$  parameter variation depending on the wood plane

The central frequency and the radiation efficiency change depending on the scenario. As it can be seen in the table on Figure 4.24, the central frequency decreases 44 MHz and the radiation efficiency for the whole scenario, improves.



PLANE	Antenna	Antenna + wood plane(0.1 cm)	Antenna + wood plane(3 cm)
Central frequency (MHz)	584	584	540
Radiation efficiency	1,119( 0.448dB )	1,084( 0.35dB )	1,075( 0,29592 dB )

Figure 4.24: Radiation efficiency and Central frequency variation with the wood plane

### 4.3.6 Q at resonance and BW resonance

As is shown in Appendix G the quality factor and the bandwidth depend on the position of the feeding point.

The book type mobile phone has the advantage that is can be possible to put the antenna far from the ground plane. The consequence of this is an improvement of the resonance BW. In Figure 4.25 it is shown a graph of the antenna that has been simulated for different distances between the antenna and the ground plane. It can be seen how the behavior of the antenna before 20 mm and after 90 mm is critic.

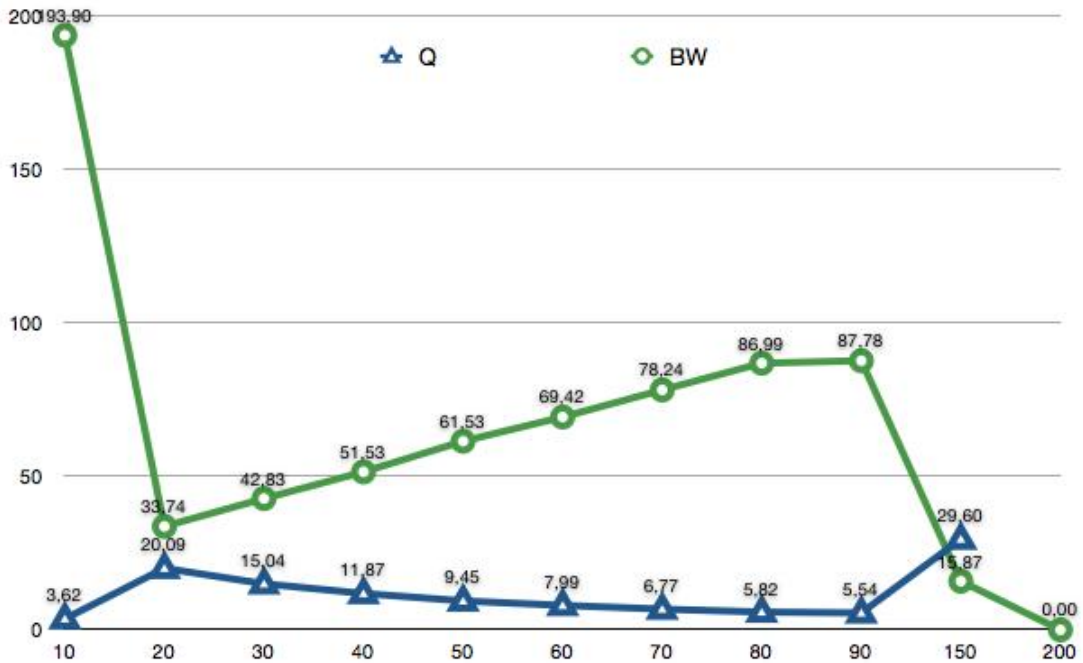


Figure 4.25: Q and resonance BW vs the distance between the ground plane and the radiator element of the antenna.

Also a study of the antenna at 50 mm from the ground plane has been done, including the variation of the position of the feeding point, in order to know its behavior.

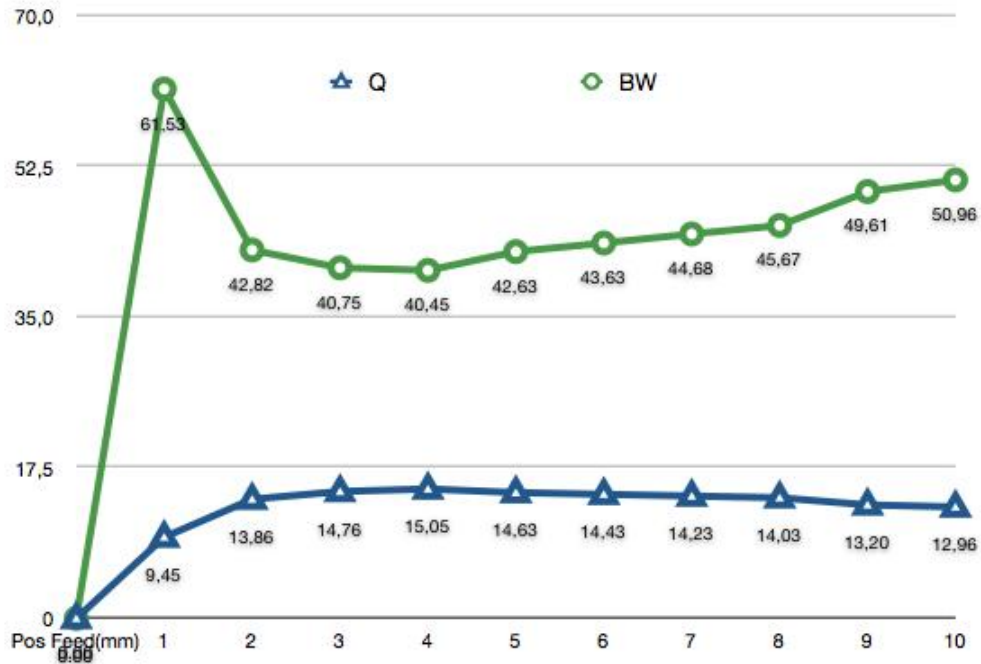


Figure 4.26: Q and BW depending on the Feed point position

Opposite to the antenna that has been shown in Section 4.2.8, which had quite narrow BW, this antenna has a resonance BW of 61,53 MHz, which allows to get more TV channels inside the antenna's BW and consequently to reduce the number of L-matching circuits needed to construct a switched monopole antenna.

#### 4.3.7 Conclusions

In this point it has been seen the second solution presented to receive DVB-H. As it was expected after the study in Section 4.2.3, the influence of the hand and the wood change the behavior of the antenna. Opposite to the Vertical Monopole Antenna, it can be seen how the BW at resonance frequency for the book-type antenna is bigger, and consequently it is possible to include more TV channels, thus reducing the number of L-matching circuits needed.

# Conclusions and Future Work

DVB-H is an extension of DVB-T that is used to cover all the handheld devices that usually are battery powered and need a low power consumption. The problem of DVB-T reception on a handheld device is that, as DVB-T is a streaming broadcast, the battery would deplete really fast as the receiver antenna would have to be powered all the time. The solution to this problem is DVB-H which uses short bursts of data to transmit the data so the receiver does not need to have the antenna turned on continuously. Additionally DVB-H also reduces the video quality as a small screen on a handheld device has not the same resolution as a big TV screen, and consequently less information needs to be transmitted.

DVB-H network topology is usually the same as the DVB-T network (shared network or hierarchical network). This is so because the DVB-T network is already deployed and the companies who own them do not want to spend a lot of money in deploying another network exclusively for DVB-H, if they can re-use the equipment they already have. Therefore the topology will have big cells covering almost all the areas and in the big cities gap fillers will be added to improve the coverage.

Some studies about DVB-H antennas were done previous to this one and, in this thesis they have been analyzed. The general sensation is that in most of them the antennas designed were bigger than most of the handheld devices in the market (cell phones, etc.) and so in this thesis one of the main objectives was to design smaller antennas. Nevertheless, some really interesting results and conclusions can be extracted from those works, like for example: matching the antennas, the influence of lumped elements on the antenna, etc.

To make the simulations a software based on FDTD was used. This software has been developed at the Antennas, Propagation and Radio Networking section of the Department of Electronic Systems at Aalborg University.

A lot of simulations have been done in this thesis to get the final results shown in Chapter 4. Although some other results are shown in Appendix G, those results are only a short sample of them. In fact more than 300 simulations have been done to obtain those results.

After studying all kinds of antenna it was decided to perform simulations on PIFA antennas and on planar monopole antennas. The first kind simulated were the PIFA antennas and, although the simulation results were good, the size of the antennas was considered to be too big compared to the size of typical handheld devices, and so they were discarded as a solution. The second and last kind of antennas simulated were the planar monopole antennas. When simulating this kind of antennas, the objective was to design two kinds of antennas: a vertical monopole and an horizontal (book-type)

monopole. Additionally it was pursued that the vertical monopole had a good behavior if used on an horizontal position.

Two types of planar monopole antennas, one vertical and one horizontal, were finally selected as the best simulations obtained. These two antennas were also simulated in different scenarios such as being hold by human hands, or laying on a wood or metallic table. The behavior of both antennas under these possible scenarios is evaluated and compared. Both designed antennas had good results in the simulations and a future work could be to build them and make real measurements as well as designing the matching network.

From the simulations under the hand influence can be concluded that in general the hand does not introduce a lot of losses. Nevertheless, in the vertical monopole antenna, when held with one hand vertically there are some points where the attenuation is quite high (up to 6.5 dB). This implies that if the phone is hold covering the radiator element of the antenna there could be some big attenuation. The simulations were done using only one model of human hand and so, a future work could consist on using different models and more accurate ways of holding the antenna, specially considering the case when the radiator element is blocked.

As a future line of work it could also be considered the fact of improving the antenna designs and to simulate the influence of additional materials to the antenna such as plastic, glass, etc. Another thing that could be done in a future is an study about the way people holds the handheld devices to improve the antenna. This could be done simply by gathering and important number of people and making them see some video on a DVB-H capable device.

# Bibliography

- [1] DVB-H Implementation Guidelines  
[[http://www.dvb-h.org/PDF/a092r2.tm2977r11.dTR102377.V1.3.1.DVB-H\\_impl\\_guide.pdf](http://www.dvb-h.org/PDF/a092r2.tm2977r11.dTR102377.V1.3.1.DVB-H_impl_guide.pdf)]  
Last visited on 11/3/2008.
- [2] DVB-H Specification: ETSI EN 302 304  
[<http://www.dvb-h.org/PDF/DVB-H%20Specification%20-%20En302304.V1.1.1.pdf>] Last visited on 11/3/2008.
- [3] DVB-H: Digital Broadcast Services to Handheld Devices  
[[http://www.dvb-h.org/PDF/01566629\\_DVB-H.pdf](http://www.dvb-h.org/PDF/01566629_DVB-H.pdf)] Last visited on 11/3/2008.
- [4] Mobile TV in Italy: A perspective on Mediaset role  
[[http://www.satexpo.it/documenti/200629ven\\_capuzzello.pdf](http://www.satexpo.it/documenti/200629ven_capuzzello.pdf)] Last visited on 11/3/2008
- [5] Texas Instrument DVB-H receiver chip: DTV1000  
[<http://focus.ti.com/general/docs/wtbuwtbu/wtbuproductcontent.tsp?templateId=6123&navigationId=12595&>
- [6] Frontier-Silicon DVB-H receiver chip: Paradiso 1 FS1030  
[[http://www.frontier-silicon.com/products/chips/briefs/Paradiso1\\_PB\\_0577.pdf](http://www.frontier-silicon.com/products/chips/briefs/Paradiso1_PB_0577.pdf)]
- [7] Microtune's DVB-H receiver chip: MT2266  
[[http://www.microtune.com/products/pdf/mt2266\\_10.pdf](http://www.microtune.com/products/pdf/mt2266_10.pdf)]
- [8] ST DVB-H receiver chip: STV0362  
[<http://www.st.com/stonline/products/literature/bd/12173.pdf>]
- [9] Analog Devices DVB-H receiver chip: ADMTV102  
[<http://www.analog.com/en/prod/0,2877,ADMTV102,00.html>]
- [10] Constantine A. Balanis, Antenna Theory: Analysis and Design, Second Edition.
- [11] Wikipedia, dipole and/or monopole
- [12] Kin-Lu Wong, Planar Antennas for Wireless communications.
- [13] *Yasuhiro Oda, Member, IEEE, Koichi Tsunekawa, Member, IEEE, and Masaharu Hata, Senior Member, IEEE*, Advanced LOS Path-Loss Model in Microcellular Mobile Communications.
- [14] Hata Model for Open Areas, [[http://en.wikipedia.org/wiki/Hata\\_Model\\_for\\_Open\\_Areas](http://en.wikipedia.org/wiki/Hata_Model_for_Open_Areas)]

- [15] *Hiroyuki Arai*, Measurement of mobile antenna systems.
- [16] ACTS - AC318 MOTIVATE (Deliverable 06): "Reference Receiver Model for Planning of Mobile TV Services".
- [17] Digital DVB-T Transmitters, Richardson Electronics.  
[<http://www.ferret.com.au/c/Richardson-Electronics/Digital-DVB-T-transmitters-n688815>]
- [18] Digital TV Transmitters, Technosystem Srl, RVR ELETTRONICA,  
[[http://www.technosystem.it/pdf/DIGITAL\\_UHF\\_VHF.pdf](http://www.technosystem.it/pdf/DIGITAL_UHF_VHF.pdf)]
- [19] Digital TV Antenna for bands IV and V, Telecomunicazione Ferrara Srl,  
[<http://www.telecfce.it/images/antenas/PANNELLO%20PUHF1.pdf>]
- [20] Muhammad Imadur Rahman, Suvra Sekhar Das, Frank H.P. Fitzek, OFDM Based WLAN Systems.
- [21] Muhammad Imadur Rahman, Basics about Multi-carrier Based Multiple Access Techniques.
- [22] Impedance matching: a primer by Electus Distribution Reference data sheet
- [23] Derive European Webpage [<http://www.derive-europe.com/main.asp>]
- [24] Amitabh Kumar, "Mobile TV DVB-H, DMB, 3G Systems and Rich Media Applications", 2007.
- [25] Kamel Haddad, "DVB-H in Denmark, Technical and Economic Aspects", Master Thesis developed at Technical University of Denmark, 2007
- [26] Aurelian Bria, "Hybrid Cellular-Broadcasting Infrastructure Systems", Licentiate Thesis, 2006.
- [27] David Gómez-Barquero & Aurelian Bria, "Feasibility of DVB-H Deployment on Existing Wireless Infrastructure", June 2005.
- [28] Kazuhiro Hirasawa, Misao Haneishi, "Analysis, Design, and Measurement of Small and Low-Profile Antennas".
- [29] David M. Pozar, "Microwave engineering", 1990 - ISBN: 0-201-50418-9 - pages 281 to 283
- [30] Y. Okumura, E. Ohmori, T. Kawano, and K. Fukuda, "Field strength and its variability in VHF and UHF land-mobile service", Rev. Elec. Comm. Lab., vol. 16, No. 9-10, pp. 825-873, 1968.
- [31] M. Hata, "Empirical formula for propagation loss in land mobile radio services", IEEE Trans. Veh. Tech., vol. 29, No. 3, pp. 317-325, 1980.
- [32] Arturas Medeisis, Algimantas Kajackas, "On the Use of the Universal Okumura-Hata Propagation Prediction Model in Rural Areas", Telecommunications Department, Kaunas University of Technology
- [33] <http://www.microwaves101.com>
- [34] Y. Okumura *et al.*, "Field Strength and Its Variability in VHF and UHF Land-Mobile Radio Service", Rev. Elec. Commun. Lab., vol. 16, 1968

- [35] M. Hata, "Empirical formula for propagation loss in Land Mobile Radio Services", *IEEE Trans. Veh. Technol.*, vol. VT-29, pp. 317-325, Aug. 1980. [<http://ieeexplore.ieee.org/iel5/25/34048/01622772.pdf?arnumber=1622772>]
- [36] Hata-Okumura Model, AWE-Communications, [<http://www.awe-communications.com/Propagation/Rural/HO/index.htm>]
- [37] Friis Transmission Equation/Free Space Radiopropagation Model, [[http://en.wikipedia.org/wiki/Friis\\_transmission\\_equation](http://en.wikipedia.org/wiki/Friis_transmission_equation)]
- Online Matlab Course, Webpage:  
 [<http://www.sdsmt.edu/syseng/ee/courses/ee622/matlab.html>], Original Code:  
 [<http://www.sdsmt.edu/syseng/ee/courses/ee622/mfiles/multipath.m>], College of Systems Engineering, South Dakota School of Mines & Technology.
- [38] John J. Egli, "Radio propagation above 40 MC over irregular terrain" U.S. Army Signal Eng. Labs., Fort Monmouth, N.J. [<http://ieeexplore.ieee.org/iel5/10933/4056388/04056397.pdf?tp=&isnumber=&arnumber=4056397>]
- [40] Notes on Okumura Propagation, Softwright LLC, Publishers of The Terrain Analysis Package, [[http://www.softwright.com/faq/engineering/prop\\_okumura.html](http://www.softwright.com/faq/engineering/prop_okumura.html)]
- [39] Alexander Schertz and Chris Weck, "Hierarchical Modulation, the transmission of two independent DVB-T multiplexes on a single frequency", Institut für Rundfunktechnik (IRT), [[www.ebu.ch/trev\\_294-weck.pdf](http://www.ebu.ch/trev_294-weck.pdf)]
- [40] "DVB-T Hierarchical Modulation, a brief introduction", DVB Group, March 2000, [[www.broadcastpapers.com/whitepapers/paper\\_loader.cfm?pid=520](http://www.broadcastpapers.com/whitepapers/paper_loader.cfm?pid=520)]
- [41] Jari Holopainen, "Antenna for Handheld DVB Terminal", Master Thesis, Helsinki University of Technology, 2005
- [42] Fredrik Persson & Mattias Wideheim, "Design of Antennas for Handheld DVB-H Terminals", Master Thesis, Lund University, January 2006
- [43] Mauro Pelosi, "Tuneable DVB-H Antenna in a Small Handheld Device", Master Thesis, Aalborg University, June 2006
- [44] Zena Fourzoli & Radwan Charafeddine, "DVB-H Antenna in a Small Handheld Device", Master Thesis, Aalborg University, June 2007
- [45] Ranga Kariyawasam & Yue Gao & Choo C. Chiau & Xiaodong Chen & Clive G. Parini & Junsheng Yu, "Dielectric Loaded Folded Half Loop Antenna for DVB-H Terminals", 2007
- [46] "Fractus® TVNow™ Mobile TV Dual-Band DVB-H (UHF + L Band) Antenna", P/N: FR01-B1-S-0-047, Fractus, 2007
- [47] William Simpson and Anton TenWolde, "Physical Properties and Moisture Relations of Wood". It is the Chapter 3 of the book "Wood handbook, Wood as an engineering material", 1999.

- [48] Allen Taflove, *Computational Electrodynamics: The Finite-Difference Time-Domain Method*, Artech House.
- [49] Gert F. Pedersen, Mathieu Tartiere, Mikael B. Knudsen, "Radiation Efficiency of Handheld Phones", Aalborg University



# List of Figures

1.1	Schematic description of the DVB-H system operating over a DVB-T system. The original figure comes from [3]. . . . .	5
1.2	Relation between burst bitrate and power saving [1] . . . . .	7
1.3	Structure of MPE-FEC error correction matrix. Obtained from [1] . . . . .	8
1.4	Spectral efficiency of OFDM signals [20][21] . . . . .	10
1.5	Delay spread and symbol duration [20][21] . . . . .	10
1.6	Inter-symbol interference[20][21] . . . . .	11
1.7	Guard time interval . . . . .	11
1.8	OFDM transceiver model [20][21] . . . . .	13
1.9	Comparison of the OFDM modes [3] . . . . .	14
2.1	DVB-H on a Shared Multiplex . . . . .	16
2.2	DVB-H using Hierarchy . . . . .	17
2.3	Hierarchical modulation example [40] . . . . .	18
2.4	Dedicated DVB-H Network . . . . .	18
2.5	Service Area vs Transmitted Power . . . . .	19
2.6	Area Coverage vs Transmitted Power for a 150 m high antenna and a 25 km service area	19
2.7	Topology of the Italian DVB-H network. Obtained from [4] . . . . .	20
2.8	Color code for the Hata model representations . . . . .	22
2.9	In-car and indoor effects on Hata propagation model . . . . .	23
2.10	In-car and indoor effects on Hata propagation model for rural areas . . . . .	24
2.11	In-car and indoor effects on Hata propagation model for suburban areas . . . . .	24
2.12	In-car and indoor effects on Hata propagation model for urban areas . . . . .	25
2.13	2-Ray model (high) and 2-Ray model with zoom (down) . . . . .	26
2.14	Comparison between the Okumura Model (outdoor, rural) and the 2-ray model (outdoor) and the Egli model (outdoor) . . . . .	27
2.15	Egli Model (green: outdoor at top, indoor bottom, incar in the middle) versus Okumura-Hata Model for Urban areas . . . . .	27
3.1	Antenna as a transition device [10] . . . . .	29
3.2	Radiation pattern according to the wavelength $\lambda$ [33] . . . . .	29
3.3	Required antenna power gain . . . . .	33
3.4	Maxwell's equations . . . . .	35
3.5	Yee cell . . . . .	36
3.6	Leapfrog chart . . . . .	37

3.7	FDTD main window . . . . .	38
3.8	Results menu . . . . .	38
4.1	Radiation Pattern of the Patch Antenna with a Ground Plane of 62 x 51mm, gap of 40 mm and the antenna with a dimensions of 36 x 51 mm. Plane X-Y (left) and X-Z (right) of the radiation pattern. . . . .	41
4.2	Meandered Monopole Vertical Antenna (values in mm) . . . . .	42
4.3	Smith Chart for the Meandered Monopole Vertical Antenna . . . . .	43
4.4	Radiation pattern of the antenna in the X-Y, Y-Z and X-Z planes in the extremes of the frequency band (470 MHz and 702 MHz) and also in the middle of it (586 MHz). . . . .	44
4.5	Values (dB) of the radiation pattern in $0^\circ$ , $90^\circ$ , $180^\circ$ and $270^\circ$ for the Meandered Monopole Vertical Antenna, also including the minimum gain of each plane. . . . .	45
4.6	Position of the hand holding the cell phone . . . . .	46
4.7	Comparative of the radiation pattern with and without the influence of the hand at 586MHz. The results of the first row are with the hand and the second row without hand. . . . .	47
4.8	Comparative table of the simulations with and without the hand . . . . .	47
4.9	Position of the hands holding the mobile phone . . . . .	48
4.10	Comparative of the radiation pattern with and without the influence of the hand at 586MHz. The results of the first row are with the hand and the second row without hand. . . . .	49
4.11	Comparative table with and without wood for the Meandered Monopole Vertical Antenna . . . . .	50
4.12	Comparative table of radiation pattern results (in dB) with the antenna under the influence of a metal plane . . . . .	50
4.13	Radiation patter of the antenna under the influence of a metal plane . . . . .	51
4.14	S <sub>11</sub> parameter variation depending on the different scenarios studied for a 586 MHz frequency. The simulations have been done using a 30 x 20 mm plane (wood and/or metal). . . . .	52
4.15	Radiation efficiency and central frequency variation on the different scenarios . . . . .	53
4.16	Meandered Monopole Book-Type Antenna . . . . .	54
4.17	Smith Chart for the Meandered Monopole Book-Type Antenna . . . . .	55
4.18	Radiation pattern of the antenna in the X-Y, Y-Z and X-Z planes in the extremes of the frequency band (470 MHz and 702 MHz) and also in the middle of it (586 MHz). . . . .	56
4.19	Values (in dB) of the radiation pattern in $0^\circ$ , $90^\circ$ , $180^\circ$ and $270^\circ$ comparative table . . . . .	57
4.20	Book Type Antenna with Hands . . . . .	57
4.21	Comparative of the radiation pattern with and without the influence of the hands at 586MHz. The results of the first row are with the hands and the second row without hand. . . . .	58
4.22	Gain in dB's for each plane depending on the angle . . . . .	59
4.23	S <sub>11</sub> parameter variation depending on the wood plane . . . . .	60
4.24	Radiation efficiency and Central frequency variation with the wood plane . . . . .	61
4.25	Q and resonance BW vs the distance between the ground plane and the radiator element of the antenna. . . . .	61
4.26	Q and BW depending on the Feed point position . . . . .	62
A.1	List of chips by manufacturer . . . . .	74
A.2	ST's DVB-H receiver chip [8] . . . . .	75

A.3	Microtune's DVB-H receiver chip [7]	76
A.4	Microtune's DVB-H receiver chip part 2 [7]	77
A.5	Paradiso's DVB-H receiver chip [6]	78
A.6	TI's DVB-H receiver chip part 1 [5]	79
A.7	TI's DVB-H receiver chip part 2 [5]	80
B.1	List of cell-phones with DVB-H capability by manufacturer	82
C.1	Typical scenario for the different radio propagation models used	84
C.2	Two ray model vs Free Space model	86
C.3	2-Ray model modeled as free space model before the breakpoint	87
C.4	Rural outdoor Okumura-Hata model compared to 2-ray model (outdoor) and Egli model (outdoor)	87
C.5	All Okumura-Hata scenarios (indoor, outdoor, incar compared with rural, urban and suburban)	88
C.6	Okumura-Hata Incar Scenario	89
C.7	Okumura-Hata Indoor Scenario	90
C.8	Okumura-Hata Outdoor Scenario	91
C.9	Okumura-Hata Rural Scenario	92
C.10	Okumura-Hata Suburban Scenario	93
C.11	Okumura-Hata Urban Scenario	94
C.12	Okumura-Hata Urban vs Suburban Scenario	95
C.13	Okumura-Hata Urban vs Rural Scenario	96
C.14	Okumura-Hata Urban vs Suburban Scenario	97
D.1	Smith Chart	98
D.2	Powers versus load resistance	99
E.1	Structure of PIFA Antenna	100
E.2	Comparison of Frequency vs L2 when different W are used	102
F.1	First case of Matching L-network	103
F.2	Second case of Matching L-network	104
G.1		106
G.2		107
G.3		108
G.4		109
G.5		110
G.6		111
G.7		112

# Table of Abbreviations

<b>DVB-T</b>	Digital Video Broadcast Terrestrial
<b>DVB-H</b>	Digital Video Broadcast Handheld
<b>OFDM</b>	Orthogonal Frequency-Division Multiplexing
<b>MPE-FEC</b>	MultiProtocol Encapsulation-Forward Error Correction
<b>MPEG-2</b>	Movies Pictures Expert Group
<b>IP</b>	Internet Protocol
<b>PID</b>	Program Identifier
<b>RF</b>	Radio Frequency
<b>RS</b>	Reed-Solomon
<b>ES</b>	Elementary Stream
<b>CRC</b>	Cyclic Redundancy Check
<b>C/N</b>	Carrier to Noise Ratio
<b>ISI</b>	Inter-Symbol Interference
<b>ICI</b>	Inter Carrier Interference
<b>CP</b>	Cyclic Prefix
<b>BER</b>	Bit Error Ratio
<b>QAM</b>	Quadrature Amplitude Modulation
<b>LOS</b>	Line of Sight
<b>HF</b>	High Frequency
<b>VHF</b>	Very High Frequency
<b>UHF</b>	Ultra High Frequency
<b>GSM</b>	Global System for Mobile Communications
<b>DCS</b>	Digital Communications system
<b>PCS</b>	Personal Communications System
<b>UMTS</b>	Universal Mobile Telecommunication System
<b>PIFA</b>	Planar Inverted-F Antenna
<b>FDTD</b>	Finite Difference Time Domain
<b>I/Q</b>	Amplitude of the “In-Phase Carrier”/Amplitude of the “Quadrature Phase Carrier”
<b>DAC</b>	Digital Analog Converter
<b>ADC</b>	Analog Digital Converter
<b>CP</b>	Cyclic Prefix
<b>IFFT</b>	Inverse Fast Fourier Transformation

## Appendix A

# List of receiver chips of DVB-H by manufacturer

This annex shows the list of receiver chips by manufacturer. The main pages of each data sheet are also included. It is important to note that Analog Devices does not have a public data sheet or whatsoever, for more information on their chip look at [9].

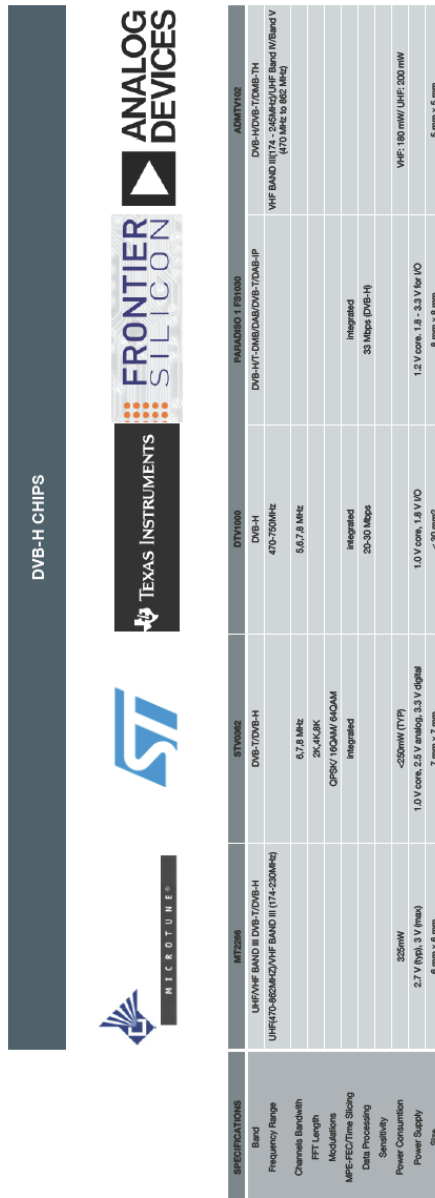


Figure A.1: List of chips by manufacturer



## STV0362

### Low-power and ultra compact DVB-T single chip receiver DVB-H broadcast compliant

Data Brief

#### Feature summary

- NorDig Unified specification (v1.0.2) capable
- Channel reception quality indicator
- Out-of-guard interval echoes superior performances
- Impulsive noise rejection capable
- Outstanding adjacent and co-channel rejection capability with integrated on-chip digital channel filters
- Digital carrier, timing and symbol recovery loops
- 2 K, 4 K, 8 K FFT length
- 6, 7 and 8 MHz channels bandwidth
- 1/4, 1/8, 1/16, 1/32 guard interval length
- QPSK - 16 QAM - 64 QAM modulations
- Hierarchical capability
- TPS decoding
- Viterbi soft decoder rate 1/2
- Puncture rates are 1/2, 2/3, 3/4, 5/6, 7/8
- Low power advanced CMOS process (90 nm)
- Power consumption: <250 mW (typ) in operation
- Multi-supply: 1.0 V core, 2.5 V analog, 3.3 V digital
- TQFP64 7 x 7 x 1.0 mm.

#### Order codes

Part number	Package
STV0362	TQFP64 (7 x 7 x 1 mm)

#### Description

The STV0362 inherits the functionality of the STV0361 device and embeds new functionalities required by the DVB-H standard at the physical layer side. The STV0362 features the full DVB-T and DVB-H standards framing structure, channel coding and modulation. The symbol, timing and carrier recovery loops are fully digital and sized in order to match the state-of-the-art RF down-converter devices.

The STV0362 is compatible with direct conversion silicon tuners and is featuring two high-performance differential 12-bit ADC for I and Q channels. The tuner baseband power is controlled by a classic AGC loop, and the RF level is monitored by a dedicated single-ended 8-bit ADC.


The terrestrial DVB-T network can be subject to several interference sources which are the neighboring digital and analog channels, as well as the in-band analog channels. The STV0362 cancels these interference sources and removes the effects of impulse noise. The channel equalization is capable of static and dynamic echo canceling even in severe urban environments.

The embedded high-performance algorithms are enhanced to cope with out-of-guard interval echoes; specific channel quality monitoring is available for acquisition and survey.

The specific power handling constraints are primarily addressed by both technology and clock rate management. The efficiency of channel acquisition and re-acquisition also minimizes power consumption.

The STV0362 relies on the decoder multimedia processor to manage the MPE-FEC and to control time slicing while operating in DVB-H mode.

Figure A.2: ST's DVB-H receiver chip [8]




**MICROTUNE®**

RF SILICON AND SUBSYSTEMS SOLUTIONS  
FOR BROADBAND COMMUNICATIONS AND AUTOMOTIVE ELECTRONICS

---

**MT2266 SINGLE-CHIP  
DUAL-BAND LOW-POWER  
DVB-T / DVB-H TUNER**  
PRODUCT BRIEF

The MT2266 is a direct conversion low-power single-chip broadband tuner for VHF Band III and UHF applications.



*MT2266 Single Chip Dual-Band Tuner*

The MicroTuner™ MT2266 is a direct conversion, low-power, single-chip broadband tuner optimized for UHF and VHF Band III DVB-T and DVB-H applications. It includes all active circuitry required to implement the complete RF-to-Baseband tuner function.

The MT2266 has been developed to give manufacturers design flexibility and low operating power, at low cost, without compromising high performance.

The MT2266 is capable of receiving UHF band and VHF Band III frequencies, enabling manufacturers to target low-power portable and low-power PCTV devices.

The combination of power management, choice of architecture, and Microtune's patents-pending ClearTune filtering technology enables the MT2266 to operate at 325 mW.

High-volume consumer markets demand low-cost products. The MT2266 was designed for low cost. The single-ended direct conversion architecture eliminates the need for baluns at the RF inputs and costly IF SAW filters. To further reduce cost and power, the UHF and VHF Band III variable gain low noise amplifiers (VLNA) and the voltage controlled oscillators (VCO) are fully integrated.

The transmission environment for mobile TV is extremely hostile. Microtune's unique patents-pending ClearTune filtering technology and the excellent performance of MT2266 will help to ensure that end users will have a superior mobile TV experience without picture interruption in the middle of tall buildings or hostile radio environments.

**APPLICATIONS**

- Portable DVB-T receivers
- PC-TV
- Notebook computer
- Dual-standard (DVB-T/DVB-H) media platforms
- Personal multimedia consoles
- PDA TV
- General DVB-T TV applications

**FEATURES**

- Fully compliant with NorDig Unified V1.0.2 and MBRAI specifications
- Integrated variable gain low noise amplifier (VLNA)
- Integrated voltage controlled oscillator (VCO)
- No RF input balun required
- No IF SAW filters required
- Low cost BOM
- 470 MHz to 862 MHz UHF frequency range
- 174 MHz to 230 MHz VHF band III frequency range
- 2.7V power supply
- Multiple power-down options
- Direct demodulator interface
- Minimal external components
- No tunable parts required
- Low phase noise for excellent COFDM performance
- One general purpose output controllable via serial control interface
- Operation with a crystal range of 8-38.4 MHz
- Crystal Oscillator LVDS or CMOS output for driving a DVB-T demodulator
- Small 6mm x 6mm 40-pin QFN package

Figure A.3: Microtune's DVB-H receiver chip [7]



**MT2266 SINGLE CHIP DUAL-BAND LOW POWER DVB-T/DVB-H TUNER**  
**PRODUCT BRIEF**

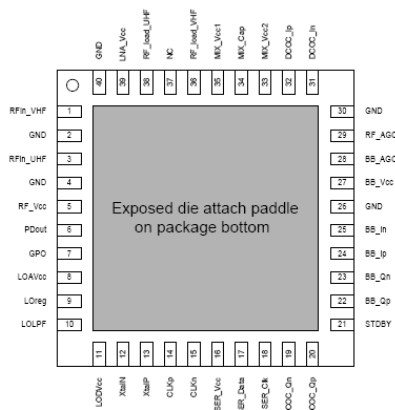
**RECOMMENDED OPERATING CONDITIONS**

PARAMETER	MIN	TYP	MAX	UNIT
UHF input frequency range	470		862	MHz
VHF III input frequency range <sup>1</sup>	174		230	MHz
Supply voltage	2.6	2.7	3.0	V
Supply voltage ripple			15	mV
Operating junction temperature	0		100	°C

1. Will also support operation at other VHF III frequency ranges with external components change.

**ABSOLUTE RATINGS**

PARAMETER	MIN	MAX	UNIT
Supply voltage		3.6	V
Storage temperature	-50	150	°C
Lead-free solder temperature for 5 seconds		260	°C
Relative humidity		95	%



MT2266 Pin Diagram

Figure A.4: Microtune's DVB-H receiver chip part 2 [7]

## Paradiso 1 FS1030

Mobile TV multistandard baseband IC for T-DMB and DVB-H





Compact footprint - 8.0 x 8.0 x 1.0 mm

### APPLICATIONS

- Mobile phone with TV
- Personal media player
- Automotive infotainment system
- Mobile/portable TV terminal
- Portable DVD player
- Mobile TV dongle
- Mobile TV enabled laptop/PC

### OVERVIEW

Paradiso 1 is an advanced multistandard baseband receiver, enabling mobile TV, audio and data services on handheld devices for worldwide markets, with industry-leading performance, size and cost.

Supporting all DVB-H, DVB-T, DAB, T-DMB and DAB-IP modes, including Chinese, European and Korean, Paradiso 1 is designed to be used with a host media processor and an RF front-end such as the Frontier Silicon *Apollo*.

Paradiso 1 offers **unmatched flexibility**, with features such as advanced Doppler and multipath channel performance, integrated RAM, variable IP stream rates, support for conditional access, and a comprehensive set of peripheral interfaces, simplifying system integration.

**Host processor interfaces** include SPI, SDIO and USB 2.0. The software data plane supports streaming outputs for TS, FIC, MSC, PSI/SI and IP data payloads. The software control plane supports remote boot and optimized baseband control. All interfaces are flexible to facilitate custom host communication protocols. Paradiso 1 can boot, stream data and be controlled through any of the above host processor interfaces, simplifying design and deployment; additional boot and control options are available through UART and SCP.

Paradiso 1 uses a 1.2 V core **power supply**, and 1.8 - 3.3 V for I/O. This can be implemented using a single 1.8 - 3.3 V input with the integrated SMPS controller, simplifying design of non-cellular products.

### KEY FEATURES

- Advanced IC for all DVB-H, T-DMB, DAB, DVB-T and DAB-IP applications
- 8 x 8 x 1 mm ultrastim 132-pin VFBGA package for slim-phones and low-profile devices
- Low power operation with advanced power management
- Supports numerous DMB variants including T-DMB, DxB, DAB-IP and BT Movio
- Enhanced packet and enhanced data group modes
- PID filtering with additional IP filtering
- Dual ADC with analog input mux supports ZIF/LIF interfaces to both single- and multi-standard tuners
- Flexible hardware-assisted DSP architecture
- Decodes multiple video, audio and data services up to maximum 1.8 Mbps (T-DMB) or 33 Mbps (DVB-H)
- Programmable communication processor has capacity for the most demanding digital receiver standards
- Flexible transport interface for data transfer to multiple video decoders
- On-chip MPE-FEC and Reed-Solomon decoder for best mobile channel performance
- Data service support to the host processor
- Supplied complete with *DeNiro* host drivers and embedded firmware
- Full evaluation system available, with flexible modular design to accept a choice of T-DMB, DVB-H and multistandard tuner ICs
- Integrated SMPS for single 1.8 - 3.6 V supply
- Wide temperature range:
  - Operation -40 to +85 °C;
  - Storage -60 to +125 °C
- Full RoHS compliance

Figure A.5: Paradiso's DVB-H receiver chip [6]


 <b>TEXAS INSTRUMENTS</b>	<b>Technology for Innovators™</b>
<h3 style="margin: 0;">Hollywood™ mobile broadcast single-chip solutions: DTV1000 and DTV1001</h3>	
	<p><u>Key features</u></p> <ul style="list-style-type: none"> <li>• First mobile DTV single chip solution—integrates RF, demod, decoder and memory</li> <li>• World's smallest footprint package—less than 30 mm<sup>2</sup> resulting in low-cost BOM</li> <li>• Low-Power Design—90 nm RF CMOS design, low 1-V core design</li> <li>• Both DVB-H (DTV1000) and ISDB-T (DTV1001) products available</li> <li>• Fast time-to-market: Development platform OS agnostic driver and API integration package</li> </ul>
<b>P R O D U C T B U L L E T I N</b>	
<p><i>Overview</i></p>	<p>Texas Instruments' (TI's) Hollywood™ family of mobile digital broadcast products provides the first ever single-chip solutions for mobile DTV standards DVB-H (DTV1000) and ISDB-T (DTV1001). Using TI's industry leading DRP™ technology, the Hollywood chips enable a single low-voltage CMOS design. TI's Hollywood solutions also simplify integration by adding intelligence to the mobile DTV chip thereby off-loading takes from the host processor (digital cellular baseband or application processor).</p>
<p><i>Product features</i></p>	<p><b>Smallest solution footprint—smaller product design</b></p> <ul style="list-style-type: none"> <li>• Single-chip solution, less than 30 mm<sup>2</sup> package</li> <li>• 51 mm<sup>2</sup> for base line configuration</li> <li>• No external memory required</li> </ul> <p><b>Low bill-of-materials count—lower solutions cost</b></p> <ul style="list-style-type: none"> <li>• Single chip—Low part count keeps solution cost low</li> <li>• Integrated LDOs and VCO/PLL (only 1 voltage and clock source needed)</li> <li>• No external memory, keeps solution cost low</li> <li>• Single-ended RF LNA (no external balun)</li> </ul> <p><b>Low power consumption—longer view time</b></p> <ul style="list-style-type: none"> <li>• Integrated data, programmable memory leads to lower power</li> <li>• Integrated on-chip smart power control—6 power modes</li> <li>• Single-chip design reduces chip-to-chip I/O consumption</li> <li>• Low 1.8 voltage peripherals and 1-volt core</li> </ul> <p><b>Reduced time-to-market</b></p> <ul style="list-style-type: none"> <li>• Common high-speed serial interfaces (SPI and SDIO)</li> <li>• Tuning, hand-over control and power control handle on chip</li> <li>• Complete SPI/SDIO driver and API sourced code package</li> <li>• Reference Development Board (RDP) available</li> <li>• Compact module available through module vendor</li> <li>• PC-based diagnostic and data/message logging tools</li> </ul>



Figure A.6: TI's DVB-H receiver chip part 1 [5]

**DTV100x specifications**

**High performance—ready for broadcaster service rollout**

- Support for 2 concurrent Elementary Streams and 8 IP filters
- 20 to 30 Mbps data processing throughput
- High sensitivity RF and low-noise figure
- Harmonic rejection filters for improved interference rejection

**Standards and bands supported**

- DVB-H: 470-750 MHz and 1.67 GHz
- ISDB-T 1-seg: 470-770 MHz
- Tunable 0.5 MHz (ISDB-T) bandwidth modes
- Tunable 5, 6, 7, 8 MHz (DVB-H) bandwidth modes

**Embedded system memory**

- MPE-FEC and Link-Layer Buffering on chip
- Built-in program and data RAM for ARM

**Host data and control interfacing**

- 48-MHz SPI
- 4-bit 25 MHz SDIO
- Driver, API source code

**Antenna control**

- 10 programmable GPIOs
- 1.8-V PWM

**Diagnostic and debug interfaces**

- PC direct connect to UART
- Also via host

**Reference input clock**

- 13, 15.36, 16.8, 19.2, 26, 38.4 MHz
- Other clocks internal

**Boot options**

- Downloaded via SPI/SDIO
- Boot loader provided

**Package and power management**

- Wafer Scale Package
- 88 balls, 0.5 mm ball pitch
- 1.8-V source (1-V core, 1.8 I/O)
- Green and lead-free compliant

**Operating temperature**

- -30°C to +85°C

Figure A.7: TI's DVB-H receiver chip part 2 [5]

## Appendix B

# List of cell-phones with DVB-H capability by manufacturer

In this chapter it is shown the different manufacturers that designed DVB-H receiver for Mobile Phone. The information have been obtained in the web page of the different chip builders.

APPENDIX B. LIST OF CELL-PHONES WITH DVB-H CAPABILITY BY MANUFACTURERS<sup>82</sup>

SPECIFICATIONS		NOKIA	NOKIA	NOKIA	NOKIA	LG	LG	LG	SAMSUNG	LG	HTC
Model	N77	182	N95	1980	1980	1980	1980	1980	EP10	6000	3399
Operating Frequency	Dual-mode, WCDMA2100/EGSM900/1800/1900 MHz or EDGE only; EGSM900/1800/1900 MHz; DVB-H 470-750 MHz	GSM 900/1800 and WCDMA 2100 networks; EDGE and DVB-H 470-750 MHz	WCDMA2100/1800/1900/1900 MHz; EGSM900/1800/1900 MHz; EDGE; DVB-H Class C, 470-750 MHz	WCDMA2100/1800/1900/1900 MHz; EGSM900/1800/1900 MHz; DVB-H	LIMITS - GSM/GPRS (900/1800/1900MHz) / HSPA, DVB-H	LIMITS - GSM/GPRS (900/1800/1900MHz) / HSPA, DVB-H	LIMITS - GSM/GPRS (900/1800/1900MHz) / DVB-H	LIMITS - GSM/GPRS (900/1800/1900MHz) / DVB-H	DVB-H - LIMITS - GSM/GPRS (900/1800/1900MHz)	GSM 850/900/1800/1900, GPRS Class 10, DVB-T / DVB-H / T-DMB	GSM 900/1800/1900
Size	114.5 (11) x 49 mm	191 x 107.4 x 18.2 mm	125 x 111 x 10 mm	103.9 x 52 x 10.7 mm	100.6x50.6x7.4 mm	102 x 42.6 x 13.3 mm	102 x 42.6 x 13.3 mm	97.6x50.7 x 4 mm	97.6x50.7 x 4 mm	110 x 56.5 x 18.5 mm	114x50x15.2mm
Battery	Mobile TV watch time, up to 3.0 hours	1000mAh	1000mAh	Normal (1000mAh)	970 mAh	950mAh	950mAh	1000 mAh	1000 mAh	1000 mAh	1100 mAh
Display	2.4"	2.8"	2.8"	2.2"	2.2"	2.4"	2.4"	2.2"	2.2"	2.6"	2.2"
Antenna	Internal	Internal	Internal	Internal	Internal	Internal	Internal	external	external	internal	internal

Figure B.1: List of cell-phones with DVB-H capability by manufacturer

## Appendix C

# Radio-propagation models

In this appendix some of the most common and simple radio-propagation models are explained. More exactly the models explained are the Okumura - Hata model, the Egli model and then the Free Space model (Friis equation [37]) as a base the two ray model is explained. All the models that are exposed have common parameters which are:

$P_R =$	<i>Reception Power</i>
$P_T =$	<i>Transmission Power</i>
$G_R =$	<i>Reception Antenna Gain</i>
$G_T =$	<i>Transmission Antenna Gain</i>
$f =$	<i>Frequency</i>
$d =$	<i>Distance</i>
$h_T =$	<i>Height of the transmitting antenna (m)</i>
$h_R =$	<i>Height of the receiving antenna (m)</i>
$\lambda =$	<i>Wavelength (m)</i>

The distance "d" between the transmitter and the receiver is expressed in km for the Okumura-Hata model and in meters in all the other models. Frequency is expressed in Hz for all the models except for the Okumura-Hata model where the frequency is expressed in MHz. The dimension of the other variables is already noted before for all the models. Figure [C.1] shows the typical scenario for the Okumura-Hata and free space models and also for the two ray model.

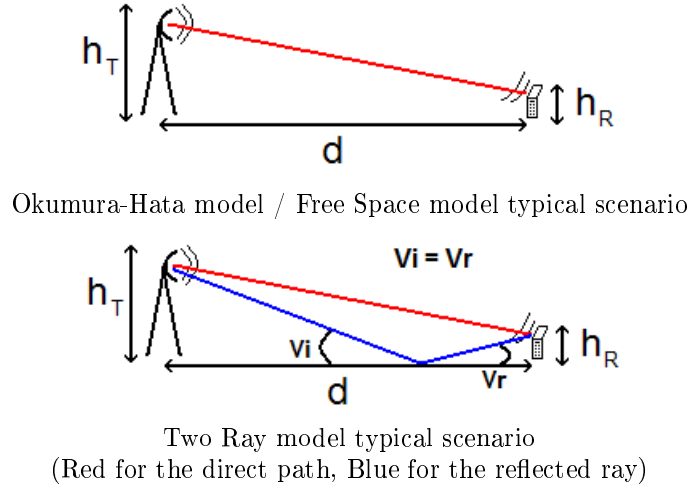


Figure C.1: Typical scenario for the different radio propagation models used

The first model explained is the Okumura-Hata which is a computation model that was first described as a result of empirical power measurements in Japan by Yoshihisa Okumura in 1968 in his publication "Field Strength and Its Variability in VHF and UHF Land-Mobile Radio Service" [34]. In 1980, Masaharu Hata simplified the considerations from Okumura and created the actual model ("Empirical formula for propagation loss in Land Mobile Radio Services" [35]). These simplifications led to the restriction that only regions with less than 20 km distance to the transmitter can be predicted.

Moreover, the model neglects the terrain profile between transmitter and receiver, i.e. hills or other obstacles between the transmitter and the receiver are not considered. As Hata and Okumura made the assumption that the transmitter would normally be located on hills, this was no disadvantage. Also phenomena like reflection and shadowing are not included. [36]. The model can be calculated as:

$$L_p(dB) = \begin{cases} A + B \log d & \text{urban} \\ A + B \log d - C & \text{suburban} \\ A + B \log d - D & \text{rural} \end{cases} \quad P_R = \frac{P_T G_T G_R}{L_P}$$

where:

$$B = 44.9 - 6.55 \log(h_T)$$

$$C = 2 \left[ \log \left( \frac{f}{28} \right) \right]^2 + 5.4$$

$$D = 4.78 [\log f]^2 - 19.33 \log f + 40.94$$

$$A = 69.55 + 26.16 \log f - 13.82 \log(h_T) - a(h_R)$$



$$a(h_R) = \begin{cases} (1.1 \log f - 0.7) h_R - (1.56 \log f - 0.8) & \textit{Little town} \\ 8.28 [\log(1.54h_R)]^2 - 1.1 & f \leq 400\text{MHz} \ \& \ \textit{Big city} \\ 3.2 [\log(11.75h_R)]^2 - 4.97 & f \geq 400\text{MHz} \ \& \ \textit{Big city} \end{cases}$$

and all the powers and gains are expressed in dBW or dBm and the gains in dBi. Another thing that can be extracted from the previous equations is the different kinds of areas. Actually Okumura describes three fundamental area types [34] [38]:

1. Urban: "Built-up city or large town crowded with large buildings and two-or-more-storied houses, or in a larger village closely interspersed with houses and thickly-grown tall trees."
2. Suburban: "Village or highway scattered with trees and houses - the area having some obstacles near the mobile radio car, but still not very congested."
3. Rural: "No obstacles like tall trees or buildings in the propagation path and a plot of land which is cleared of anything 300 to 400m ahead, as, for instance, farm-land, rice field, open fields, etc."

To calculate the results the equation has been introduced to an algebraic software such as Derive [23] which can evaluate the variables and give the answer of the equation easily.

The second model used is the Free Space model which is nothing else than the Friis equation [37]:

$$P_R = P_T G_T G_R \left( \frac{\lambda}{4\pi d} \right)^2$$

where the powers are expressed as Watts and the gains are dimensionless.

The third model used is the 2-ray model. This model is based on the line of sight between the transmitter and the receiver and considers that the receiver gets the signal from the direct path between both (receiver and transmitter) and also one reflection through the ground. For short distances the model oscillates because the addition of the 2 rays can be constructive or destructive depending on the phase. Moreover, when a certain distance is achieved (breakpoint) the model stops oscillating and decreases proportionally inverse to  $d^4$ .

Figure [C.2] shows this oscillations as a relative power gain  $\left( \frac{P_R}{P_T} \right)$  and compares the 2-ray model to the Free Space model (frequency = 586 MHz, transmitter antenna height = 100 m, receiver antenna height = 1.5 m, both antenna gains = 1). This figure has been obtained modifying a Matlab code obtained from [37] to suit the adequate frequency and antenna heights. The conclusion of the comparison between the two models is that the two ray model can be approximated using the free space model for short distances (before the breakpoint) if the power fadeouts are not considered.

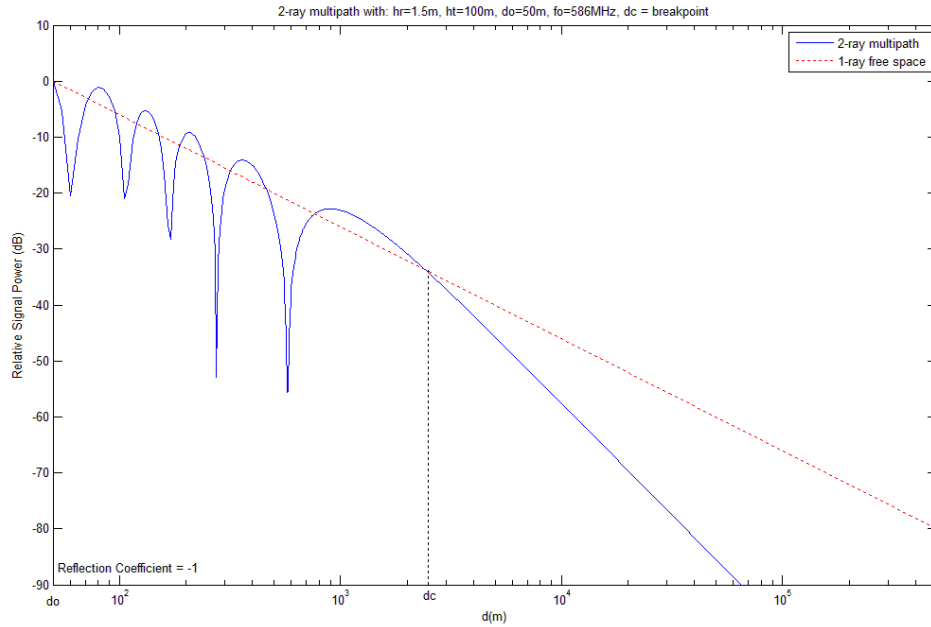


Figure C.2: Two ray model vs Free Space model

For long distances (after the breakpoint) the two ray model can be formulated as:

$$P_R = P_T G_T G_R \left( \frac{h_T h_R}{d^2} \right)^2$$

Actually, the breakpoint where the 2-ray model stops behaving like the free space model and starts behaving as the previous equation can be found using the following equation as it is the point where the two models (two ray for long distances and free space model) intersect:

$$d_c = \frac{4\pi h_T h_R}{\lambda}$$

Finally the Egli model has been used too. This model originates when in contrast to the theoretical two ray model, J.J. Egli measured a significant increase of the path loss with the carrier frequency "f" for ranges  $1 < d < 50$  km [38]. He proposed the next semi-empirical model:

$$P_R = P_T G_T G_R \left( \frac{h_T h_R}{d^2} \right)^2 \left( \frac{40}{f} \right)^2$$

Next all the additional graphic representations about the propagation models can be found.

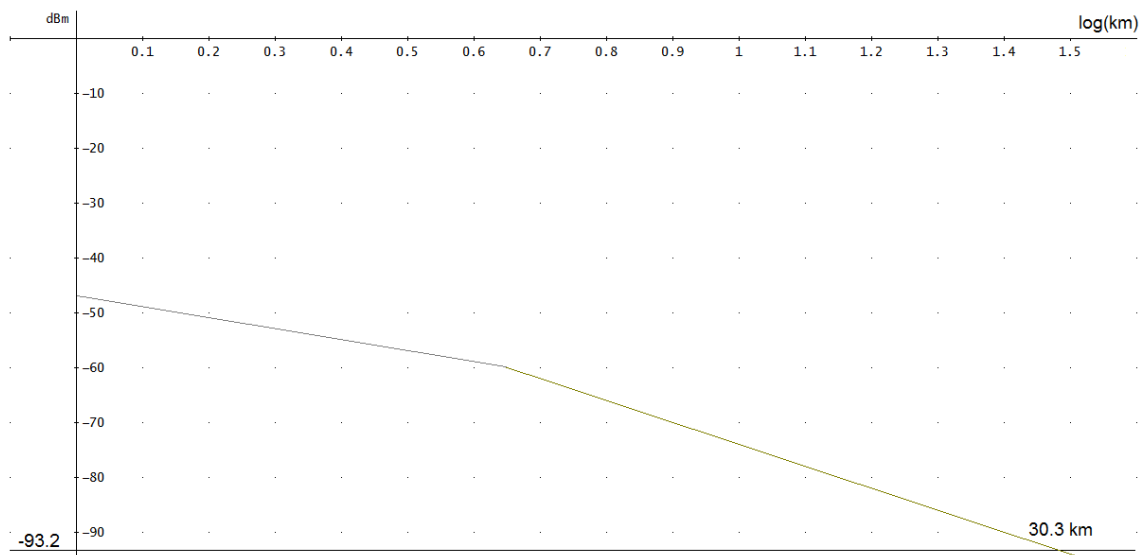


Figure C.3: 2-Ray model modeled as free space model before the breakpoint

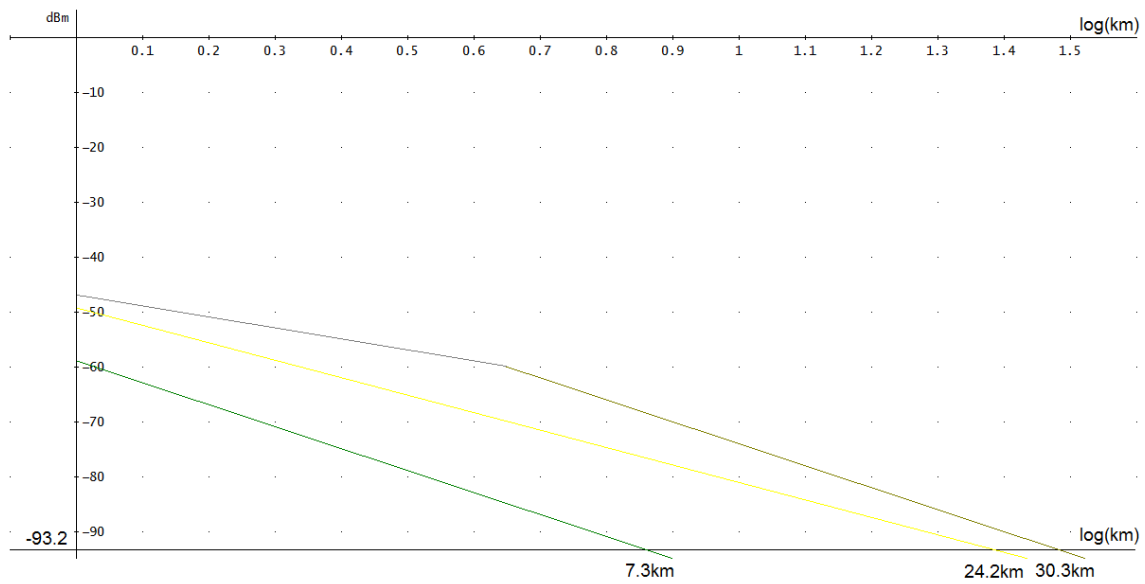


Figure C.4: Rural outdoor Okumura-Hata model compared to 2-ray model (outdoor) and Egli model (outdoor)

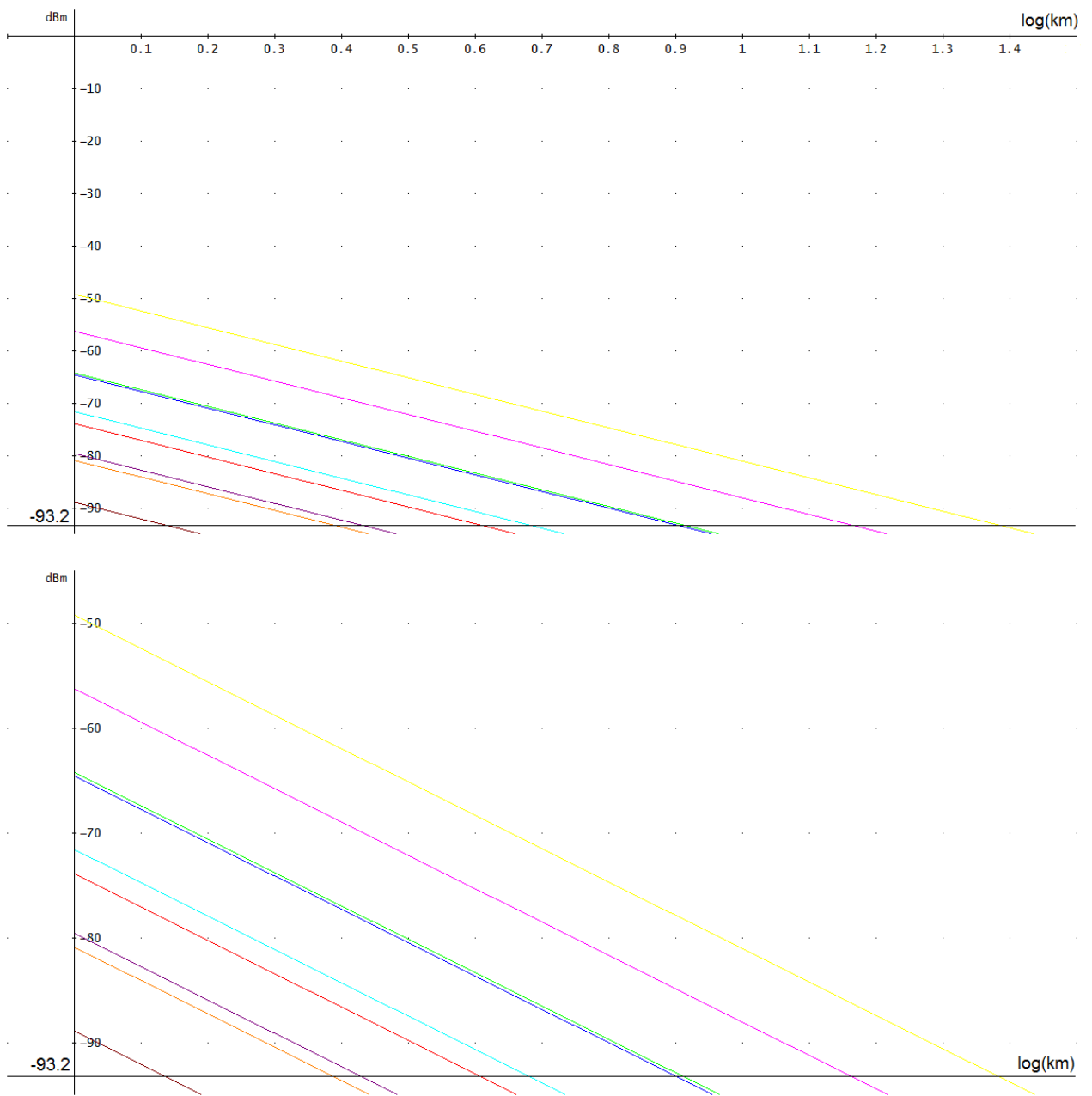


Figure C.5: All Okumura-Hata scenarios (indoor, outdoor, incar compared with rural, urban and suburban)

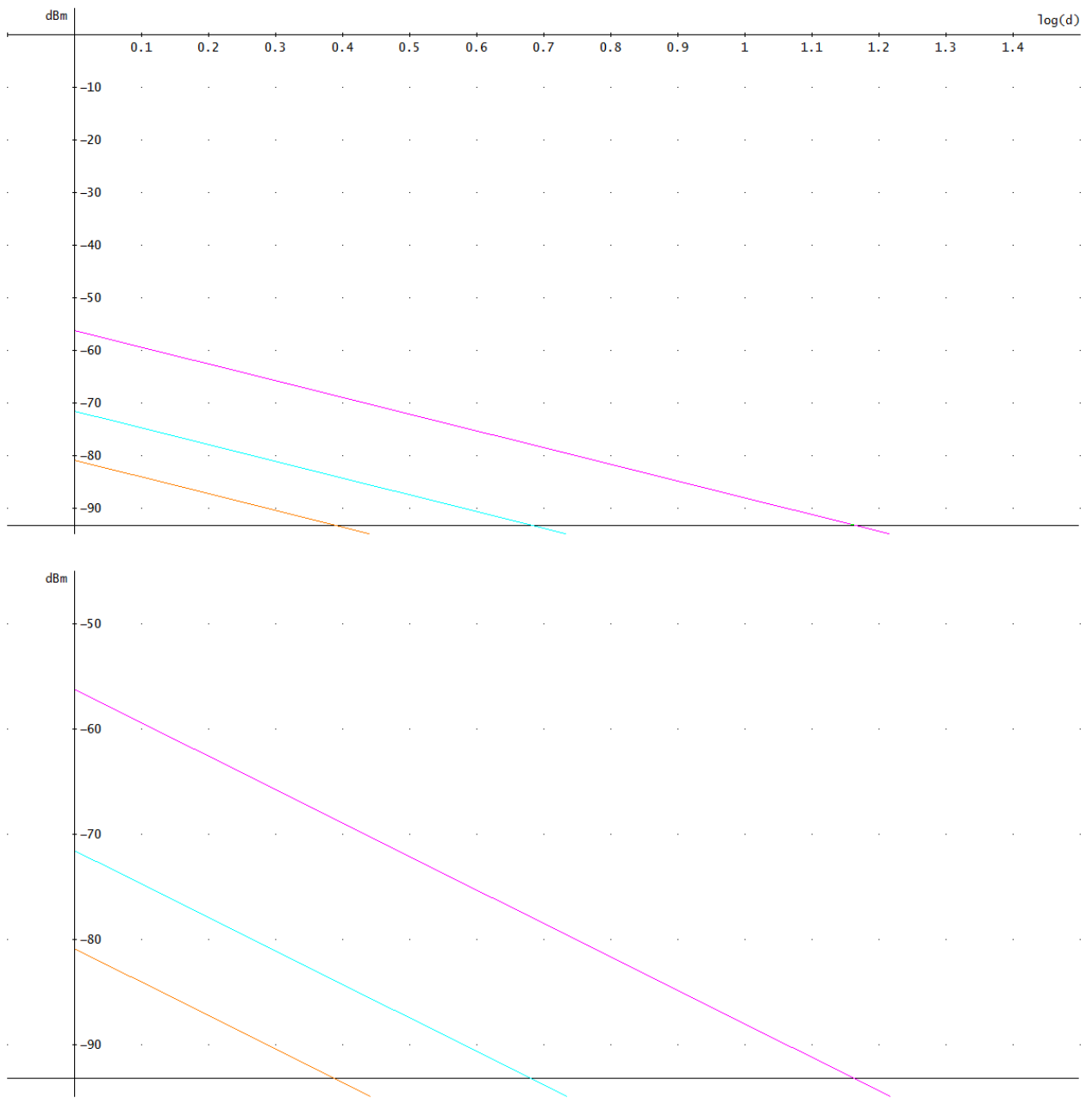


Figure C.6: Okumura-Hata In-car Scenario

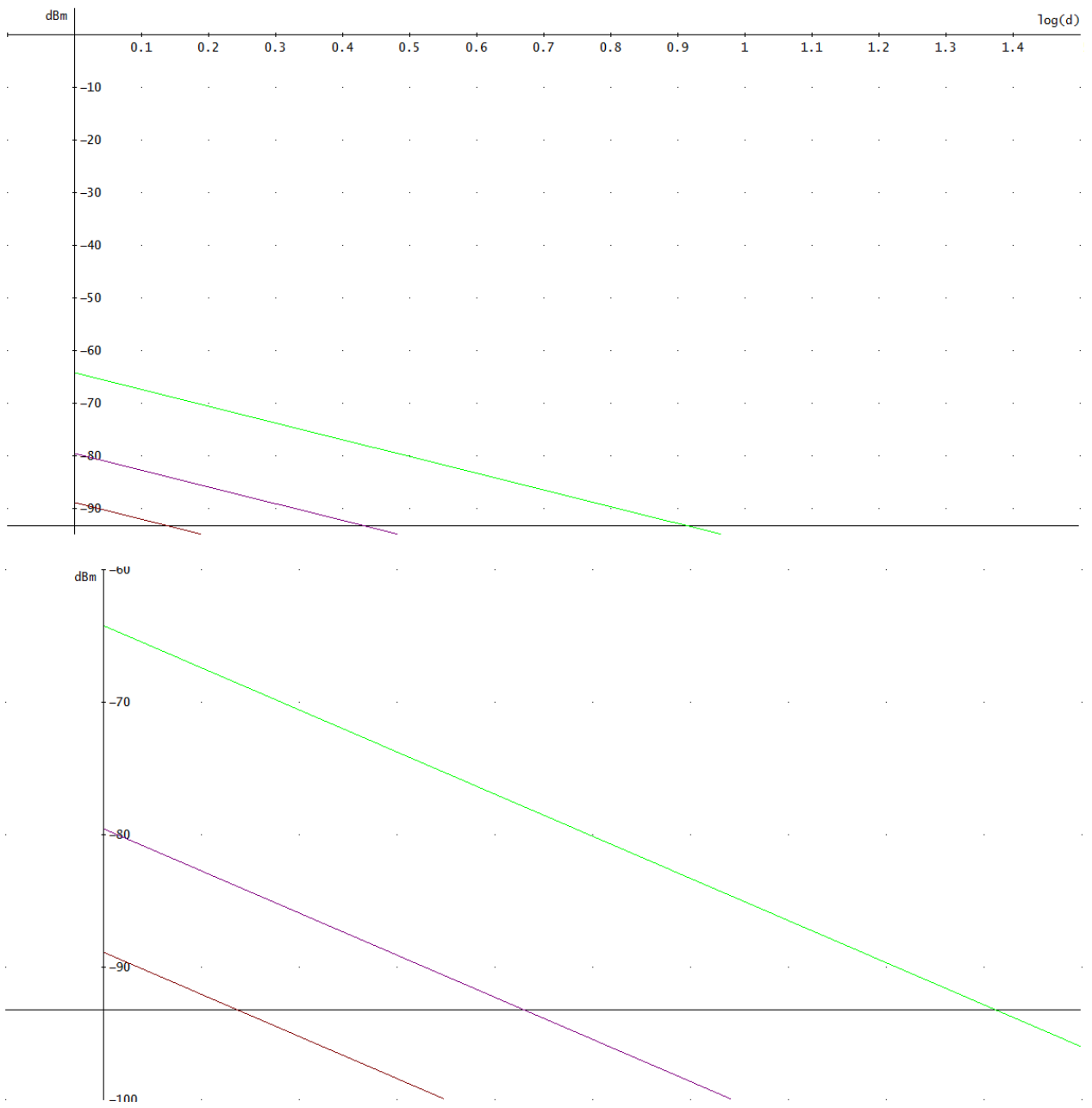


Figure C.7: Okumura-Hata Indoor Scenario

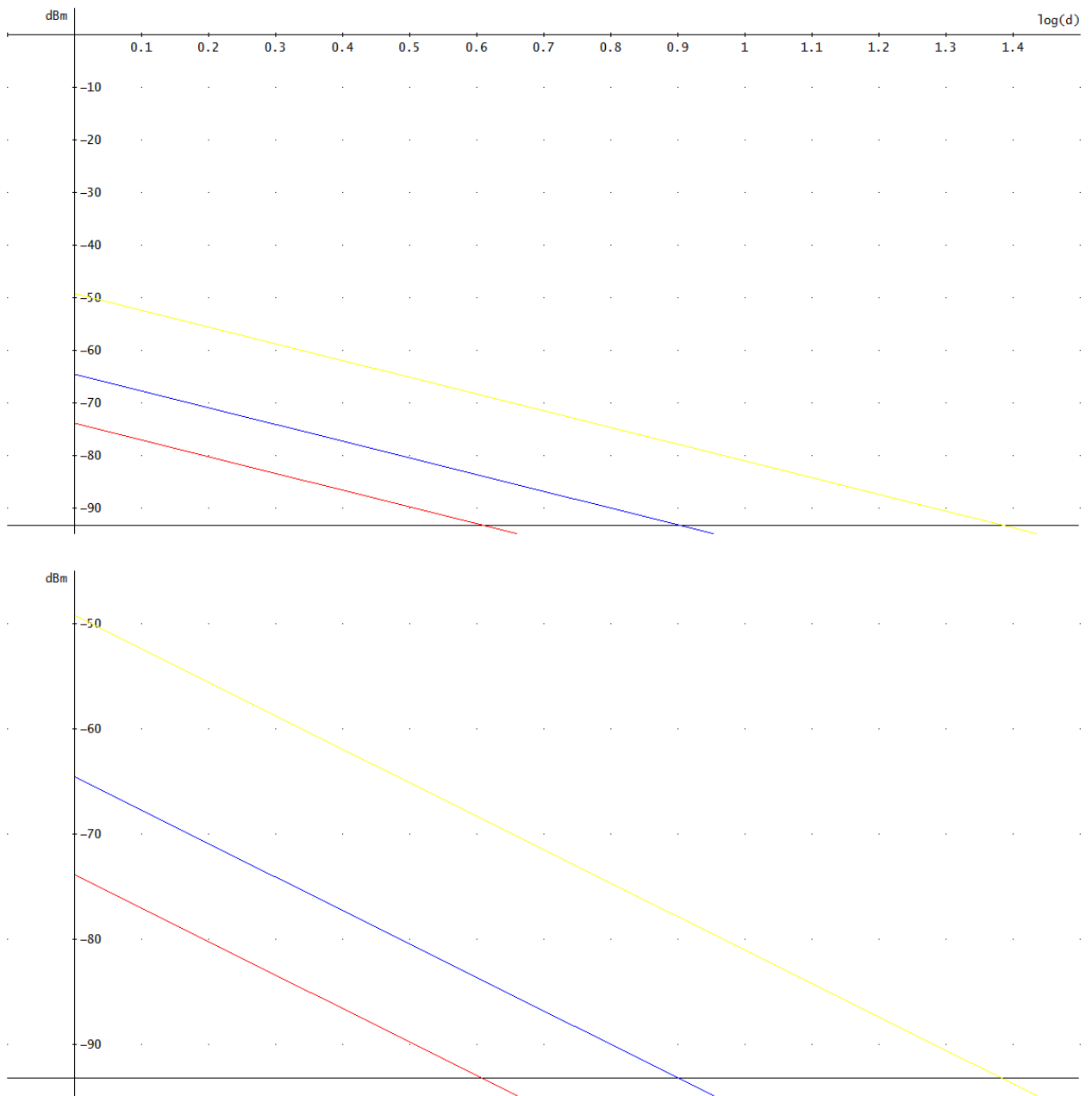


Figure C.8: Okumura-Hata Outdoor Scenario

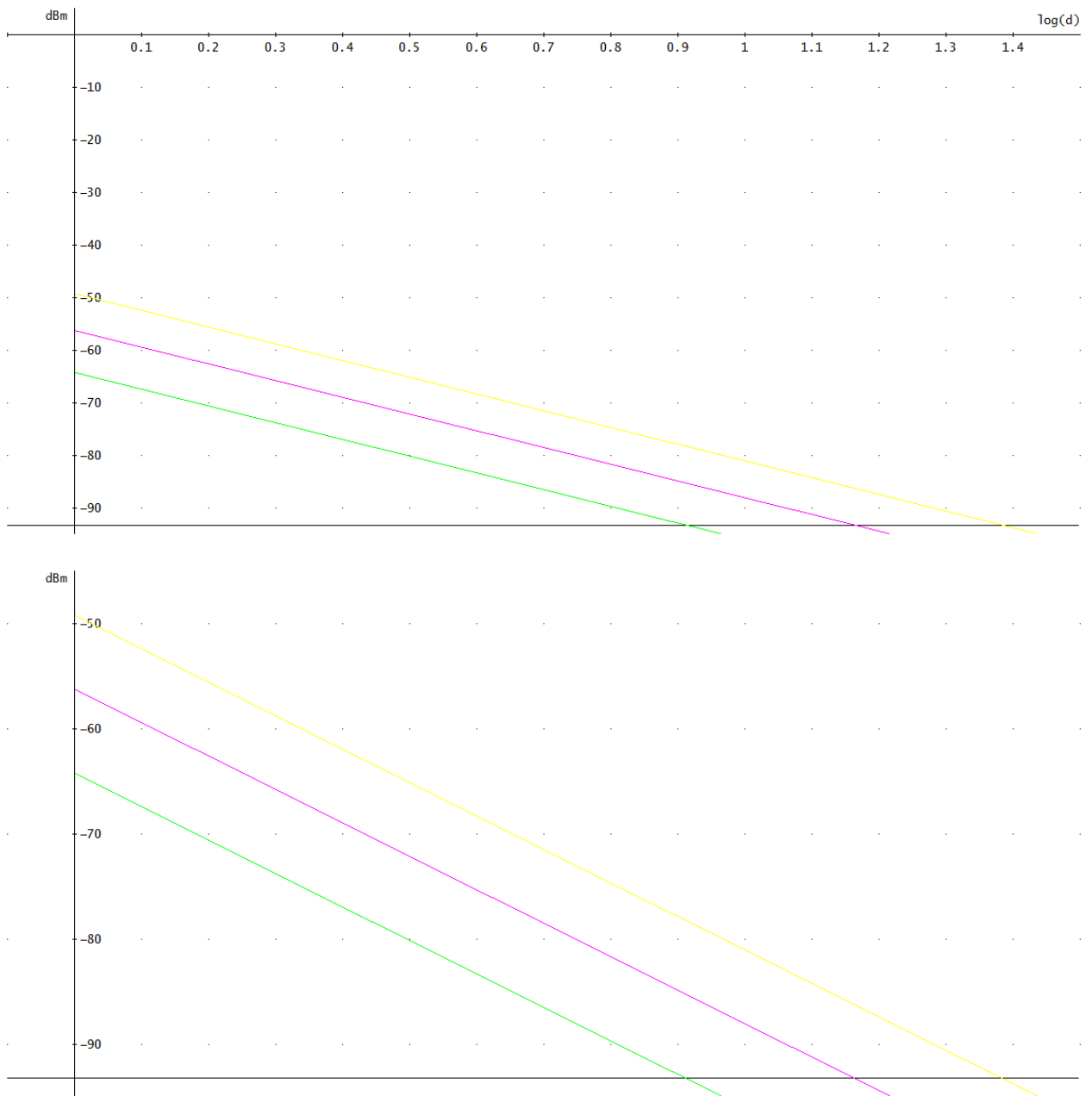


Figure C.9: Okumura-Hata Rural Scenario



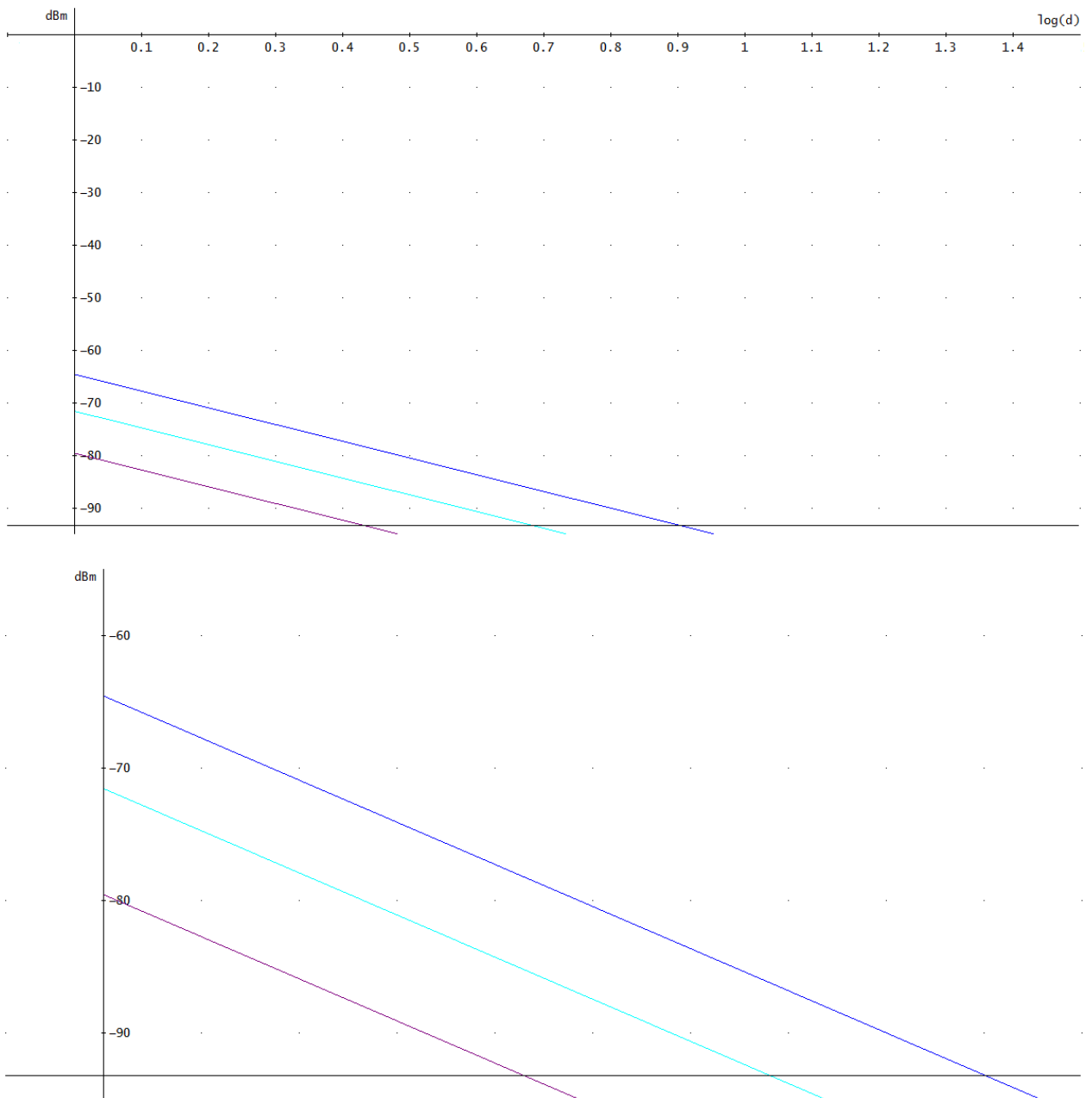


Figure C.10: Okumura-Hata Suburban Scenario

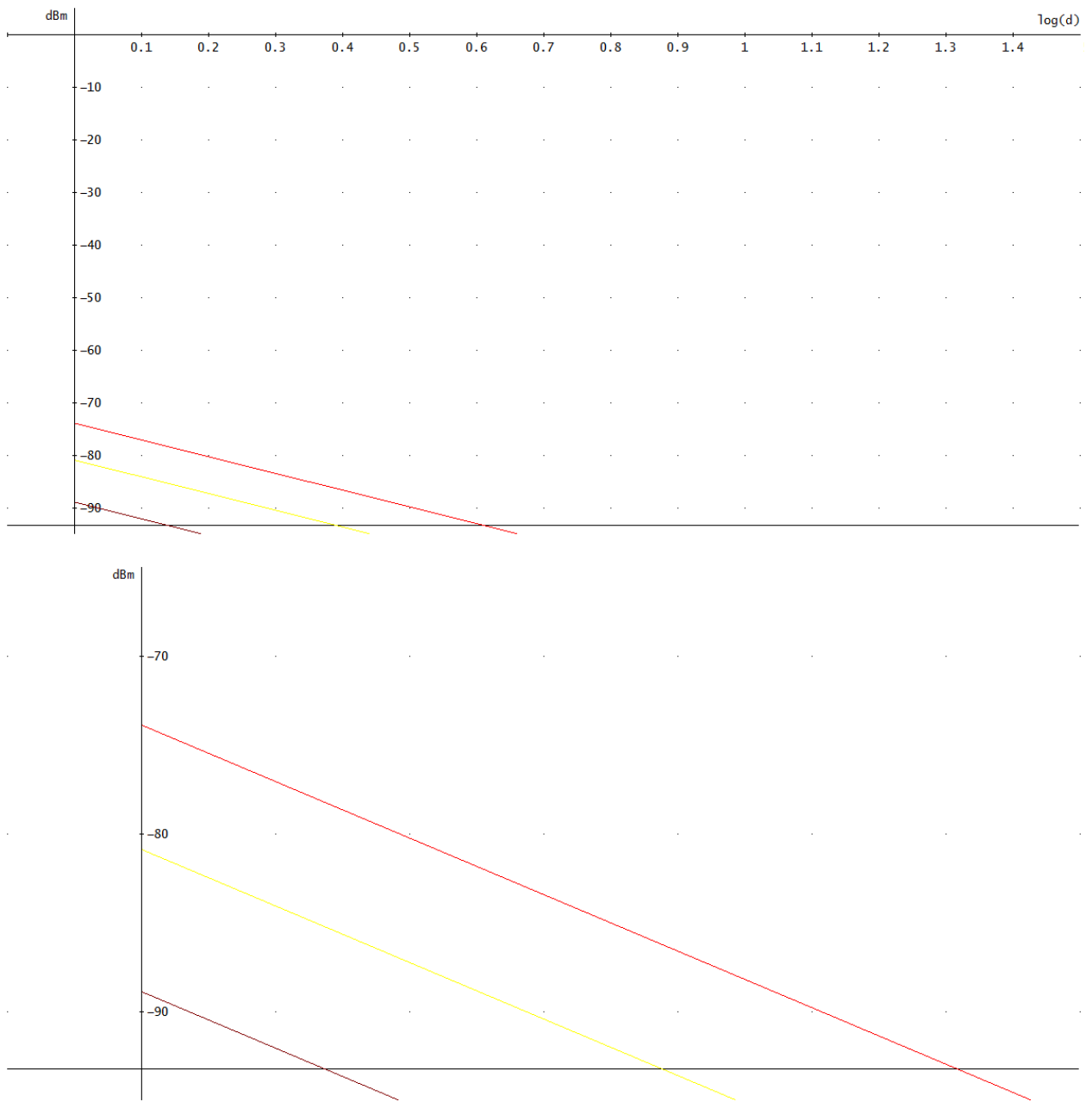


Figure C.11: Okumura-Hata Urban Scenario

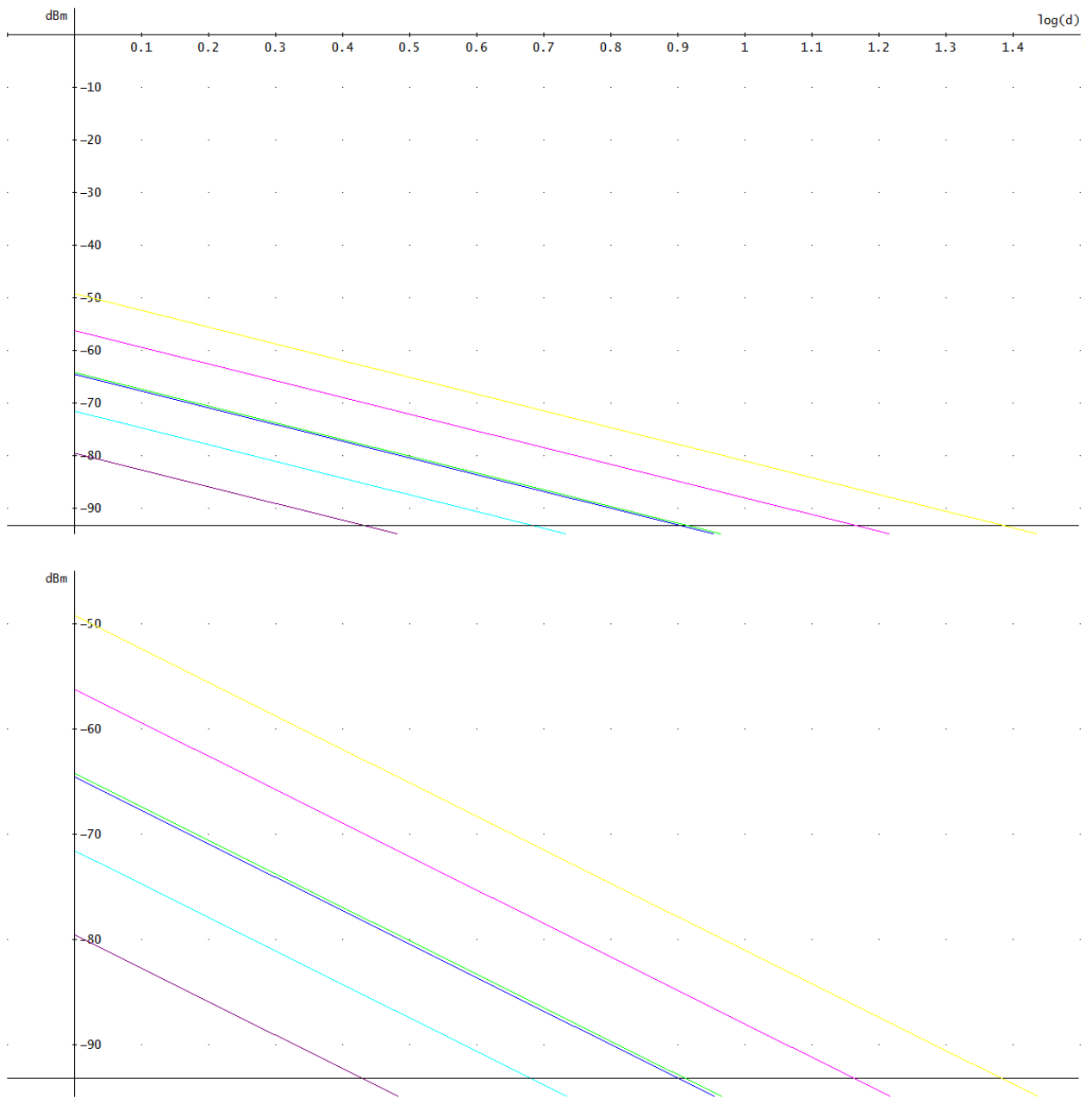


Figure C.12: Okumura-Hata Urban vs Suburban Scenario

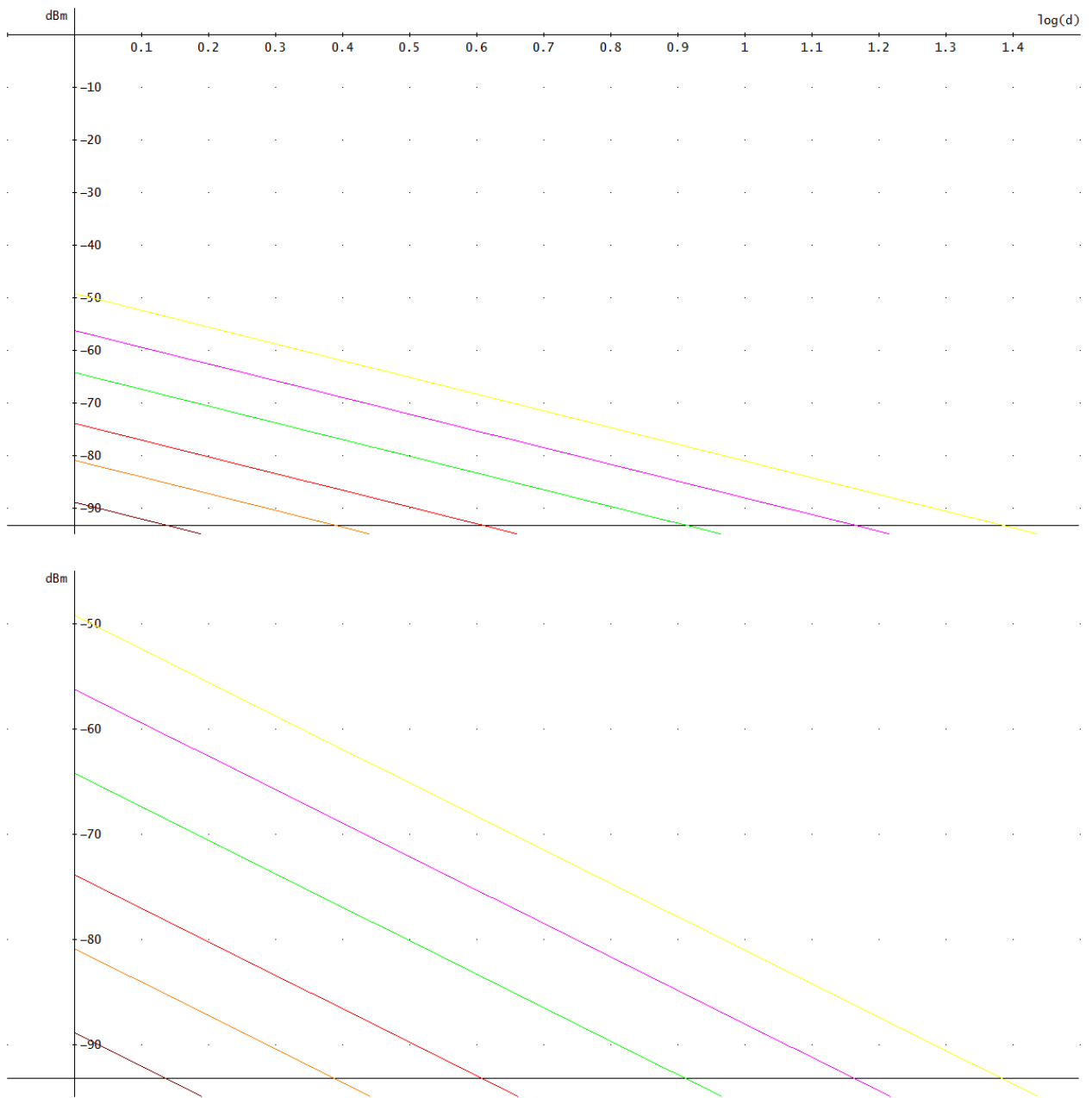


Figure C.13: Okumura-Hata Urban vs Rural Scenario

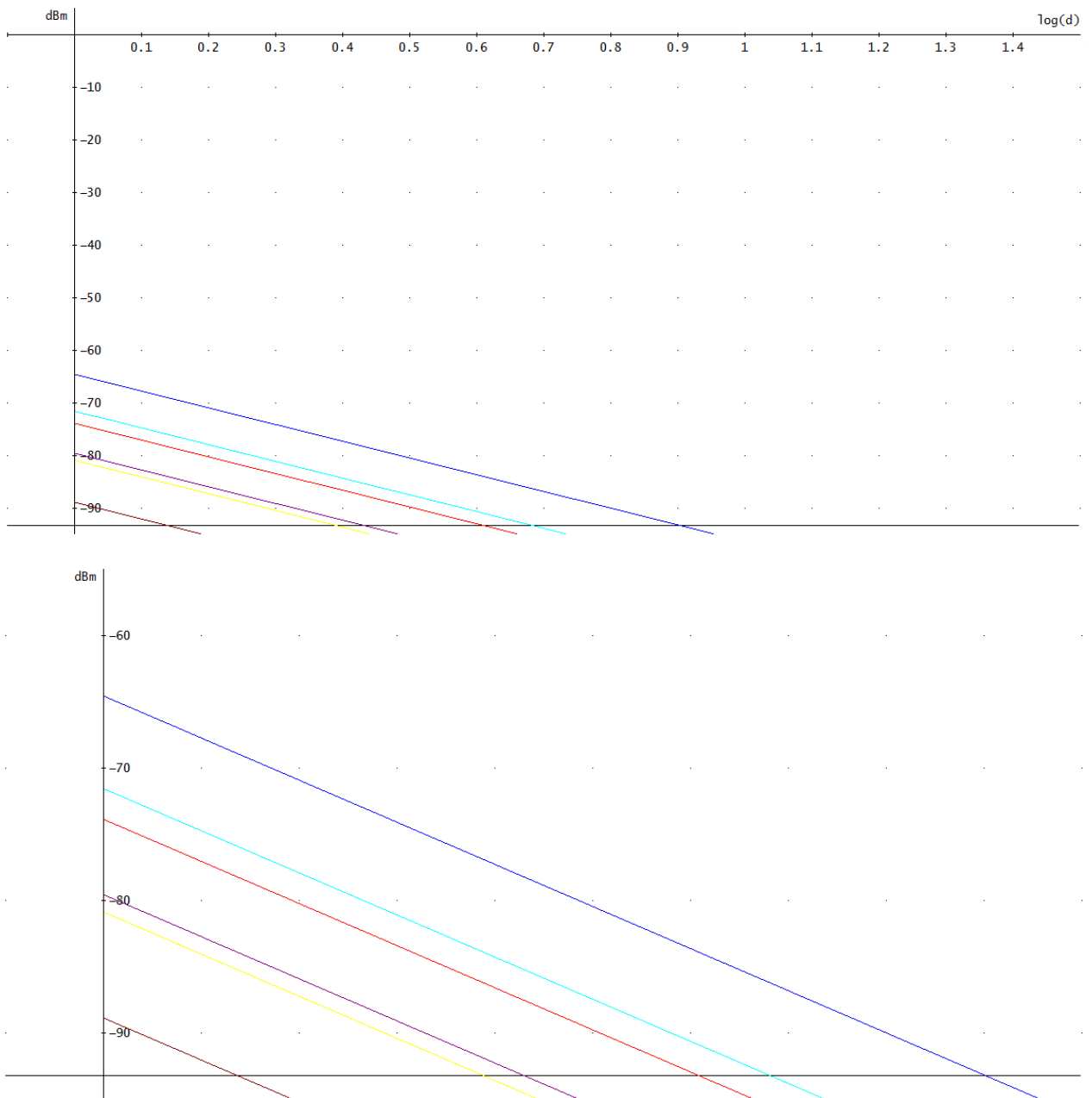


Figure C.14: Okumura-Hata Urban vs Suburban Scenario

# Appendix D

## Smith Chart

The first important output parameter of the simulations is the Smith Chart which is a representation of the resistance and the reactance in the logarithm scale graph. All this information has been extracted from [22].

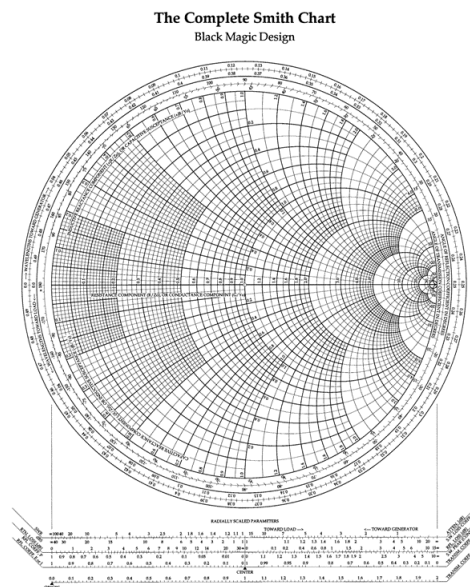


Figure D.1: Smith Chart

Thanks to this device, we can easily see if the load impedance  $R_L$  can be matched with the source impedance  $R_S$ . This matching parameter is really important in order to maximize the power transfer and also to minimize reflections. As read at the beginning of the chapter, the impedance is composed of the resistance (real part) and the reactance (imaginary part). In the ideal case, load and source resistance are in phase and the load reactance is in quadrature with the source one.

In the simple cases, the reactance is close to zero and so can be neglected and the impedance is considered as a pure resistance. If not, signal reflection occurs because of the imperfections in the cable which cause impedance mismatch. This reflection can be measured with the reflection coefficient:

$$\Gamma = \frac{R_L - R_S}{R_L + R_S}$$

Impedance discontinuities involve a degradation of the signal quality (attenuation, distortion...). The following graph displays the variation of power lost in the generator according to the variation of the load resistance. The ideal matched load resistance is determined when the power lost in the generator is equal to the power transferred to load. This matched resistance involves a maximization of the power transferred.

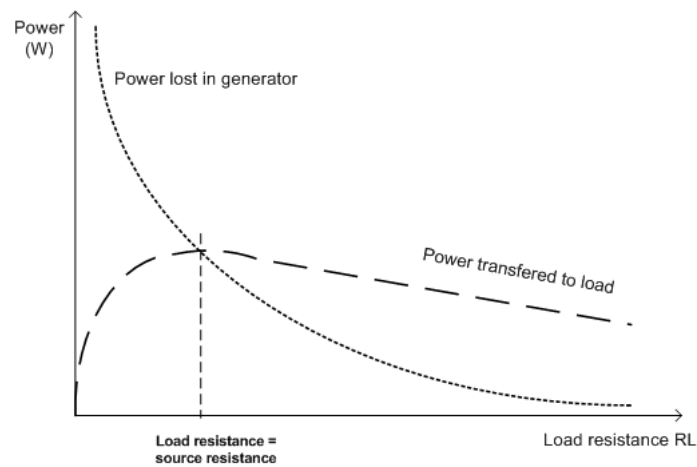


Figure D.2: Powers versus load resistance

Many radio frequency systems tend to use a  $50\Omega$  reference impedance.

## Appendix E

# Resonant frequency in PIFA antennas

In Planar Inverted F Antennas (PIFA), the resonant frequency is affected by the ratio  $\frac{L1}{L2}$  (see the structure of a PIFA antenna in Figure E.1). In [28] it can be seen that the more the ratio increases, the higher the drop in the ratio  $\frac{W}{L1}$  will be, and so the PIFA resonance frequency is proportional to the current distribution effective length.

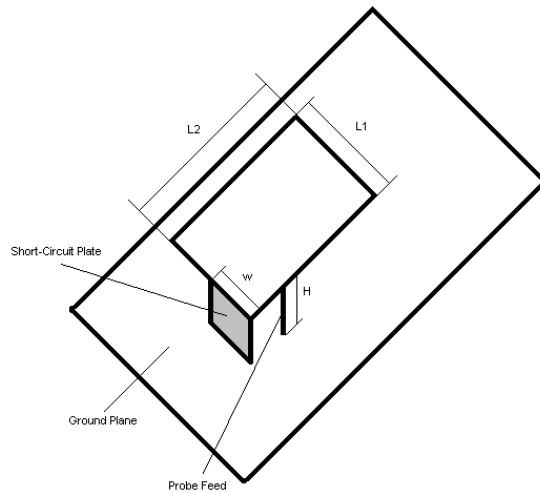


Figure E.1: Structure of PIFA Antenna

If the width of the shortcircuit plate and the length of the antenna's plate are equal i.e.  $\frac{W}{L1} = 1$ , then it results in an antenna of  $\frac{\lambda}{4}$ . The resonance frequency of the antenna can be expressed by

$$f_{r1} = \frac{c}{4*(L2+H)}$$

where

$$L2 + H = \frac{\lambda}{4}$$



The extreme case happens when  $W=0$ . This case can be represented by an infinitesimal short circuit pin. The expression can be expressed by

$$f_{r_2} = \frac{c}{4*(L_1+L_2+H)}$$

where

$$L_1 + L_2 + H = \frac{\lambda}{4}$$

When  $0 < W < L_1$

$$f_r = \frac{c}{4*(L_1+L_2+H-W)}$$

Finally, when  $0 < \frac{W}{L_1} < 1$  the resonance frequency can be approximated with a linear interpolation operation where

$$f_r = R * f_{r_1} + (1 - R) * f_{r_2} \text{ for } \frac{L_1}{L_2} \leq 1$$

and

$$f_r = R^k * f_{r_1} + (1 - R^k) * f_{r_2} \text{ for } \frac{L_1}{L_2} > 1$$

where

$$R = \frac{W}{L_1} \text{ and } k = \frac{L_1}{L_2}.$$

Figure [E.2] shows how changes the frequency vs  $L_2$  in the different cases that have been shown in this appendix. The constant values that have been used for this study are  $L_1 = 80 \text{ mm}$ ,  $H = 5 \text{ mm}$  and  $W = 50 \text{ mm}$ .

As it is also shown in Figure [E.2] the resonance frequency is always growing when the size of  $L_2$  also increases.

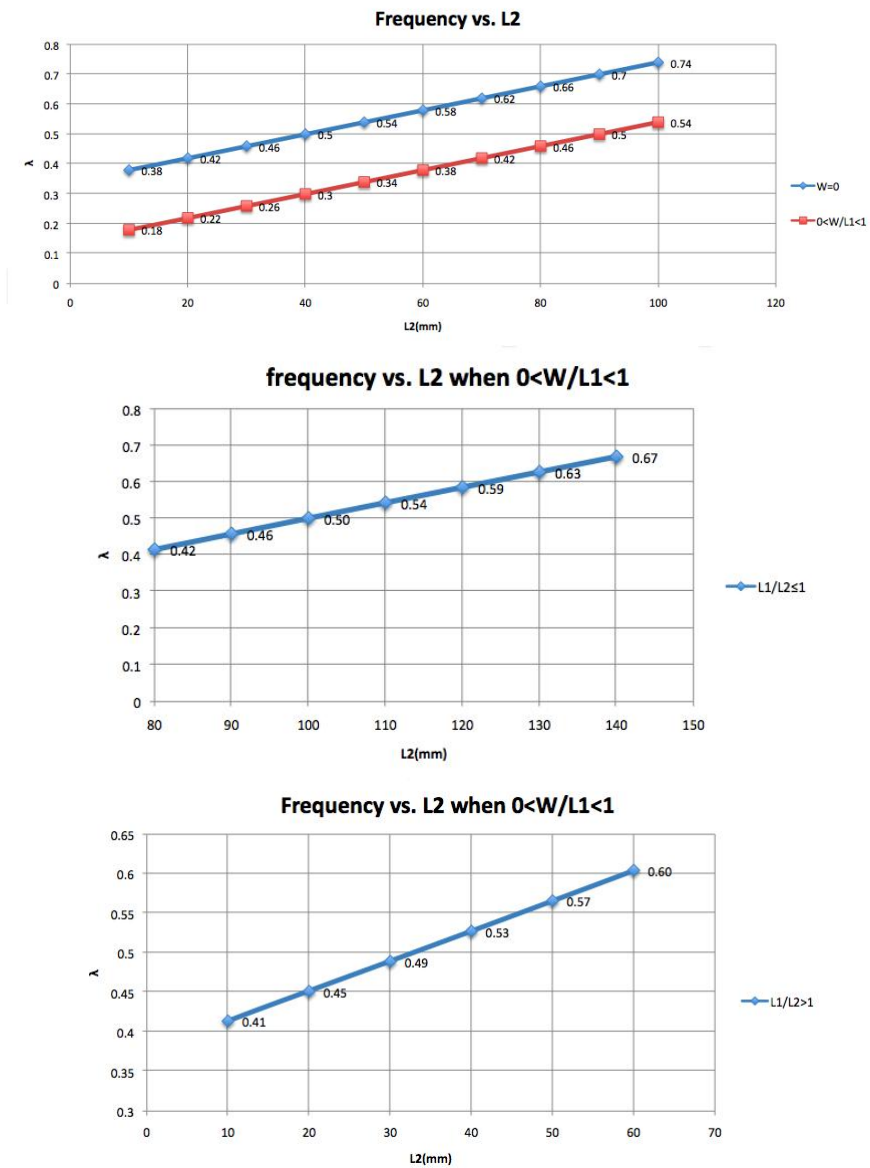


Figure E.2: Comparison of Frequency vs L2 when different W are used

# Appendix F

## Antenna Matching

One of the biggest problems when designing an antenna is to match its impedance to the transmission line, but not in the sense of designing the matching circuit but instead if it can be really matched. This means that ideally all impedances can be matched but in reality, to match the antenna, capacitors and inductors will be used and these components have some physical limitations which also limits their real (commercial) values. This commercial values can be seen in Table F.1.

	Capacitor	Inductor
Maximum	1 mF	39 mH
Minimum	0.5 pF	1 nH

Table F.1: Surface mount commercial capacitors and inductors

To do the matching a simple matching L-network has been used [29]. This kind of matching network has two configurations shown in Figures F.1 and F.2, which also show that both elements used for the impedance matching are only reactive components (inductors and capacitors) and consequently there will be no losses ideally.

Definitions:

$Z_L$  its the impedance to be matched (the load impedance)

$R_L$  its the real part of the load impedance (resistance)

$X_L$  its the imaginary part of the load impedance (reactance)

$Z_0$  its the characteristic impedance of the transmission line

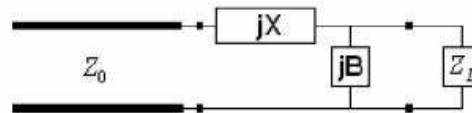


Figure F.1: First case of Matching L-network

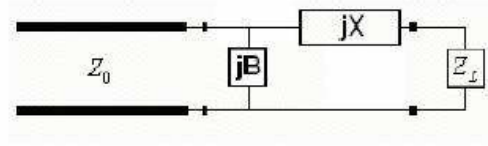


Figure F.2: Second case of Matching L-network

There are two possible configurations for this matching network, depending on the value of the load impedance [29]. In both cases is wanted the load impedance to equal  $Z_0$  if it is looked from before the matching network.

If  $R_L > Z_0$  the network looks like in Figure F.1, and solving the impedance equation, B and X can be found as:

$$B = \frac{X_L \pm \sqrt{\frac{R_L}{Z_0} (R_L^2 + X_L^2 - Z_0 R_L)}}{R_L^2 + X_L^2}$$

$$X = \frac{1}{B} + \frac{X_L Z_0}{R_L} - \frac{Z_0}{B R_L}$$

If B is positive, the element in parallel is a capacitor. If B is negative, it is an inductor. If X is positive, the element in series is an inductor. If X is negative, it is a capacitor [29].

If  $R_L < Z_0$  the network looks like in Figure F.2 and now B and X can be found as:

$$B = \pm \frac{1}{Z_0} \sqrt{\frac{Z_0 - R_L}{R_L}}$$

$$X = \pm \sqrt{R_L (Z_0 - R_L)} - X_L$$

If B is positive, the element in parallel is a capacitor. If B is negative, it is an inductor. If X is positive, the element in series is an inductor. If X is negative, it is a capacitor [29].

From these equations and different cases the values of B and X can be calculated and from these two, the values of the capacitors and inductors can be found as:

if B or X are capacitors, then:  $B$  or  $X = \frac{1}{j\omega C}$

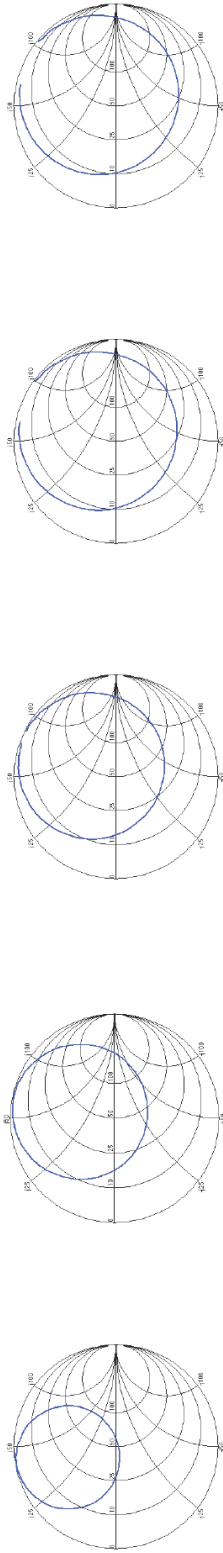
if B or X are inductors, then:  $B$  or  $X = j\omega L$

## Appendix G

# Design and Simulation of different antennas

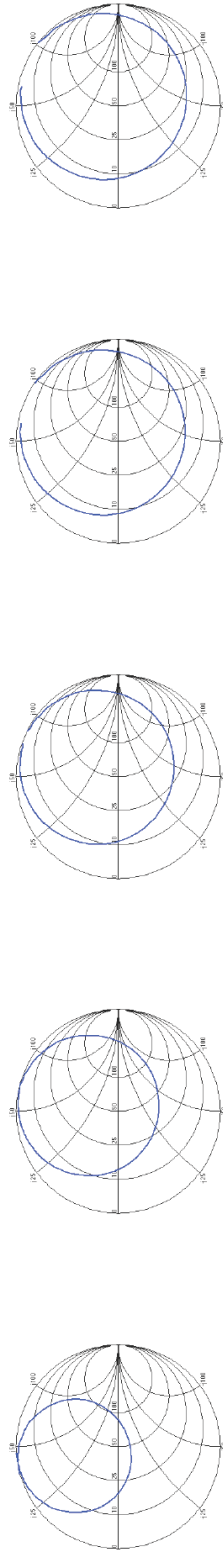
Next, it will be shown all the main results of the antennas that are presented in Chapter 4. Further, it can be seen some extra simulations with lumped elements.

Meandered\_Monopole\_Vertical\_Antenna\_100x40 mm



SPECIFICATIONS	1 MM	2 MM	3 MM	4 MM	5 MM
Radiation Efficiency	1.2303	1.2042	1.2095	1.2225	1.2184
Radiation Efficiency(dB)	0.90017	0.80704	0.826	0.87256	0.85799
Resonance found at frequency (MHz)	543	551	560	575	578
Q at Resonance	15,1762	34,6126	42,21	41,2823	40,9441
BW resonance(MHz)	35,77	15,91	13,26	13,92	14,11

Meandered\_Monopole\_Vertical\_Antenna\_90x40 mm



SPECIFICATIONS	1 MM	2 MM	3 MM	4 MM	5 MM
Radiation Efficiency	1.1763	1.2053	1.1982	1.2078	1.2022
Radiation Efficiency(dB)	0.70518	0.81082	0.78529	0.81983	0.7989
Resonance found at frequency (MHz)	548	556	565	580	584
Q at Resonance	6,739	46,538	52,6829	50,7643	50,1397
BW resonance(MHz)	81,31	11,947	10,72	11,42	11,64

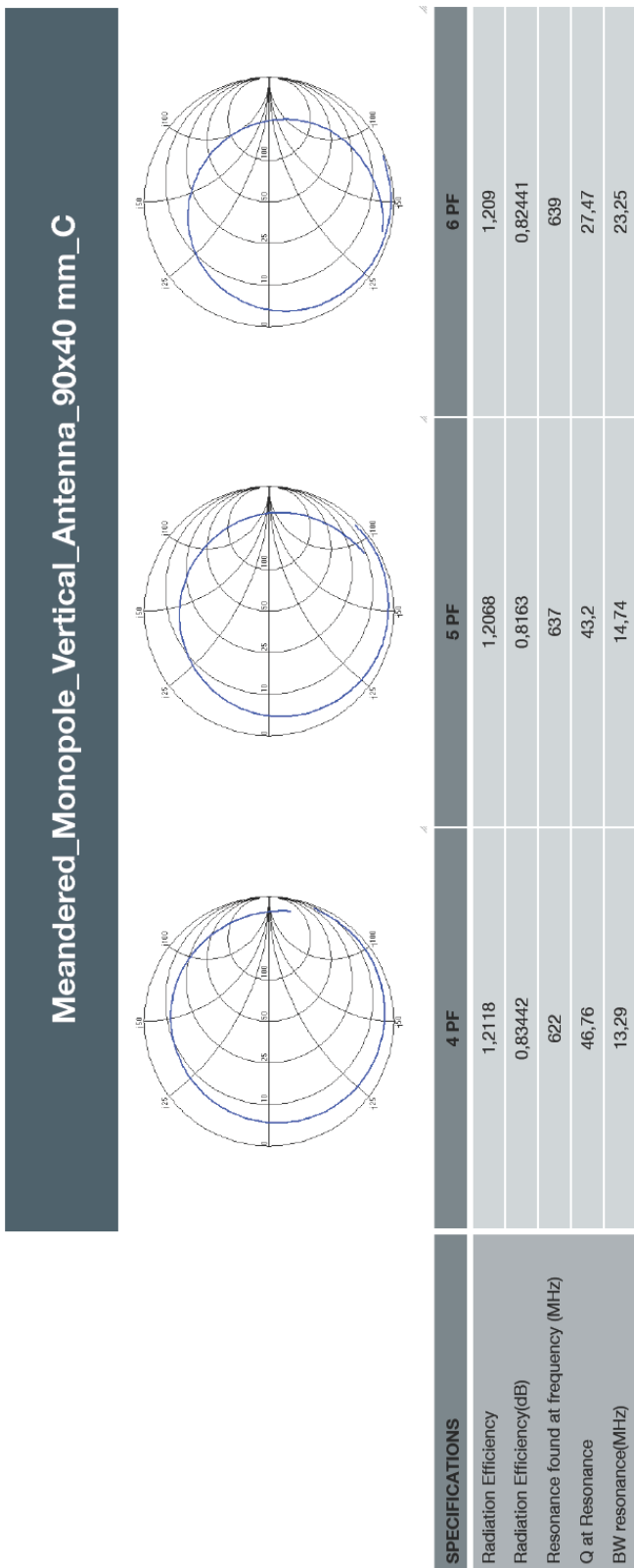
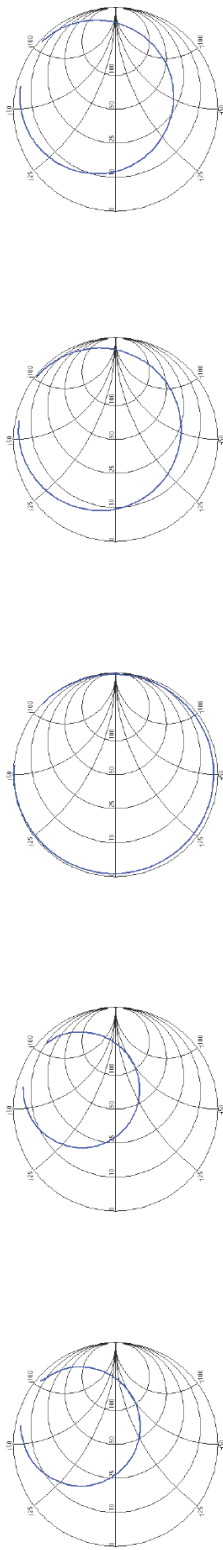


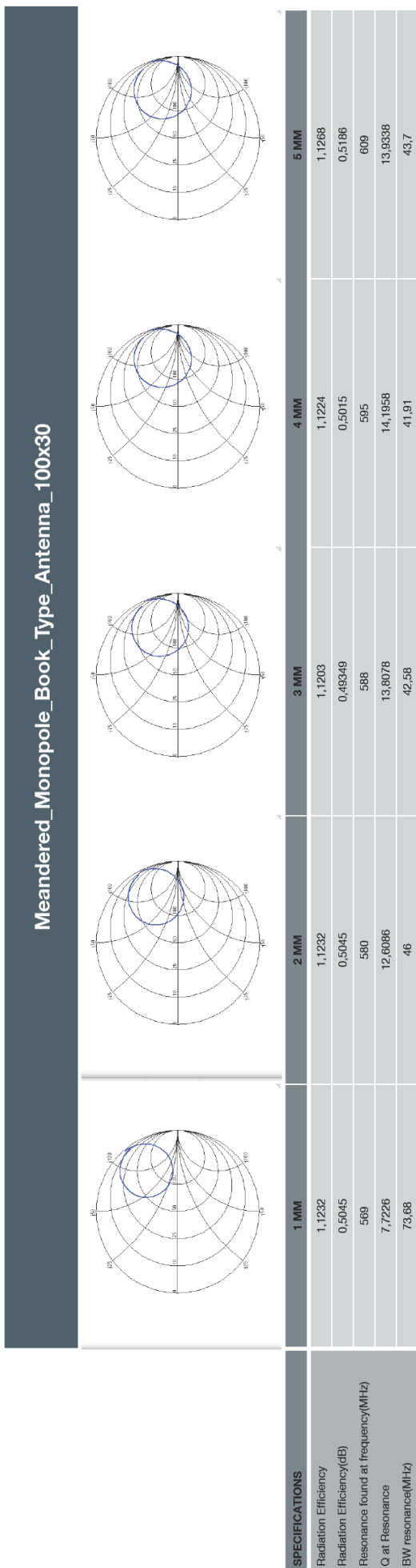
Figure G.2:

Meandered\_Monopole\_Vertical\_Antenna\_90x40mm  
\_Hands\_Wood\_Plans\_and\_Metal

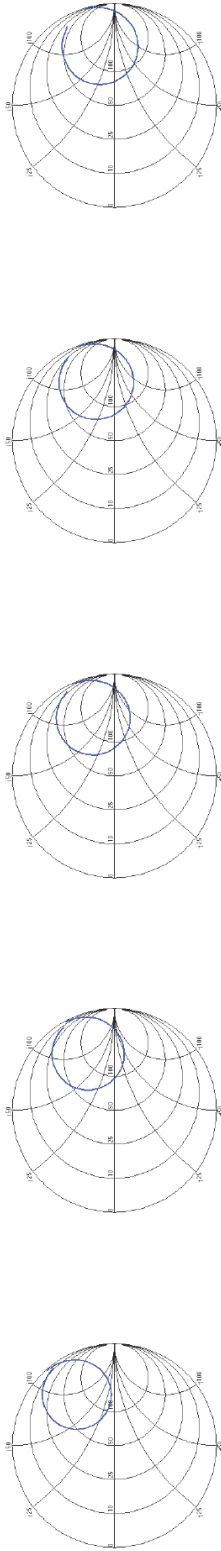


SPECIFICATIONS	HAND	DOUBLE HAND	METAL (1 CM)	WOOD (0,1 CM)	WOOD (3 CM)
Radiation Efficiency	1,2118	0,64398	1,064	1,0976	1,0929
Radiation Efficiency(dB)	0,83442	-1,9113	0,27	0,40455	0,38375
Resonance found at frequency (MHz)	622	563	574	584	569
Q at Resonance	46,76	11	423	45,49	33,4961
BW resonances(MHz)	13,29	51,2	1,356	12,83	16,98



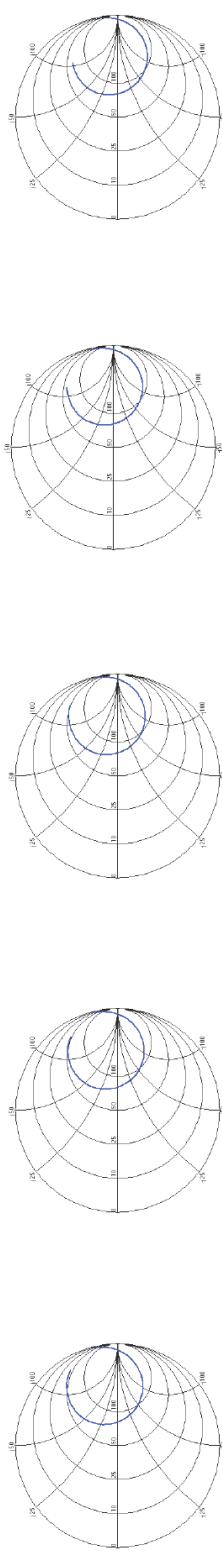


**Meandered\_Monopole\_Book\_Type\_Antenna\_90x30\_Different\_Position\_Feed**



	1 MM	2 MM	3 MM	4 MM	5 MM
<b>SPECIFICATIONS</b>					
Radiation Efficiency	1,1191	1,1185	1,1231	1,1223	1,1164
Radiation Efficiency(dB)	0,48884	0,4864	0,50427	0,50127	0,478
Resonance found at frequency(MHz)	582	594	602	609	624
Q at Resonance	9,4582	13,8694	14,76	15,0541	14,636
BW resonance(MHz)	61,53	42,82	40,75	40,45	42,63

**Meandered\_Monopole\_Book\_Type\_Antenna\_90x30\_Different\_Position\_Feed**



	6 MM	7 MM	8 MM	9 MM	10 MM
<b>SPECIFICATIONS</b>					
Radiation Efficiency	1,165	1,119	1,1217	1,1258	1,1263
Radiation Efficiency(dB)	0,47844	0,48834	0,49874	0,51467	0,5165
Resonance found at frequency(MHz)	630	636	641	655	661
Q at Resonance	14,438	14,237	14,0353	13,202	12,9688
BW resonance(MHz)	43,63	44,68	45,67	49,61	50,98

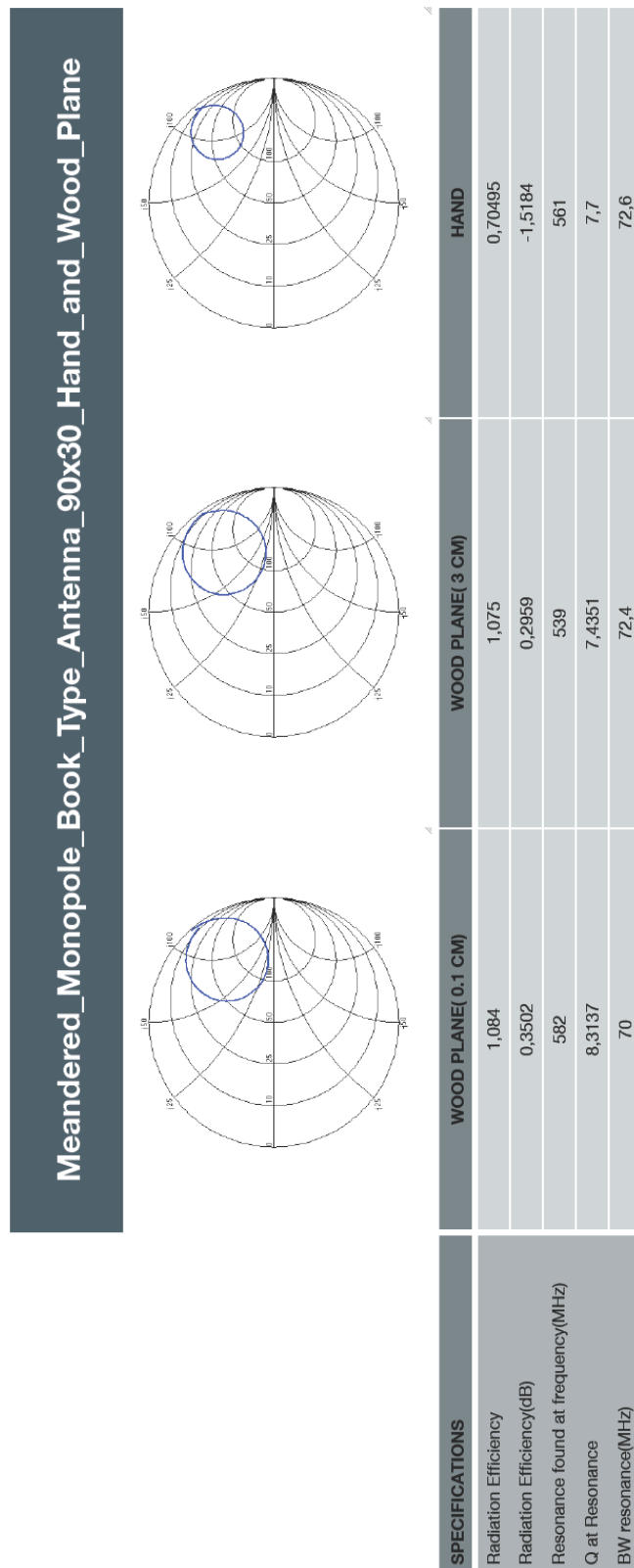


Figure G.6:

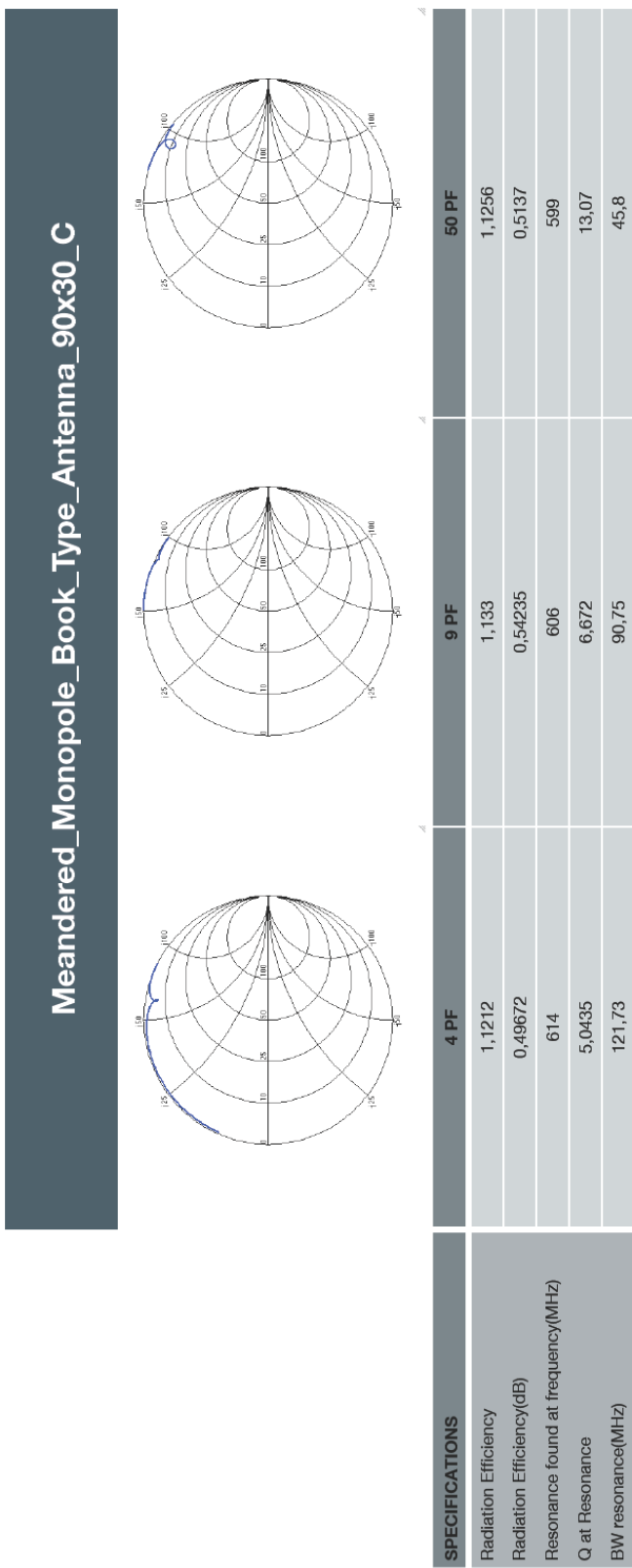


Figure G.7: